BIOGEOCHEMICAL CYCLING OF POLYAMINES IN A COASTAL MARINE ENVIRONMENT

by

QIAN LIU

(Under the Direction of James T. Hollibaugh)

ABSTRACT

Polyamines are a group of short-chain aliphatic compounds containing multiple primary or secondary amine groups. They are ubiquitous in aquatic environments with concentrations in the sub-nanomolar range, while concentrations in cells are at millimolar levels. They are commonly regarded as important osmolytes, synthesized or assimilated by osmotrophs, like bacterioplankton. They play a key role in cellular growth and synthesis of nucleic acids and proteins. However, few studies have examined the role of polyamines in oceanic N cycling.

In this study, I hypothesized that polyamines contributed a significant amount of nitrogen to bacterial N production because of greater N: C ratio in polyamines than other labile organic nitrogen compounds. I determined turnover rates of three polyamines (putrescine, spermidine and spermine) in water samples using ^{3}H-labeled compounds and measured their concentrations by HPLC in the South Atlantic Bight (SAB) and in salt marsh estuaries. The data showed that polyamines were rapidly assimilated by bacterioplankton, especially in samples from salt marshes and the inner-shelf of the SAB. However, low ambient concentrations of polyamines limited their contribution to bacterioplankton C and N demands compared to dissolved free amino acids that were used as controls. My study of polyamine metabolism in phytoplankton suggested that bacterial uptake of polyamines was limited by sources of polyamines. I found low concentrations (nmol L^{-1}) of dissolved polyamine pools in media of phytoplankton cultures, similar to concentrations measured in the field. My data suggested that the composition and concentration of dissolved polyamines was a result of low diffusion from intracellular pools, selective release and uptake by healthy phytoplankton cells, as well as modifications by bacterioplankton uptake.

Thaumarchaeota have been shown to oxidize polyamine nitrogen. This dissertation investigated the spatial and seasonal variability of abundances and activity of Thaumarchaeota in the SAB by quantitative PCR of Thaumarchaeota 16S rRNA and Archaea ammonia monooxygenase subunit A (*amoA*) genes and simulated *in situ* incubations with $^{15}NH_4Cl$. I found a peak in Thaumarchaeota abundance (>1000-fold increase) in mid-summer at inshore and nearshore stations, but rapid ammonia oxidation was constrained to the inner-shelf at the mouth of the estuaries, probably driven by the substrate availability.

INDEX WORDS: Polyamines, Putrescine, Spermidine, Spermine, Turnover rates, Uptake rates, HPLC, Bacterial Production, Phytoplankton, Diatom, Environmental variables, Thaumarchaeota, Ammonia-oxidizing Archaea, Nitrification, South Atlantic Bight

BIOGEOCHEMICAL CYCLING OF POLYAMINES IN A COASTAL MARINE ENVIRONMENT

by

QIAN LIU

B.S., Shandong University of Technology, China, 2005

M.S., Central Michigan University, 2009

A Dissertation Submitted to the Graduate Faculty of The University of Georgia in Partial Fulfillment of the Requirements for the Degree

DOCTOR OF PHILOSOPHY

ATHENS, GEORGIA

2016

BIOGEOCHEMICAL CYCLING OF POLYAMINES IN A COASTAL MARINE ENVIRONMENT

by

QIAN LIU

Major Professor:	James T. Hollibaugh
Committee:	Brian Binder
	Brian Hopkinson
	Patricia Medeiros
	Xiaozhen Mou

Electronic Version Approved:

Suzanne Barbour
Dean of the Graduate School
The University of Georgia
May 2016

DEDICATION

To my dear parents, Zhongqiu Liu and Yuhua Li

ACKNOWLEDGEMENTS

I would like to give my deepest gratitude to my Ph.D. advisor, Dr. James T. Hollibaugh, for his tremendous support through my doctoral study. It is him who brings me to the world of ocean and expands my vision in sciences. The graduate study could have been much harder without the numerous advice and discussion with him in these years. He never told me what I should do, instead, he encouraged me to propose an idea and think in my ways to solve the problems. His enthusiasm and attitude in science have influenced my perspectives in my future career. I wish to become a scientist and educator like him, dedicating myself to the scientific research and teach the future scientists. I would like to also thank my Ph.D. advisory committee –Drs. Brian Binder, Brian Hopkinson, Patricia Medeiros and Xiaozhen Mou, for their timely advice and input to my research work. I am really grateful to all of them for allowing me to access to their laboratory equipments and devoting their precious time to teach me the laboratory techniques. My research would not be done without their assist.

I also owe thanks to all the people of the Hollibaugh Laboratory, who have shared their experience, knowledge and friendship through all these years. Many thanks to Dr. Carrie Givens, Dr. Bradley Tolar, Dr. Christian Edwardson, Chris Abin, Meredith Ross, Jelani Cheek and Corinne Sweeney. Without their support, this work could not be finished successfully. I would like to especially thank Dr. Bradley Tolar, who is always patient and happy to answer all my questions in the laboratory. He assisted me in experiments and data analysis on cruises and shared with me all his knowledge without the reservation. I also thank all my collaborators-Dr. Xinxin Lu (Kent State University), who hosted me when I spent a summer in Dr. Xiaozhen

Mou’s laboratory and taught me to use HPLC for sample analysis; Drs. Nishibori Naoyaoshi and Ichiro Imai from Japan, who spent substantial times to help with measuring polyamine samples even though we have never met; Dr. Brian Popp and Natalie Wallsgrove from University of Hawaii for helping measure the ammonia-oxidation rates in samples that I collected from the cruises. I would like to give many thanks to the captain and crew members of R/V Savannah for taking me to the ocean expedition and the UGA Marine Institute at Sapelo Island for providing laboratory space for my research.

I am very grateful to the people of the Department of Marine Sciences. I really enjoy studying and working in this “small family”. The faculty and staffs are always kind and helpful. I would like to specially thank Dr. Mary Ann Moran, who is giving me a lot of advices not only in my research but also in my future career development. I also give many thanks to Sharon Barnhart, Jackie Fortson and Cat Mills, who help me with all the technology and document problems, which I am not good at outside the science. I am very lucky to have many close friends, Chen Shen, Yuntao Wang, Yeping Yuan, Jing Chen, Linquan Mu, Fang Cao and Shalabh Sharma, who share the happiness, struggles and encouragements with me.

Beyond the work and science, I am so thankful to my dear parents. Without their support, I would not come to the U.S.A. to continue my graduate study. It has been a hard time for them without me around in these years, but they give me all their love and support. They are the ones who deserve all the honors I received from this degree.

TABLE OF CONTENTS

Page

APPENDICES

CHAPTER 1

INTRODUCTION AND LITERATURE REVIEW

Nitrogen is a common factor limiting the primary and secondary productivity in the upper ocean (Carpenter and Capone 1983). Concentrations of inorganic nitrogen (DIN) are low in surface waters due to the high assimilation by phytoplankton. In coastal waters, DIN can be supplied by upwelling and runoff, stimulating high primary productivity (Zehr and Ward 2002). In less productive open ocean, the processes of microbial degradation of organic nitrogen compounds provide regenerated N to the environment to fuel productivity (Dugdale and Goering 1967, Azam et al. 1983). Although heterotrophic bacteria can also use DIN (Kirchman 1994, Allen et al. 2001), their roles in assimilating and degrading organic nitrogen to recycle DIN is their most important contribution to the N cycle in the upper ocean (e.g. Diaz and Raimbault 2000, Kerner and Spitzy 2001, Varela et al. 2003). The nitrogen regeneration by bacteria or microzooplankton grazing depends on the availability of these substrates as well as the ratio of carbon to nitrogen in labile organic matter (Caron and Goldman 1990, Kirchman 2000). Therefore, regenerated nitrogen provided by heterotrophic bacteria may have spatial and seasonal variability (Kirchman 2000). Heterotrophic bacteria can use a variety of dissolved organic nitrogen compounds, such as proteins, amino acids, urea, taurine, glycine betaine and polyamines (Hollibaugh and Azam 1983, Höfle 1984, Fuhrman 1987, 1990, Suttle et al. 1991, Keil and Kirchman 1991, Lee 1992, Lee and Jørgensen 1995, Moran et al. 2004, Poretsky et al. 2010, Mou et al. 2010, Williams et al. 2012). Dissolved free amino acids (DFAA) are readily used by bacteria and the turnover of DFAA is rapid, proceeding within only a few hours

(Fuhrman 1987, 1990, Suttle et al. 1991). However, DFAA can supply < 40% of the nitrogen required by bacterioplankton, and the remaining requirement is assumed to be met by uptake of other organic nitrogen compounds or DIN, based on the detection of transporters and assimilation genes in genomes of bacterioplankton and from field experiments (Höfle 1984, Lee and Jørgensen 1995, Kirchman 2000, Allen et al. 2001, Williams et al. 2012).

The small organic nitrogen compounds found in seawater, such as taurine, glycine betaine and polyamines, have similar intracellular concentrations (mmol L^{-1}) to amino acids and their biogeochemical characteristics in seawater are assumed to resemble the amino acids. I focused on the role of polyamines, a group of organic nitrogen compounds, in bacterial nitrogen demand in different regions of the SAB since 1) the high N content ($C:N \geq 2$) of polyamines makes them ideal as organic nitrogen sources for bacterioplankton; 2) genes for polyamine transporters and catabolic pathways are widespread in marine bacterioplankton such as SAR 11 (Moran et al. 2004, Poretsky et al. 2010, Mou et al. 2010); 3) the assimilation of putrescine has been detected previously in waters with high productivity (Höfle 1984, Lee and Jørgensen 1995).

Polyamine Characteristics

Polyamines are a group of short-chain aliphatic organic compounds containing multiple amine groups. They have been found in all domains of life (Tabor and Tabor 1985). Polyamines include 1,3 diaminopropane (DAP), 1,4 diamino butane (putrescine, PUT), 1,5 diamino pentane (cadaverine, CAD), spermidine (SPD), spermine (SPM), norspermidine (NSPD) and norspermine (NSPM). Their chemical structures are given in Table 1.1 with pKa values for each amine group. PUT, SPD and SPM are the most common polyamines found in living cells and environment (Tabor and Tabor 1985, Rodriguez-Garay et al. 1989, Hamana and Matsuzaki 1992, Márian et al. 2000, Nishibori et al. 2001a, 2001b, Lu and Hwang 2002, Kusano et al. 2007, Incharoensakdi et al. 2010). Their functions have been studied in different organisms, from bacteriophages to mammals. They are cations at physiological pH and contribute to stabilizing cells membranes and aid the syntheses of DNA, RNA and proteins (Tabor and Tabor 1985). They affect the syntheses of proteins and DNA by decreasing polypeptide elongation rate and synthesis and translation of mRNA, and slowing the rate of movement of the DNA replication fork, respectively (Morris and Hansen1973, Geiger and Morris 1980). They have been shown to enhance growth because the growth rate of mutant of *E. coli* strains lacking polyamines is 70% lower than in wild type cells (Hafner et al. 1979, Tabor et al. 1980). Long-chain polyamines induce rapid silica precipitation and interact with silica-precipitating proteins to form species-specific patterns of biomineralization in diatom cell walls (Kröger et al. 2000). Long-chain or branched polyamines are also synthesized in the thermophilic bacterium *Thermus thermophiles* as well as by thermophilic and hyperthermophilic Crenarchaeota to protect cells from the denaturing effects of high temperature (Oshima 1979, 1982, Oshima and Baba 1981, Carteni-Farina et al. 1985, Knott 2007). Polyamines also serve as osmolytes, playing an important role in preventing cell lysis in hypotonic medium. They are also synthesized in cells living in hypertonic environments (e.g. seawater, salt lakes) to maintain normal physiological functions of these cells (Tabor 1960, Tabor and Tabor 1985). Polyamine synthesis responds to environmental stresses. Genes of polyamine synthesis pathways are overexpressed under conditions of extreme temperature, drought, salinity and toxicity (Kasukabe et al. 2004, Urano et al. 2004, Kusano et al. 2007).

Polyamine Metabolism in Microorganisms

Polyamines can be produced by *de novo* biosynthesis in the cell or taken up from the environment. The *de novo* biosynthesis of polyamines starts with the synthesis of PUT by two different metabolic pathways, either from ornithine via ornithine decarboxylase (ODC, EC 4.1.1.17), which is mostly used by eukaryotes (e.g. fungi and algae) (Theiss et al. 2002, Kusano et al. 2007), or from arginine via arginine decarboxylase and agmatine ureohydrolase (ADC, EC4.1.1.19), found mostly in prokaryotes and plants (Fig. 1.1; Tabor and Tabor 1985, Incharoensakdi et al. 2010). PUT is used as a substrate to form SPD via SPD synthase (EC 2.5.1.16), and then converted to SPM or thermospermine by SPM synthase (EC 2.5.1.22) by the addition of aminopropyl groups from decarboxylated S-adenosyl methionine (Fig. 1.1). Oxidation of SPD or SPM produces DAP, which is subsequently converted to the triamine NSPD, and then the tetraamine NSPM (Tabor et al. 1958, Tabor and Tabor 1966, 1985, Bagga et al. 1991, Fuell et al. 2010).

Uptake systems for polyamines have been identified in many different microorganisms (Tabor and Tabor 1966). Uptake systems for putrescine (PotFGHI) and spermidine (PotABCD) have been found in *E. coli*, yeast, cyanobacteria and most of marine bacterial groups (Igarashi and Kashiwagi 1999, Moran et al. 2007, Incharoensakdi et al. 2010, Mou et al. 2010, 2011), suggesting the use and selective uptake of exogenous polyamines. SAR 11 and roseobacter taxa have been identified as the significant contributors to polyamine uptake by marine bacterioplankton because a large number of polyamine transporter genes from these groups were detected in metatranscriptomes of polyamine-amended coastal marine bacterioplankton samples (Poretsky et al. 2010, Mou et al. 2010). These organisms degrade polyamines through a transamination pathway and produce succinate, an intermediate of TCA cycle, while the nitrogen assimilated from polyamines may be used to synthesize amino acids (Mou et al. 2011).

Hölfe (1984) found that most of the carbon from PUT and CAD amendments was not incorporated into bacterial cells (< 10%) and growth was not enhanced by the addition of putrescine; thus, most of the carbon in putrescine may be respired or excreted and not contribute to biomass production. The fate of polyamine nitrogen in these cells is not clear, but may depend on nitrogen availability in the water column. PUT has been studied most thoroughly so far, but all data suggest that the low concentrations of polyamines in the environment could be a result of bacterial uptake (Höfle 1984, Lee and Jørgensen 1995, Mou et al. 2011).

Polyamine Distributions in Marine Environments

Concentrations and the composition of polyamine pools have been determined by high performance liquid chromatography (HPLC) in both cells and seawater. Intracellular polyamines pools are much larger (mmol L^{-1}) in bacteria and algae (Hamana and Matsuzaki 1985, 1992, Nishibori et al. 2006, Nishibori and Nishijima 2007, Incharoensakdi et al. 2010) than in the water column (nmol L^{-1}; Lee and Jørgensen 1995, Nishibori et al. 2001a, 2001b, Nishibori et al. 2003). As discussed above uptake by bacteria may be responsible for maintaining low concentrations of polyamines in seawater. Most of the few studies of polyamine concentrations in seawater have been conducted in coastal waters or salt ponds with high primary productivity. These studies found that dissolved polyamine concentrations ranged from undetectable to hundreds of nmol L^{-1}, with high concentrations corresponding to algal blooms or high primary production (Lee and Jørgensen 1995, Nishibori et al. 2001a, 2001b, Nishibori et al. 2003). PUT and SPD are the most common polyamines detected in seawater, while other polyamines are detected only occasionally

(Nishibori et al. 2001a, 2001b, 2003). In order to better assess the significance of polyamines in the ocean, more studies of polyamine distributions in oligotrophic offshore waters were necessary.

Ammonia-oxidizing Archaea Proposed to Oxidize Reduced N in DON Compounds

Detection of mesophilic Archaea in the ocean has changed our view that they only live in extreme environments (Delong 1992, Fuhrman et al. 1992). Karner et al. (2001) found that the relative abundance of Archaea increased from surface to the bottom of the ocean (~ 40% of total prokaryotes), comparable to the abundance of bacteria at depth. Archaea can also take up organic compounds, such as amino acids, as nutrient and energy sources (Ouverney and Fuhrman 2000). However, in recent decades, physiological and genomic studies of Archaea have shown that one clade, the marine group I Archaea, can grow as chemoautotrophs, oxidizing ammonia to nitrite to generate the reducing equivalents needed to fix carbon through the 3-hydroxypropionate/4-hydroxybutyrate pathway (Schleper et al. 2005, Könneke et al. 2005, Hallam et al. 2006a, 2006b, Berg et al. 2007, Martens-Habbena et al. 2009). Previously only two clades of Bacteria were considered to be capable of oxidizing ammonia, the first step of nitrification; however, since Archaea ammonia monooxygenase (*amo*) genes were detected in DNA sequences retrieved from the Sargasso Sea (Venter et al. 2004), the role of Archaea in nitrification has been investigated widely. These studies have shown that ammonia-oxidizing Archaea (now called Thaumarchaeota) outnumbered ammonia-oxidizing Bacteria (AOB) in most marine environments by up to 1000-fold (Wuchter et al. 2006, Mincer et al. 2007, Santoro et al. 2010, Newell et al. 2013). Moreover, Thaumarchaeota have a high affinity for ammonia and can outcompete AOB for the substrate (Martens-Habbena et al. 2009), suggesting that Thaumarchaeota are the dominant ammonia-oxidizer in the ocean.

Although Thaumarchaeota can survive in the water column with extremely low ammonium concentrations (10 nmol L^{-1}; Martens-Habbena et al. 2009), it has been suggested that Thaumarchaeota can use urea as an alternative source of reduced N to fuel nitrification (Hallam et al. 2006b, Alonso-sáez et al. 2012, Connelly et al. 2014, Tolar 2014). The *ureC* gene, which is found widely distributed in bacteria and phytoplankton (Collier et al. 2009, Baker et al. 2009, Su et al. 2013), is used as an indicator of the potential to use urea. *ureC* genes have been identified in the genome of '*Cenarchaeum symbiosum*' and in the environment, suggesting the significance of this gene to Thaumarchaeota (Hallam et al., 2006b, Alonso-sáez et al. 2012, Tolar 2014). In high latitude environments, some evidence has suggested that Thaumarchaeota are involved in uptake of urea, hydrolyzing urea and subsequently oxidizing ammonia (Alonso-sáez et al. 2012, Connelly et al. 2014). However, in Georgia coastal waters, urea oxidation is low and it has been suggested that urea hydrolysis happens extracellularly and the released ammonium is then oxidized by Thaumarchaeota (Tolar 2014). Preliminary experiments performed by amending coastal seawater samples with ^{15}N-labeled urea and putrescine have shown that the oxidation of ^{15}N supplied as putrescine could be 2-order of magnitude larger than the oxidation of ammonium and urea, and polyamine-N appeared to be oxidized directly to NOx (Hollibaugh lab, unpublished). This did not occur in amino acid-N and urea-N; thus, polyamine oxidation changed our traditional view that bacteria are mainly responsible for polyamine removal. Low polyamine concentrations (sub-nmol L^{-1} level, ~1-order of magnitude lower than dissolved free amino acids) may also be explained by the direct oxidation by Thaumarchaeota.

OBJECTIVES

The first objective of my work was to determine the distribution and composition of dissolved polyamines in the SAB. A second objective was to determine their turnover rate in situ by measuring uptake by bacteria. A third objective was to determine the contribution of polyamines to bacterial N demand. These objectives are addressed in Chapter 2, which reports turnover rates and concentrations of putrescine, spermidine and spermine in the South Atlantic Bight (SAB), from inner shelf to the shelf-break. These data were used to calculate polyamine uptake rates. I determined the same variables for two dissolved free amino acids (glutamate and arginine) to better understand the relative contributions of polyamines to bacterial carbon and nitrogen demands, which were estimated from L-leucine incorporation. Environmental variables (e.g. T, S, dissolved oxygen, light attenuation and DIN concentrations) were measured to evaluate the impact of environmental conditions on the cycling of polyamines in seawater.

Previous studies (Lee and Jørgensen 1995, Nishibori et al. 2003), and the results described in Chapter 2 suggested that the abundance and composition of phytoplankton control the concentration and composition polyamines in the water column. My fourth objective was to determine the composition and concentration of intracellular pools of polyamines in 4 representative phytoplankton (a cyanobacterium, 2 different centric diatoms and a dinoflagellate), while the 5th objective was to determine how environmental conditions (stress, nutrient limitation) affected polyamine pools in phytoplankton and the 6th was to evaluate uptake or loss of polyamines from phytoplankton into the culture medium. Experiments to address these objectives are described in Chapter 3. I designed experiments using laboratory cultures of pure phytoplankton species (diatoms *Thalassiosira pseudonana* and *Chaetoceros* sp.; the cyanobacterium *Synechococcus* sp. and the dinoflagellate *Amphidinium carterae* Hulburt) to determine the intracellular concentration and composition of polyamines in these species. I used the model diatom species *T. pseudonana* for more detailed studies of variation of polyamine pools in different growth phases of *T. pseudonana*. Another set of experiments with *T. pseudonana* manipulated environmental (T and S) conditions and nutrient limitation to observe the changes of the intracellular and extracellular polyamine pools. Since phytoplankton have been reported to take up DON in the ocean (Bronk et al. 2007), we used ^{14}C-labeled PUT to track the uptake of PUT by *T. pseudonana*. The information on polyamine synthesis, release and uptake by phytoplankton addressed in Chapter 3 will help us better understand the spatial and temporal variability of polyamines in the ocean.

As discussed above, preliminary data suggest that Thaumarchaeota are able to use the N in polyamines in place of ammonia to generate energy. A 7th objective of my work, then, was to determine the spatial and temporal distribution of Thaumarchaeota in the SAB. Thaumarchaeota have been detected in Georgia coastal waters previously and their abundance has been found to vary seasonally, with a mid-summer peak of $> 10^8$ 16S rRNA gene copies L^{-1} (Hollibaugh et al. 2011, 2014, Tolar 2014). I repeated some of the survey work conducted in 2011 and expanded our sampling sites into coastal waters of the SAB out to the shelf-break to determine the spatial and seasonal distribution of Tharmarchaeota there. I measured the abundance of Thaumarchaeota 16S rRNA and ammonia monooxygenase subunit A (*amoA*) genes, as well as Betaproteobacteria *amoA* and *Nitrospina* sp. 16S rRNA genes. I measured nitrification rate by *in situ* incubation of ^{15}N-labeled NH_4Cl at selected stations from inshore to offshore. I constructed clone libraries of Thaumarchaeota 16S rRNA and Archaea *amoA* genes to assess the distribution of Thaumarchaeota ecotypes and their diversity of in different water mass. A better understanding of the seasonal and spatial variability of ammonia-oxidizing Archaea in the SAB will lay the foundation for future studies of polyamine distributions in the SAB.

REFERENCES

Allen AE, Booth MG, Frischer ME, Verity PG, Zehr JP, Zani S (2001) Diversity and detection of nitrate assimilation genes in marine bacteria. Appl Environ Microbiol 67:5343-5348

Alonso-Saez L, Waller AS, Mende DR, Bakker K, Farnelid H, Yager PL, Lovejoy C, Tremblay JE, Potvin M, Heinrich F, Estrada M, Riemann L, Bork P, Pedros-Alio C, Bertilsson S (2012) Role for urea in nitrification by polar marine Archaea. Proc Natl Acad Sci U S A 109:17989-17994

Azam F, Frenchel T, Field JG, Gray JS, Meyer-Reil LA, Thingstad F (1983) The ecological role of water-column microbes in the sea. Mar. Ecol. Prog. Ser 10: 257-263

Bagga S, Dharma A, Phillips GC, Kuehn GD (1991) Evidence for the occurrence of polyamine oxidase in the dicotyledonous plant *Medicago sativa* L. (alfalfa). Plant Cell Rep 10:550-554

Baker KM, Gobler CJ, Collier JL (2009) Urease gene sequences from algae and heterotrophic Bacteria in axenic and nonaxenic phytoplankton cultures. J Phycol 45:625-634

Berg IA, Kockelkorn D, Buckel W, Fuchs G (2007) A 3-hydroxypropionate/4-hydroxybutyrate autotrophic carbon dioxide assimilation pathway in Archaea. Science 318: 1782-1786

Bronk DA, See JH, Bradley P, Killberg L (2007) DON as a source of bioavailable nitrogen for phytoplankton. Biogeosciences 4:283-296

Caron DA, Goldman JC (1990) Protozoan nutrient regeneration. In: Capriulo GM (ed) Ecology of marine protozoa. Oxford University Press, New York, p 283-306

Carpenter EJ, Capone, DG (1983) Nitrogen in the Marine Environment. Academic Press.

Carteni-Farina M, Porcelli M, Cacciapuoti G, De Rosa M, Gambacorta A, Grant WD, Ross HNM (1985) Polyamines in halophilic archaebacteria. FEMS Microbiol. Lett. 28: 323-327.

Collier JL, Baker KM, Bell SL (2009) Diversity of urea-degrading microorganisms in open-ocean and estuarine planktonic communities. Environ Microbiol 11:3118-3131

Connelly TL, Baer SE, Cooper JT, Bronk DA, Wawrik B (2014) Urea uptake and carbon fixation by marine pelagic bacteria and archaea during the Arctic summer and winter seasons. Appl Environ Microbiol 80:6013-6022

DeLong EF (1992) Archaea in coastal marine environments. Proc Natl Acad Sci 89:5685-5689

Diaz F, Raimbault P (2000) Nitrogen regeneration and dissolved organic nitrogen release during spring in a NW Mediterranean coastal zone (Gulf of Lions): implications for the estimation of new production. Mar Ecol Prog Ser 197:51-65

Dugdale RC, Goering JJ (1967) Uptake of new and regenerated forms of nitrogen in primary productivity. Limnol Oceanogr 12:196-206

Fuell C, Elliott AK, Hanfrey CC, Franceschetti M, Michael AJ (2010) Polyamine biosynthesis diversity in plants and algae. Plant Physiology and Biochemistry 48:513-520

Fuhrman J (1987) Close coupling between release and uptake of dissolved free amino acids in seawater studied by an isotope dilution approach. Mar. Ecol. Prog. Ser 37: 45-52

Fuhrman J (1990) Dissolved free amino acids cycling in an estuarine outflow plume. Mar. Ecol. Prog. Ser 66: 197-203

Fuhrman JA, McCallum K, Davis AA (1992) Novel major archaebacterial group from marine plankton. Nature. 356: 148-149

Geiger LE, Morris DR (1980) Stimulation of deoxyribonucleic acid replication fork movement by spermidine analogs in polyamine-deficient *Escherichia coli.* J. Bacteriol. 141:1192-1198

Hafner EW, Tabor CW, Tabor H (1979) Mutants of *Escherichia coli* that do not contain 1,4-diaminobutane (putrescine) or spermidine. J. Biol. Chem. 254: 12419-12426

Hallam SJ, Konstantinidis KT, Putnam N, Schleper C, Watanabe Y, Sugahara J, Preston C, de la Torre J, Richardson PM, DeLong EF (2006a) Genomic analysis of the uncultivated marine crenarchaeote Cenarchaeum symbiosum. Proc Natl Acad Sci U S A 103:18296-18301

Hallam SJ, Mincer TJ, Schleper C, Preston CM, Roberts K, Richardson PM, DeLong EF (2006b) Pathways of carbon assimilation and ammonia oxidation suggested by environmental genomic analyses of marine Crenarchaeota. PLoS Biol 4:e95

Hamana K, Matsuzaki S (1985) Further study on polyamines in primitive unicellular eukaryotic algae. J. Biochem 97: 1311-1315

Hamana K, Matsuzaki S (1992) Polyamines as a chemotaxonomic marker in bacterial systematics. Critical Reviews in Microbiology 18:261-283

Hollibaugh JT, Azam F (1983) Microbial degradation of dissolved proteins in seawater. Limnol Oceanogr 28:1104-1116

Hollibaugh, J.T., Gifford, S.M., Moran, M.A., Ross, M.J., Sharma, S., and Tolar, B.B. (2014) Seasonal variation in the metatranscriptomes of a Thaumarchaeota population from SE USA coastal waters. *ISME J* **8**: 685-698.

Hollibaugh, J.T., Gifford, S., Sharma, S., Bano, N., and Moran, M.A. (2011) Metatranscriptomic analysis of ammonia-oxidizing organisms in an estuarine bacterioplankton assemblage. *ISME J* **5**: 866-878.

Höfle MG (1984) Degradation of putrescine and cadaverine in seawater cultures by marine bacteria. Applied and Environmental Microbiology 47:843-849

Igarashi K, Kashiwagi K (1999) Polyamine transport in bacteria and yeast. Biochem. J. 344:633-642

Incharoensakdi A, Jantaro S, Raksajit W, Mäenpää P (2010) Polyamines in cyanobacteria: biosynthesis, transport and abiotic stress. Current Research, Technology and Education Topics in Applied Microbiology and Microbial Biotechnology 23-32

Karner MB, DeLong EF, Karl DM (2001) Archaeal dominance in the mesopelagic zone of the Pacific Ocean. Nature 409:507-510

Kasukabe Y, He LX, Nada K, Misawa S, Ihara I, Tachibana S (2004) Overexpression of spermidine synthase enhances tolerance to multiple environmental stresses and up-regulates the expression of various stress regulated genes in transgenic Arabidopsis thaliana. Plant Cell Physiol 45:712-722

Keil RG, Kirchman DL (1991) Contribution of dissolved free amino-acids and ammonium to the nitrogen requirements of heterotrophic bacterioplankton. Mar Ecol Prog Ser 73:1-10

Kerner M, Spitzy A (2001) Nitrate regeneration coupled to degradation of different size fractions of DON by the picoplankton in the Elbe Estuary. Microb Ecol 41:69-81

Kirchman DL (1994) The uptake of inorganic nutrient by heterotrophic bacteria. Microbial Ecology 28:255-271

Kirchman DL (2000) Uptake and regeneration of inorganic nutrients by marine heterotrophic bacteria. Microbial Ecology of the Oceans, 1st edn. Wiley-Liss, pp. 261-288.

Knott JM, Romer P, Sumper M (2007) Putative spermine synthases from Thalassiosira pseudonana and Arabidopsis thaliana synthesize thermospermine rather than spermine. FEBS Letters 581:3081-3086

Konneke M, Bernhard AE, de la Torre JR, Walker CB, Waterbury JB, Stahl DA (2005) Isolation of an autotrophic ammonia-oxidizing marine archaeon. Nature 437:543-546

Kröger N, Deutzmann R, Bergsdorf C, Sumper M (2000) Species-specific polyamines from diatoms control silica morphology. PNAS 97: 14133-14138

Kusano T, Yamaguchi K, Berberich T, Takahashi Y (2007) Advances in polyamine research in 2007. J Plant Res 120: 345-350

Lee C (1992) Controls on organic carbon preservation: The use of stratified water bodies to compare intrinsic rates of decomposition in oxic and anoxic systems. Geochimica et Cosmochimica Acta 56: 3323-3335

Lee C, Jørgensen NOG (1995) Seasonal cycling of putrescine and amino acids in relation to biological production in a stratified coastal salt pond. Biogeochemistry 29:131-157

Lu Y, Hwang D (2002) Polyamine profile in the paralytic shellfish poison-producing alga *Alexandrium minutum.* Journal of Plankton Research 24 (3): 275-279

Marián FD, García-Jiménez P, Robaina RR (2000) Polyamines in marine macroalgae: Levels of putrescine, spermidine and spermine in the thalli and changes in their concentration during glycerol-induced cell growth in vitro. Physiologia Plantarum 110: 530-534

Martens-Habbena W, Berube PM, Urakawa H, de la Torre JR, Stahl DA (2009) Ammonia oxidation kinetics determine niche separation of nitrifying Archaea and Bacteria. Nature 461:976-979

Mincer TJ, Church MJ, Taylor LT, Preston C, Karl DM, DeLong EF (2007) Quantitative distribution of presumptive archaeal and bacterial nitrifiers in Monterey Bay and the North Pacific Subtropical Gyre. Environ Microbiol 9:1162-1175

Moran MA, Buchan A, Gonzalez JM, Heidelberg JF, Whitman WB, Kiene RP, Henriksen JR, King GM, Belas R, Fuqua C, Brinkac L, Lewis M, Johri S, Weaver B, Pai G, Eisen JA, Rahe E, Sheldon WM, Ye W, Miller TR, Carlton J, Rasko DA, Paulsen IT, Ren Q, Daugherty SC, Deboy RT, Dodson RJ, Durkin AS, Madupu R, Nelson WC, Sullivan SA, Rosovitz MJ, Haft DH, Selengut J, Ward N (2004) Genome sequence of Silicibacter pomeroyi reveals adaptations to the marine environment. Nature 432:910-913

Moran MA, Belas R, Schell MA, González JM, Sun F, Sun S *et al.* (2007) Ecological genomics of marine roseobacters. Appl Environ Microbiol 73: 4559–4569

Morris DR, Hansen MT (1973) Influence of polyamine limitation on the chain growth rates of β-galactosidase and of its messenger ribonucleic acid. J. Bacteriol. 116: 588-592

Mou X, Sun S, Rayapati P, Moran MA (2010) Genes for transport and metabolism of spermidine in Ruegeria pomeroyi DSS-3 and other marine bacteria. Aquatic Microbial Ecology 58: 311-321

Mou X, Vila-Costa M, Sun S, Zhao W, Sharma S, Moran MA (2011) Metatranscriptomic signature of exogenous polyamines utilization by coastal bacterioplankton. Environmental Microbiology Reports 3: 798–806

Newell SE, Fawcett SE, Ward BB (2013) Depth distribution of ammonia oxidation rates and ammonia-oxidizer community composition in the Sargasso Sea. Limnology and Oceanography 58:1491-1500

Nishibori N, Fujihara S, Nishijima T (2006) Changes in intracellular polyamine concentration during growth of *Heterosigma akashiwo* (Raphidophyceae). Fisheries Science 72: 350-355

Nishibori N, Matuyama Y, Uchida T, Moriyama T, Ogita Y, Oda M, Hirota H (2003) Spatial and temporal variations in free polyamine distributions in Uranouchi Inlet, Japan. Marine chemistry 82(3): 307-314

Nishibori N, Nishii A, Takayama H (2001a) Detection of free polyamine in coastal seawater using ion exchange chromatography. ICES Journal of Marine Science 58: 1201-1207

Nishibori N, Nishijima T (2007) Changes in polyamine levels during growth of a red-tide causing phytoplankton *Chattonella antiqua* (Raphidophyceae). European Journal of Phycology 39: 51-55

Nishibori N, Yuasa A, Sakai M, Fujihara S, Nishio S (2001b). Free polyamine concentrations in coastal seawater during phytoplankton bloom. Fisheries Science 67: 79-83

Oshima T (1979) A new polyamine, thermospermine, 1,12-diamino-4,8-diazadodecane, from an extreme thermophile. J. Biol. Chem. 254 (18): 8720-8722

Oshima T (1982) A pentaamine is present in an extreme thermophile. J. Biol. Chem. 257 (17):9913-9914

Oshima T, Baba M (1981) Occurrence of sym-homospermidine in extremely thermophilic bacteria. Biochem Biophys Res Commun. 103(1):156-160

Ouverney CC, Fuhrman JA (2000) Marine planktonic archaea take up amino acids. Appl Environ Microbiol 66:4829-4833

Poretsky RS, Sun S, Mou X, Moran MA (2010) Transporter genes expressed by coastal bacterioplankton in response to dissolved organic carbon. Environ Microbiol 12:616-627

Rodriguez-Garay B, Phillips GC, Kuehn GD (1989) Detection of norspermidine and norspermine in *Medicago sativa* L. (Alfalfa). Plant physiology 89:525-529

Santoro AE, Casciotti KL, Francis CA (2010) Activity, abundance and diversity of nitrifying archaea and bacteria in the central California Current. Environ Microbiol 12:1989-2006

Schleper C, Jurgens G, Jonuscheit M (2005) Genomic studies of uncultivated archaea. Nat Rev Microbiol 3:479-488

Su J, Jin L, Jiang Q, Sun W, Zhang F, Li Z (2013) Phylogenetically diverse ureC genes and their expression suggest the urea utilization by bacterial symbionts in marine sponge Xestospongia testudinaria. PLoS One 8:e64848

Suttle CA, Chan AM, Fuhrman JA (1991) Dissolved free amino acids in the Sargasso Sea: uptake and respiration rates, turnover times, and concentrations. Mar. Ecol. Prog. Ser. 70: 189-199

Tabor H (1960) Stabilization of bacteriophage T5 by spermine and related polyamines. Biochem. Biophys. Res. Commun. 3:382-385

Tabor H, Hafner EW, Tabor CW (1980) Construction of an *Escherichia coli* strain unable to synthesize putrescine, spermidine, or cadaverine: characterization of two genes controlling lysine decarboxylase. J. Bacteriol. 144: 952-956

Tabor H, Rosenthal, SM, Tabor CW (1958) The biosynthesis of spermidine and spermine from putrescine and methionine. The Journal of Biological Chemistry 233: 907-914

Tabor CW, Tabor H (1966) Transport systems for 1,4-Diaminobutane, Spermidine, and Spermine in *Escherichia coli.* The Journal of Biological Chemistry 241: 3714-3723

Tabor CW, Tabor H (1985) Polyamines in microorganisms. Microbiological Reviews. 49: 81-99.

Theiss C, Bohley P, Voigt J (2002) Regulation by polyamines of ornithine decarboxylase activity and cell division in the unicellular green alga Chlamydomonas reinhardtii. Plant physiology 128:1470-1479

Tolar, B. B. (2014). The influence of environmental factors including reactive oxygen species on the spatial and temporal distribution of marine Thaumarchaeota (Doctoral dissertation).

Urano K, Yoshiba Y, Nanjo T, Ito T, Yamaguchi-Shinozaki K, Shinozaki K (2004) Arabidopsis stress-inducible gene for arginine decarboxylase AtADC2 is required for accumulation of putrescine in salt tolerance. Biochem Bioph Res Co 313:369-375

Varela MM, Barquero S, Bode A, Fernandez E, Gonzalez N, Teira E, Varela M (2003) Microplanktonic regeneration of ammonium and dissolved organic nitrogen in the upwelling area of the NW of Spain: relationships with dissolved organic carbon production and phytoplankton size-structure. J Plankton Res 25:719-736

Venter JC, Remington K, Heidelberg JF, Halpern AL, Rusch D, Eisen JA, Wu D, Paulsen I, Nelson KE, Nelson W, Fouts DE, Levy S, Knap AH, Lomas MW, Nealson K, White O, Peterson J, Hoffman J, Parsons R, Baden-Tillson H, Pfannkoch C, Rogers YH, Smith HO (2004) Environmental genome shotgun sequencing of the Sargasso Sea. Science 304:66-74

Williams TJ, Long E, Evans F, Demaere MZ, Lauro FM, Raftery MJ, Ducklow H, Grzymski JJ, Murray AE, Cavicchioli R (2012) A metaproteomic assessment of winter and summer bacterioplankton from Antarctic Peninsula coastal surface waters. ISME J 6:1883-1900

Wuchter C, Abbas B, Coolen MJ, Herfort L, van Bleijswijk J, Timmers P, Strous M, Teira E, Herndl GJ, Middelburg JJ, Schouten S, Sinninghe Damste JS (2006) Archaeal nitrification in the ocean. Proc Natl Acad Sci U S A 103:12317-12322

Zehr JP, Ward BB (2002) Nitrogen cycling in the ocean: new perspectives on processes and paradigms. Appl Environ Microbiol 68:1015-1024

Table 1.1: Structures and pKa values of polyamines.

Polyamine	Chemical Structure	pKa			
		①	②	③	④
Cadaverine	$\underset{①}{H_2N}\text{-}(CH_2)_5\text{-}\underset{②}{NH_2}$	10.25	9.13		
Putrescine	$\underset{①}{H_2N}\text{-}(CH_2)_4\text{-}\underset{②}{NH_2}$	10.8	9.63		
1,3-Diaminopropane	$\underset{①}{H_2N}\text{-}(CH_2)_3\text{-}\underset{②}{NH_2}$	8.76	10.56		
Spermidine	$\underset{①}{H_2N}\text{-}(CH_2)_4\text{-}\underset{②}{NH}\text{-}(CH_2)_3\text{-}\underset{③}{NH_2}$	10.95	8.56	9.98	
Spermine	$\underset{①}{H_2N}\text{-}(CH_2)_3\text{-}\underset{②}{NH}\text{-}(CH_2)_4\text{-}\underset{③}{NH}\text{-}(CH_2)_3\text{-}\underset{④}{NH_2}$	10.9	8.4	7.9	10.1
Norspermidine	$\underset{①}{H_2N}\text{-}(CH_2)_3\text{-}\underset{②}{NH}\text{-}(CH_2)_3\text{-}\underset{③}{NH_2}$	10.65	7.69	9.57	
Norspermine	$\underset{①}{H_2N}\text{-}(CH_2)_3\text{-}\underset{②}{NH}\text{-}(CH_2)_3\text{-}\underset{③}{NH}\text{-}(CH_2)_3\text{-}\underset{④}{NH_2}$	10.46	8.54	7.21	9.82

Figure 1.1: Two polyamine *de novo* biosynthesis pathways. SAMS, S-adenosylmethionine synthetase; SAMD, S-adenosylmethionine decarboxylase; *ldcC*, lysine decarboxylase.

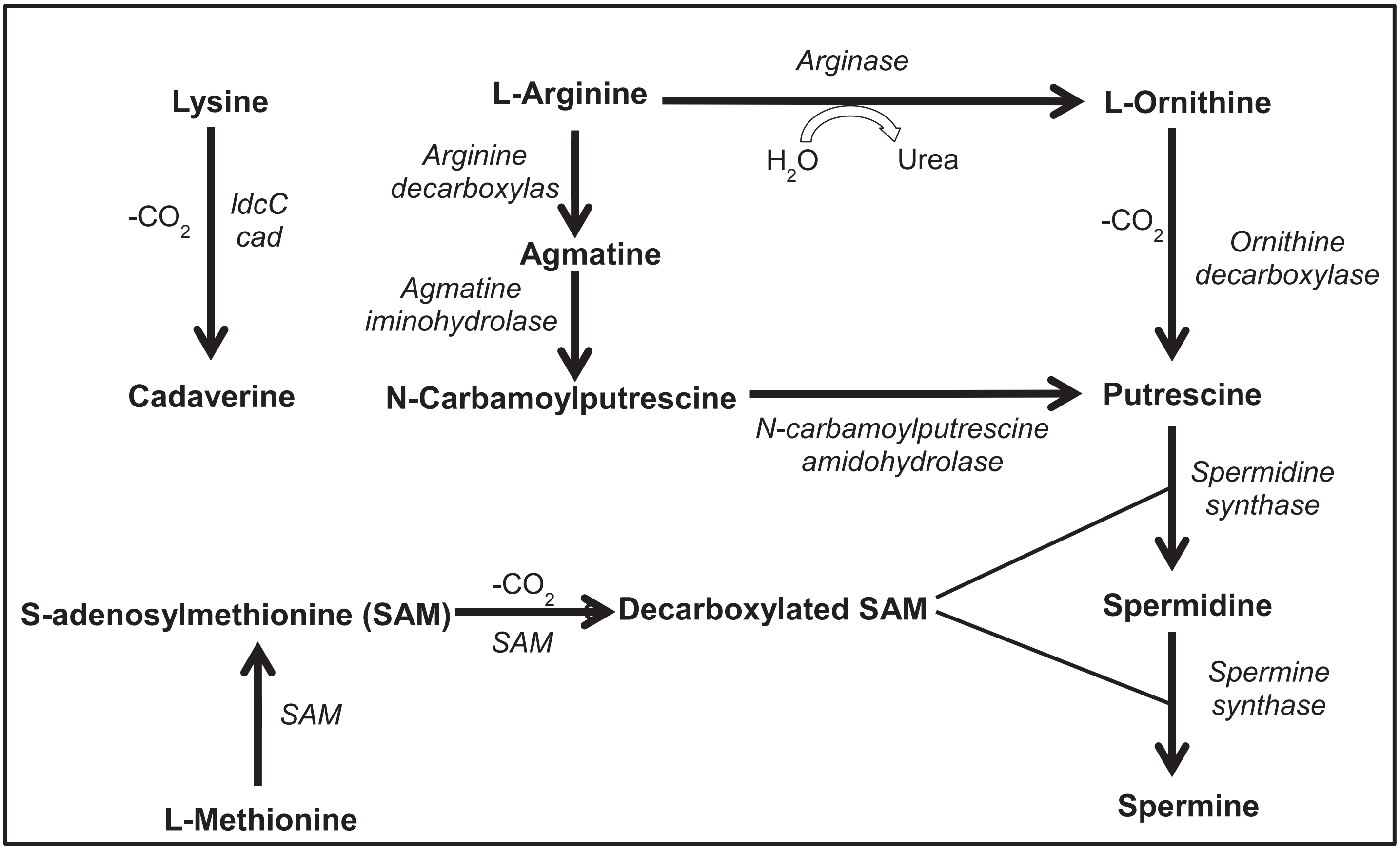
Lysine
-CO2
ldcC
cad
Cadaverine
L-Arginine
Arginine
decarboxylas
Agmatine
Agmatine
iminohydrolase
N-Carbamoylputrescine
Arginase
H2O
Urea
L-Ornithine
-CO2
Ornithine
decarboxylase
Putrescine
N-carbamoylputrescine
amidohydrolase
Spermidine
synthase
Spermidine
Spermine
synthase
Spermine
S-adenosylmethionine (SAM)
-CO2
SAM
Decarboxylated SAM
SAM
L-Methionine

CHAPTER 2

CONCENTRATIONS, TURNOVER RATES AND FLUXES OF POLYAMINES IN COASTAL WATERS OF THE SOUTH ATLANTIC BIGHT[1]

---

[1] Liu, Q., X.X. Lu, B.B. Tolar, X. Mou, and J.T. Hollibaugh. 2015. Biogeochemistry. 123:117-133. Reprinted here with permission of publisher.

ABSTRACT

Polyamines are short-chain aliphatic compounds containing multiple amine groups. They are important components of the cytosol of eukaryotes and are present at mmol L^{-1} concentrations inside phytoplankton cells, while complex polyamines play a role in biosilica deposition. Concentrations of polyamines measured in seawater are typically in the sub-nmol L^{-1} range, implying rapid and efficient uptake by osmotrophs, likely bacterioplankton. We measured turnover rates of 3 polyamines (putrescine, spermidine and spermine) using ^{3}H-labeled compounds and determined their concentrations by HPLC to estimate polyamine contributions to dissolved organic matter and bacterioplankton carbon and nitrogen demand. These measurements were made on transects from the inner shelf to the Gulf Stream across the South Atlantic Bight (SAB) during April and October of 2011 and in salt marsh estuaries on the Georgia coast during August of 2011 and April of 2012. We found that turnover rates of polyamines were similar to those of amino acids (arginine and glutamic acid) measured in the same samples; however, fluxes of polyamines into bacterioplankton were much lower than amino acid fluxes as a result of low ambient concentrations. Turnover rates and fluxes of polyamines decreased from near-shore waters to the shelf-break, following the pattern of chlorophyll a concentration. Polyamine uptake accounted for less than 10% of bacterial N demand and 5% of bacterial C demand on average, with a large variation among water masses.

INTRODUCTION

Dissolved organic matter (DOM) released directly from phytoplankton or as a result of grazing or viral lysis is the main source of carbon and nitrogen for heterotrophic bacteria in the sea (Ducklow et al. 2001; Agustí and Duarte 2013), fueling the “microbial loop” (Azam et al.

1983). Heterotrophic bacteria assimilate and catabolize organic compounds from DOM and simultaneously release inorganic C, N and P produced through cellular respiration. DOM is a complex mixture of compounds of varying reactivities. Within this mixture, dissolved free amino acids (DFAA) constitute a small (~1%) but very labile pool of compounds with rapid turnover rates, contributing significantly to bacterial C and N requirements (Fuhrman 1987, 1990; Suttle et al. 1991). Taurine, glycine betaine, dimethylsulfoniopropionate and polyamines have molecular weights and intracellular concentrations similar to amino acids. These compounds have various metabolic functions in cells, ranging from osmolytes to DNA stabilization. Metabolic pathways for their degradation have been identified in bacterioplankton and they can produce TCA cycle intermediates, indicating their potential to contribute to bacterial biomass production (Mou et al. 2010; Denger et al. 2006; Moran et al. 2007); however, their concentration and turnover in the environment have received less attention than amino acids.

Polyamines are short-chain aliphatic organic compounds containing multiple amine groups. Putrescine (PUT), spermidine (SPD) and spermine (SPM) are typically the dominant polyamines found in living cells and in seawater (Tabor and Tabor 1985; Incharoensakdi et al. 2010; Kusano et al. 2007; Lu and Hwang 2002; Márian et al. 2000; Nishibori et al. 2001a; Nishibori et al. 2001b). Polyamines are involved in a wide variety of biological reactions, including the synthesis of DNA, RNA and proteins. They contribute to membrane stability and stress responses in higher plants, fungi and bacteria (Tabor and Tabor 1985; Incharoensakdi et al. 2010; Jantaro et al. 2003; Alcázar et al. 2006). In seawater, polyamines are found mostly in algae and bacteria (Hamana and Matsuzaki 1985, 1992; Nishibori et al. 2006; Nishibori and Nishijima 2007; Incharoensakdi et al. 2010). Polyamine pools are maintained in cells by *de novo* biosynthesis and by uptake of exogenous compounds. Biosynthesis starts with the formation of PUT either from ornithine via ornithine decarboxylase (ODC) or arginine via arginine decarboxylase and agmatine ureohydrolase (ADC). PUT can then be used as a substrate to form SPD, followed by synthesis of SPM (Tabor and Tabor 1958, 1966, 1985; Fuell et al. 2010). Putrescine (PotFGHI) and spermidine-preferential uptake systems (PotABCD) have been found in *E. coli*, yeast, cyanobacteria and most of marine bacterial groups (Incharoensakdi et al. 2010; Igarashi and Kashiwagi 1999; Moran et al. 2007; Mou et al. 2010, 2011), indicating that these organisms can use exogenous polyamines.

Polyamines measured in seawater could come directly from living or dead organisms or be produced from protein and amino acid degradation (Höfle 1984). Polyamine concentrations are reported to reach 30 nmol L^{-1} in coastal seawater during algal blooms and have been reported to be as high as 250 nmol L^{-1} in a coastal salt pond (Nishibori et al. 2001a; Lee and Jørgensen 1995). The relative distribution of polyamines between organisms and seawater is similar to that of DFAA, suggesting similarities in their geochemical processing. As with DFAA, heterotrophic bacteria may catabolize polyamines for carbon and nitrogen or as sources of energy, in addition to using them directly in other metabolic processes as mentioned above (Lee 1992; Höfle 1984).

Previous studies of polyamine cycling in seawater are few in number and were mainly conducted in near-shore coastal waters or semi-enclosed marine basins (Lee 1992; Lee and Jørgensen 1995). Measuring turnover rates of polyamines in a broader range of water masses will help in elucidating their role in marine C and N cycling. Based on their turnover rates, polyamine fluxes into bacterioplankton and their contributions to bacterial C and N demand can also be estimated for comparison with other compounds. In this study, we determined turnover rates, concentrations and uptake of polyamines along an inshore to offshore transect and compared them to similar measurements made with select amino acids. We used our data to estimate the potential contribution of polyamines to bacterial C and N demand to obtain a general idea of the contribution of polyamines to bacterial production. We correlated these parameters with biological and environmental conditions across our study areas and used these analyses to identify factors potentially driving spatial variability of polyamine cycling.

MATERIALS AND METHODS

Sampling locations

Samples were collected on two cruises of the R/V Savannah in the South Atlantic Bight (SAB) on 18-22 April and 2-6 October 2011. A total of 13 stations were occupied along 3 inshore-offshore transects of the SAB between Savannah, Georgia and Jacksonville, Florida (Fig. A.1a). Sample sites covered the near-shore, middle shelf and the shelf-break at the edge of the Gulf Stream along the SAB. Water properties at near-shore stations were influenced by river inflow and tidal exchange with salt marshes and estuaries. In contrast, offshore stations, especially those along the shelf-break, were oceanic and influenced by the Gulf Stream. Station locations and sampling depths are given in Table A.1. Seawater samples were collected using 12 L Go-Flo bottles mounted on a CTD rosette. Because the SAB shelf is shallow, samples were only collected at the surface and near the bottom except at shelf-break stations where mid-depth samples were also collected. Profiles of environmental variables (temperature, salinity, dissolved oxygen, relative fluorescence and photosynthetically active radiation - PAR) were taken by sensors mounted on the CTD during hydrocasts to collect water samples.

Inshore samples were collected during 13-16 August 2011 and 17-20 April 2012 at Georgia Coastal Ecosystems - Long Term Ecological Research (GCE-LTER) sampling sites, located on the Georgia, USA coast adjacent to the SAB (http://gce-lter.marsci.uga.edu/ and Fig. A.1b). We collected 2 L of near-bottom water during high and low tide from Sapelo Sound (SP, GCE stations 1, 2 and 3) and Altamaha Sound (AL, GCE stations 7, 8 and 9). We also collected surface water samples from a floating dock at Marsh Landing (ML) on the Duplin River every 3 hours over 24-hour periods. The water passing the dock on flood tide comes from Doboy Sound, which receives input both from the Atlantic Ocean and Altamaha River, while the Duplin River drains a salt marsh with limited input of groundwater from Sapelo Island on ebb tide. The Sapelo Island National Estuarine Research Reserve (SINERR) maintains an observatory at Marsh Landing that collects meteorological, water quality and nutrient data (available at http://cdmo.baruch.sc.edu, station LD). Profiles of temperature and salinity were measured at other stations using a CTD and discrete samples were taken to measure nutrients, chlorophyll and other water quality variables (http://gce-lter.marsci.uga.edu/).

Turnover Rate, Concentration and Uptake Rate of Polyamines and Amino acids

Seawater samples were drawn directly from Go-Flo bottles into clean, acid-washed 500 mL polypropylene bottles. A series of 10 mL subsamples were quickly transferred to 15 mL snap-cap, disposable test tubes. Radiolabeled polyamines [2, 3-^{3}H(N)]-putrescine (80 Ci mmol^{-1}, American Radiolabeled Chemicals (ARC)); [terminal methylene-^{3}H]-spermine (50 Ci mmol^{-1}, ARC); [terminal methylene-^{3}H (N)]-spermidine (39 Ci mmol^{-1}, PerkinElmer) and two amino acids L-[2,3,4-^{3}H]-arginine (54.6 Ci mmol^{-1}, PerkinElmer); and L-[3,4-^{3}H]-glutamic acid (51.1 Ci mmol^{-1}, PerkinElmer) were added to five replicate subsamples to final concentrations of 5 nmol L^{-1} (~1 µCi tube^{-1}). Arginine (ARG) and glutamic acid (GLU) were chosen as representatives of DFAA in seawater because they are readily processed by microbial communities (Crawford et al. 1974; Hollibaugh 1979) and have distinct functional groups. In addition, Ferguson and Sunda (1984) showed that the turnover rate of GLU in samples from the Gulf of Mexico approximated that of the turnover rate of an amino acid mixture based on regression analysis (slope =1.04, intercept=0.076, r = 0.94). Note that measured polyamine concentrations were generally <5 nmol L^{-1} (see below), so that the amendments we used are not tracer additions, especially for polyamines. We used these amendments to obtain reliable counts in small volume, short duration incubations and because we had no information, in advance, on polyamine concentrations in our samples. The turnover rates we measured are thus approximations of turnover rates that would have been measured in a true tracer experiment: they may be elevated if uptake *in situ* was limited by substrate concentration, or they may be depressed because the substrate pool is larger than *in situ*. As a consequence, our estimates of polyamine fluxes and the contributions of polyamines to bacterial C and N demand are also likely biased; however, we assume that the spatial and temporal patterns of activity we observed reflect underlying ecosystem processes.

Duplicate control samples were filtered immediately after the addition of the substrate. The remaining triplicates of each substrate were incubated in the dark for ~1 hour at the *in situ* temperature. Incubations were terminated by filtering samples through 0.45 µm pore size Millipore filters (type HA) held on a 1225 Sampling Manifold (Millipore). Each filter was rinsed with 10 mL of unlabeled seawater to wash out unincorporated substrate, and then placed in a 7 mL scintillation vial. Ethyl acetate was added immediately to stop biological activity and to dissolve the filters, then scintillation cocktail was added prior to counting on a Beckman Coulter LS 6500. CPM were converted to DPM using counting efficiencies determined by the instrument using an external standard, then turnover rates were calculated by equation (1)

Turnover rate = $(\text{dpm}_{\text{experimental}} - \text{dpm}_{\text{control}})/ (\text{dpm}_{\text{added}} \times \text{incubation time})$ (1)

A second water sample was collected for determining concentrations of dissolved polyamines and DFAA. The sample was filtered through 3 μm and then 0.2 μm pore size membrane filters at low vacuum (~1 cm Hg) and the filtrate was frozen at -80 °C until analysis. Concentrations of polyamines and DFAA were determined by high-pressure liquid chromatography (HPLC) following derivitization with *o*-phthaldialdehyde/ethanethiol (OPA/ET) and 9-fluorenylmethyl chloroformate (FMOC) reagents (Lu et al. 2014; Körös et al. 2008). The limits of detection for PUT, SPD and SPM were 0.05, 0.01 and 0.1 nmol L^{-1}, respectively, and 0.01 – 0.1 nmol L^{-1} for DFAA species. Uptake rates were calculated by multiplying turnover rates (d^{-1}) from Equation 1 by concentrations (nmol L^{-1}) we measured in the same sample (S_n) plus the 5 nmol L^{-1} added as tracer (S_a).

Fate of Polyamine Carbon

We quantified respiration of polyamine C using putrescine as a model compound. [2, 3-^{14}C]- putrescine (100 mCi $mmol^{-1}$, ARC) and [1,4-^{14}C]- putrescine (110 mCi $mmol^{-1}$, ARC) were mixed in equimolar proportions and added to 10 mL seawater samples to a final concentration of 50 nmol L^{-1} (~0.1 μCi $tube^{-1}$). After incubation in the dark at the *in situ* temperature for ~0.5 hour, samples were filtered through 0.45 μm pore size Millipore filters (type HA) and the radioactivity of ^{14}C collected on the filter was determined by liquid scintillation counting as above. The ^{14}C retained by the filter was considered to be incorporated carbon. One milliliter of 1N Na_2CO_3 was added to the filtrate which was then frozen and held at -80 °C until analysis. In the laboratory, dissolved inorganic ^{14}C was stripped from the filtrate and trapped on a phenethylamine-saturated filter following Hobbie and Crawford (1969). The trapped ^{14}C was quantified by liquid scintillation counting. Phenethylamine-captured ^{14}C was confirmed to be respired carbon from control experiments with labeled substrate added to filtered sterilized seawater. The percentages of C incorporated and respired were calculated by dividing the radioactivity from filter and filtrate, respectively, by their sum.

Bacterial Production and Abundance

Bacterial Production (BP) was determined from ^{3}H-L-leucine incorporation into bacterial protein (Kirchman et al. 1985; Simon and Azam 1989). L- [4,5-$^{3}H(N)$]-leucine (60 Ci mmol^{-1}, ARC) was added to 4 replicate 5 mL water samples to a final concentration of 20 nmol L^{-1} (~5 μCi tube^{-1}). Two control tubes were filtered through 0.45 μm-pore size Millipore filters immediately after adding ^{3}H-L-leucine. Duplicate experimental samples were incubated for ~1 hr in the dark at the *in situ* temperature, and then filtered as above. Samples were extracted with cold 5% trichloroacetic acid (TCA) and 80% ethanol after filtration (Hollibaugh and Wong 1992) and filters were radioassayed by liquid scintillation counting as above. L-leucine incorporation rate was converted to bacterial protein production (BPP) using a factor of 3565 g protein (mole leucine incorporated)$^{-1}$ (Simon and Azam 1989). The BPP measurement can be converted to the rate of dry weight production by multiplying by 1.6, and into bacterial carbon demand (BCD) by multiplying the rate of dry weight production by 0.54 (Simon and Azam 1989). Bacterial nitrogen demand (BND) was estimated from BCD assuming that the C: N ratio of bacterial cells is 5:1 (Lee and Jørgensen 1995).

Bacterial abundance was determined by quantitative PCR of 16S rRNA genes using an iCycler iQ5 qPCR System (BioRad) and 2X SYBR® Green I Dye (BioRad) following previously described protocols (Buchan et al. 2009). Samples (~1L) for DNA extraction were collected at each station and depth on both cruises. They were pressure filtered (at ~60 kPa) through 0.22 μm Durapore filters (Millipore) and frozen in 2 mL of lysis buffer (0.75 mol L^{-1} sucrose, 40 mmol L^{-1} EDTA, 50 mmol L^{-1} Tris, pH 8.3). DNA was extracted and purified by phenol-chloroform extraction as described previously (Tolar et al. 2013; Bano and Hollibaugh 2000). Triplicate 25 μL reactions containing 2 μL of template DNA were run with gene-specific primers (BACT1369F: 5'-CGGTGAATACGTTCYCGG-3' and PROK1492R: 5'-GGWTACCTTGTTACGACTT-3') for each sample (Suzuki et al. 2000). Samples were run alongside standards (ranging from $10\text{-}10^7$ copies μL^{-1}) and checked for PCR inhibition by comparing 10-fold dilutions of DNA run on the same plate. Specificity of each reaction was confirmed with a melt curve. The detection limit was 9.12×10^4 copies L^{-1} with qPCR efficiency ranging from 95.6 to 106 %. Gene abundance was converted to copies L^{-1} of sample filtered by assuming 100% extraction efficiency and calculated as in Tolar et al. (2013).

Chemical Analyses

The concentration of biogenic silica (BSi) was measured as an estimate of the abundance of diatoms in SAB samples (Nelson et al. 1995; Brzezinski et al. 1997). BSi was analyzed following the protocol described in Brzezinski and Nelson (1989), modified from Strickland and Parsons (1977) and Paasche (1973). Briefly, a total volume of 0.6 to 1 L of water was filtered through a 0.6 μm pore size polycarbonate membrane filter, which was then frozen at -80 °C until analysis. Filters were placed in 4 mL of 0.2 N NaOH, heated to 95°C for 40 min, then the solution was neutralized by adding 1 mL of 1 N HCl. The sample was centrifuged for 10 min at 1000 x g, and then the supernatant was used to quantify silicic acid following Brzezinski and

Nelson (1989). Extracts from coastal seawater samples were diluted 10-fold for BSi measurement. Samples for nutrient determination were filtered through 0.22 µm Durapore filters (Millipore) immediately after collection and stored frozen at -80 °C until analysis. Ammonium (NH_4^+) was measured using a fluorometric method described in Holmes et al. (1999). Nitrate plus nitrite (NO_x^-) was analyzed by reducing nitrate to nitrite with cadmium (Jones 1984), and nitrite (NO_2^-) was determined following Strickland and Parsons (1972).

Statistical Analyses

Principal Components Analysis (PCA) of biological (bacterial production and abundance) and environmental data (relative fluorescence, dissolved oxygen, attenuation coefficient, temperature and salinity) was used to group SAB stations for better understanding of the patterns of polyamine cycling. The average PAR attenuation coefficient (K) at each station was calculated from PAR profiles collected with other environmental data during CTD casts (Lin et al. 2009). Redundancy analysis (RDA) was applied to identify factors that might influence turnover rates, concentrations and fluxes of polyamines and amino acids. RDA is a canonical analysis that combines regression and ordination in a multivariate model. Linear relationships are assumed between response and explanatory variables in RDA (Legendre and Legendre 2012). The log-transformed nutrient data (NH_4^+, NO_2^-, NO_x^-), biological data (BSi concentrations, bacterial production and abundances) and environmental variables (relative fluorescence, temperature and salinity) measured during the two cruises were analyzed with 999 Monte-Carlo permutations using the software package CANOCO (4.5; ter Braak and Šmilauer 2002). Individual *t*-tests run in R (http://www.r-project.org/) were used to test the statistical significance of spatial differences in turnover rates, concentrations and uptake rates of polyamines and amino acids using log-transformed data.

RESULTS

Water Column Characteristics

The temperature and salinity of surface water encountered on the April cruise ranged from 19 °C and 29 at near-shore stations to 27 °C and 36.7 at shelf-break stations, respectively. Bottom water (~450 m) temperature was 7.9 °C at shelf-break stations. In October, the salinity was uniformly ~36 across the SAB except at station 1 (surface: 23.5, bottom: 27.6). Surface water temperature ranged from 24.2 °C at near-shore stations to 29.2 °C at the shelf-break and decreased to 7.3 °C at 450 m. The water column was well mixed at near-shore and mid-shelf stations (< 50 m) during both cruises, while the water column at the shelf-break was weakly stratified during April and well stratified in October with a thermocline at ~50 m. Temperature was uniform at inshore GCE-LTER sites (April: 23 ± 0.5°C; August: 31 ± 0.6°C); however, salinity varied significantly between sites (SP: 31 ± 1, ML: 30.3 ± 0.1 and AL: 8.9 ± 9.9 in April; SP: 35.6 ±0.2, ML: 32.2±0.4 and AL: 14.7±11.2 in August) due to tidal mixing and variable riverine freshwater input, especially at AL stations 7-9.

Relative fluorescence (RF) and BSi, representing chlorophyll a (Chl a) and the abundance of diatoms, respectively, decreased from near-shore to offshore waters during both cruises (Fig. A.2a, c). Relative fluorescence was highest at mid-depth at shelf-break stations, comparable to or even higher than those measured at the mid-shelf stations. L-leucine incorporation rates and the abundance of bacterial 16S rRNA genes also decreased from inshore to offshore (Fig. A.2b, d). L-leucine incorporation rates and bacteria 16S rRNA gene abundance covaried in April but not in October; for example, bacterial abundance was low at Gray's Reef (GR) in October, yet bacterial production was extremely high.

We used PCA of biological and environmental variables to group similar stations in the SAB (Fig. 2.1). The first two PCA axes explained 88.0% of the variation between stations in April and 94.8% of the variation between stations in October. The contribution of each variable to principal components axes is given in Table A.2. Overall, the analysis supported separating the stations into 3 groups: near-shore, mid-shelf and shelf-break. Environmental conditions at GR varied between cruises so GR was grouped with mid-shelf stations in April and near-shore stations in October.

Turnover Rates of Polyamines and Amino acids

Turnover rates of polyamines (PUT, SPD and SPM) and amino acids (ARG and GLU) were faster at near-shore stations and decreased rapidly offshore in the SAB during both cruises (Fig. 2.2 and Table 2.1). Polyamine turnover varied similarly to that of amino acids but the difference between near-shore and offshore waters was greater. Polyamine turnover rates at mid-shelf and shelf-break stations in April were 6.7% and 1.3%, respectively, of those at near-shore stations. Turnover rates of polyamines measured on the October cruise were similar to those measured on the April cruise, while amino acids turned over slower than April (*t*-test, $p = 0.005$; Fig. 2.2 and Table 2.1). On both cruises, turnover rates of SPD and SPM were faster than those of PUT at nearly all stations (*t*-test, $p < 0.05$; Fig. 2.2).

The turnover rates of polyamines and amino acids in samples collected from inshore GCE-LTER sites also varied spatially (Fig. 2.3 and Table 2.1). Polyamine turnover rates were relatively faster in samples from the riverine estuary Altamaha Sound (AL) than other areas, especially PUT turnover rates. As with samples collected on the cruises, the turnover rates of SPD and SPM were greater than the turnover of PUT in April samples (*t*-test, $p < 0.05$), but in August PUT turnover rate was similar to the other two species (*t*-test, $p > 0.05$), with relatively faster turnover rates in some samples collected at AL (Fig. 2.3). Polyamine turnover rates were significantly faster (*t*-test, $p = 0.002$) at inshore GCE sites in April when compared to turnover rates measured at near-shore SAB stations (Table 2.1).

Concentrations of Polyamines and DFAA

Polyamine concentrations were very low compared to total DFAA concentrations measured in the same samples (Fig. 2.4 and Table 2.1). Concentrations of individual polyamines were typically <1 nmol L^{-1} (Fig. 2.4). On the April cruise, the summed concentrations of polyamines were similar in near-shore and mid-shelf samples but increased ~3-fold at shelf-break stations. In contrast, higher concentrations of DFAA were found at near-shore stations. DFAA pools were 1 to 2 orders of magnitude greater than polyamine pools in SAB samples (Fig. 2.4a, b; Table 2.1). PUT and SPD were detected in all samples, but SPM was only detected in samples from the shelf-break. SPD was the most abundant polyamine encountered on the October cruise. Relatively high concentrations of SPD were found in surface samples from near-shore stations 3 (3.3 ± 0.2 nmol L^{-1}, mean ± SE) and GR (5.3 ± 4.2 nmol L^{-1}), as well as in one mid-shelf sample (Stn 8; 7.0 nmol L^{-1}; Fig. 2.4c). DFAA were uniformly distributed with concentrations < 400 nmol L^{-1} (Fig. 2.4d), except for one extremely high concentration found in surface water of Stn 8 ($2{,}210 \pm 493$ nmol L^{-1}) where polyamine concentrations were also elevated. DFAA concentrations were significantly greater in October versus April (*t*-test, p =

0.0006) and the DFAA pool was more than 2 orders of magnitude larger than the polyamine pool, which did not change significantly between the two cruises (*t*-test, $p > 0.05$).

Concentrations of polyamines and DFAA were only measured at inshore GCE-LTER sites in April of 2012 (Fig. 2.4e, f) and SPD was the most abundant polyamine species detected in those samples. PUT was only detected in samples collected during low tide at GCE 2 in SP but the concentration in this sample was > 4 nmol L^{-1}. On average, the concentrations of polyamines at inshore sites were similar to those measured at near-shore and mid-shelf stations of the SAB on the April cruise, with concentrations of individual polyamines consistently <1 nmol L^{-1}. DFAA concentrations were significantly higher at inshore GCE sites than at near-shore SAB stations (*t*-test, $p< 0.05$).

Uptake Rates of Polyamines and Amino Acids

Uptake rates of polyamines (Fig. 2.5a, c) and amino acids (Fig. 2.5b, d) were highest at near-shore stations and decreased at mid-shelf and shelf-break stations on both cruises, a distribution similar to turnover rates. Uptake rates of polyamines and amino acids at near-shore stations were 2-fold higher in April cruise than October, but were similar at mid-shelf and shelf-break stations on both cruises (Table 2.1). The summed uptake rates of ARG and GLU were approximately 3-fold, 8-fold and 5-fold greater than polyamine uptake rates at near-shore, mid-shelf and shelf-break stations, respectively (Table 2.1). On average, uptake rates of all substrates were higher at inshore GCE-LTER stations than at near-shore SAB stations in April (*t*-test, $p < 0.05$; Fig. 2.5e, f; Table 2.1).

Fate of Putrescine Carbon

We found that 26 ±17% (mean ± SD) of PUT carbon processed (uptake plus respiration) was released as $^{14}CO_2$ in samples collected during the April cruise. A larger fraction (51 ± 8.8%) of PUT carbon was respired in samples collected in October, and elevated respiration of PUT carbon was observed primarily at near-shore and mid-shelf stations. Compared to the low respiration of PUT C detected across the SAB on the April cruise, a large fraction of the PUT carbon was respired by samples collected in April at inshore GCE sites (Table 2.2); however, the respiration of PUT carbon decreased in samples collected at Marsh Landing during August (Table 2.2).

Contributions to Bacterial Demand

The contributions of polyamines and DFAA to BCD and BND were compared using fluxes calculated as the product of measured turnover rates and measured *in situ* substrate concentrations (S_n). Our analysis indicated that C and N supplied by polyamines accounted for only a small proportion of the total bacterial demand for C and N in these samples, in contrast to a much larger contribution supplied by ARG plus GLU (Table 2.3). Polyamines contributed <4% of BCD and 8% of BND in samples collected in the SAB. Maximum contributions were at shelf-break stations on the April cruise and at near-shore stations on the October cruise (Table 2.3). Polyamine contributions to BND were highest at inshore GCE-LTER sites, especially at Marsh Landing (ML) where 14% of BND could be supplied by polyamines. In contrast, the contribution of polyamine C to BCD was low (<3%) at inshore stations and similar to those we measured in the SAB (Table 2.3).

Environmental Factors versus Turnover Rates, Concentrations and Uptake of Polyamines and Amino acids

RDA was only applied to samples collected in the SAB due to incomplete coverage of ancillary environmental variables at other stations. The RDA biplot (Fig. 2.6a) showed that 72% of the variability in the turnover rate - environment relationship was explained by canonical axis 1 (RDA 1). Adding the second axis (RDA 2) increased the variance explained to 76%. Bacterial 16S rRNA gene abundance was omitted from subsequent statistical analyses due to its low contribution to the turnover rate - environment model. Chlorophyll fluorescence (RF, $p = 0.001$) and salinity ($p = 0.003$) contributed significantly to RDA1 while nitrite concentration contributed significantly to RDA 2 ($p = 0.002$). Turnover rates of polyamines and amino acids were both positively correlated with chlorophyll fluorescence and negatively correlated with salinity on RDA1. SPD turnover rate was correlated with the concentrations of biogenic silica (BSi) and ammonium, while turnover rates of the other four substrates we measured (PUT, SPM, ARG and GLU) were more closely associated with L-leucine incorporation rates (LEU), a proxy for bacterial production.

The first two canonical axes only explained 25.5% of the variability in the concentration-environment relationship (17.8% for RDA1 and 7.7% for RDA2; Fig. 2.6b). RDA 1 was not statistically significant ($F = 6.78$, $p = 0.37$); however, polyamine concentrations were shown to cluster closely with NO_2^- concentrations and bacterial 16S rRNA gene abundance, while DFAA concentrations varied with temperature, bacterial production, salinity and NO_x^- concentrations.

The uptake-environment relationship shown in Figure 2.6c indicates that 82.3% of the variability was explained by RDA1 and only 2.1% of the variability was explained by RDA 2. Chlorophyll fluorescence ($p = 0.001$) and bacterial production ($p = 0.003$) contributed significantly to RDA 1; the former was more closely correlated with polyamine uptake while the latter was strongly associated with amino acid uptake. Although BSi was not a significant factor in uptake-environment model, it showed a stronger correlation with polyamine uptake than chlorophyll fluorescence. Weightings for all four canonical axes are given in Table A.3.

DISCUSSION

Polyamine Pool

Polyamine concentrations were very low (N.D. to nmol L^{-1}) at our study sites, <1% of the total DFAA concentrations in most of samples. Our findings are similar to those reported for Japanese coastal waters (mostly <5 nmol L^{-1}; Nishibori et al. 2001a, b and 2003), but were much lower than the concentrations of PUT measured in an eutrophic salt pond (N.D. to 250 nmol L^{-1}; Lee and Jørgensen 1995); indicating significant spatial variability in polyamine concentrations. Instead of PUT, which is usually reported to dominate the polyamine pool in seawater (Nishibori et al. 2001a, b and 2003), SPD was the dominant polyamine in our samples and was widely distributed across our study area. PUT was detected frequently on the April cruise but was only detected occasionally on the October cruise and at GCE-LTER sites; however, when present it contributed significantly to total polyamine concentrations. The predominance of SPD and PUT was possibly due to their distribution in algal cells, especially diatoms (Hamana and Matsuzake 1985), and variation in the species composition of phytoplankton biomass. SPD is also abundant in cyanobacteria, in some species of green algae and in members of the Raphidophyceae (Hamana and Matsuzake 1982, 1992; Jantaro et al. 2003; Badini et al. 1994; Nishibori et al. 2006). The occasional detection of SPM at low concentrations in our samples may reflect its distribution in specific eukaryotes, because the free SPM has only been found in yeast and a few eukaryotic algae (Hamana and Matsuzaki 1982, 1985). Thus, detection of different polyamine species in our samples could be as much due to the diversity of their sources as to removal by selective uptake (Nishibori et al. 2003).

Polyamine Turnover and Uptake Rates

The similarity in the distribution of polyamine and DFAA turnover rates in our samples suggest that a similar mechanism (bacterial uptake) controls their distribution and that polyamines are a biologically active fraction of DOM. However, as discussed above, the supply of polyamines may be as important as uptake in determining composition and distributions. Our RDA analysis showed that the turnover rates of both polyamines and amino acids correlated significantly with chlorophyll fluorescence and salinity. The close coupling between polyamine turnover and chlorophyll fluorescence implies a link to phytoplankton, presumably as a potential source of polyamines (Lee and Jørgensen 1995), in the biogeochemical cycling of polyamines in seawater. Higher phytoplankton biomass could result in more polyamines released to seawater, stimulating polyamine uptake by bacterioplankton, while the composition or physiological condition of the phytoplankton crop may affect the composition of the polyamine pool. We did not collect samples for chlorophyll measurements at inshore sites. GCE-LTER data indicates that chlorophyll concentrations are higher at freshwater stations in Altamaha Sound (AL, GCE Stn 7-9) than in the more saline water of Sapelo Sound (SP, GCE 1-3) during April and August, consistent with the pattern of polyamine turnover rates we found. However, elevated chlorophyll concentrations and low salinity tend to co-occur in near- and in-shore waters; thus, it was not surprising that turnover rates correlated with both variables.

We measured BSi (Fig. A.2a, c) to estimate the abundance of diatoms and found a strong correlation between SPD turnover rates and BSi, suggesting a link between diatoms and the supply of SPD. Long-chain polyamines (LCPAs) have been detected in diatom frustules as a component of silafins, a silica-precipitating protein. In LCPAs, putrescine, spermidine and spermine moieties are attached to N-methylated derivatives of polypropyleneimine units (Kröger et al. 2000; Bridoux and Ingalls 2010). However, whether the simple, short-chain polyamines in seawater originate from these long-chain polyamines, and the possible biochemical processes linking these two polyamine pools, have not been studied.

As we expected, the patterns of polyamine and amino acid turnover rates across the SAB were similar to the pattern of bacterioplankton heterotrophic activity measured as L-leucine incorporation rate (LEU). Previous studies focused on the cycling of PUT, partly as a consequence of the availability of labeled substrates. The turnover rates of PUT we measured are comparable to those reported previously (Table 2.4; Lee and Jørgensen 1995; Lee 1992), which were faster in more productive water (>0.1 d^{-1}) and slower in stratified or less productive waters (0.001-0.1 d^{-1}). Pools of the other two polyamine species we measured (SPD and SPM) turned over more rapidly than PUT in most of our samples. The K_m of SPD uptake by the energy-dependent polyamine uptake system in *E.coli* is about 10-fold less than that of PUT, indicating more effective uptake of SPD at low substrate concentrations (Tabor and Tabor 1966). Although SPM was undetectable in samples from most stations, we measured rapid turnover of SPM in SAB samples suggesting that heterotrophic bacteria may use it preferentially. Previous studies with *E.coli* found that SPM was taken up more rapidly than other polyamines at the pH of seawater (Tabor and Tabor 1966, 1985), consistent with results from our study.

The turnover rates and uptake rates we calculated are underestimates because we did not correct them for respiration. However, our studies showed that a larger fraction of PUT carbon was incorporated than respired, comparable to the results of a previous study (Lee and Jϕrgensen 1995) showing that 40 - 100% of PUT carbon was incorporated into biomass by bacteria from a salt pond. Our incubations were of <1 h duration and Höfle (1984) suggested that a longer incubation period (>6 h) was required before PUT carbon was respired significantly and concluded that the uptake of radiolabeled polyamines can be regarded as a reasonable estimate of bacterial polyamine utilization, as long as short incubations are used to make the measurements (Lee 1992).

Variability in polyamine uptake was determined primarily by variability in turnover rates, rather than variability in concentration. Polyamine concentrations were generally low and uniform in our samples, thus polyamine concentrations in incubations to determine turnover rates were determined primarily by the concentration of added radiolabeled substrate (5 nmol L^{-1}). Because we were unable to add truly tracer concentrations of radiolabeled substrates to our samples, to some extent these measurements may approach "potential uptake" rates rather than "*in situ* uptake" rates. We assumed that the spatial and temporal distribution of the uptake rates we measured approximate the spatial and temporal distribution of true *in situ* rates. These uptake rates were then used in statistical analyses in an effort to elucidate the patterns of polyamine utilization. As a conservative measure, we used the polyamine concentrations we measured, rather than the sum of the measured plus the added tracer ($S_n + S_a$ in the parlance of Hobbie et al. 1968), in our calculations of BCD and BND. Using the total pool size ($S_n + S_a$) would increase calculated fluxes into bacterioplankton by orders of magnitude in some cases (Table 2.1).

The similarity of the patterns of polyamine and amino acid uptake in the study area suggest similar pathways of biogeochemical cycling. The primary source of both classes of compounds in the environment is likely phytoplankton biomass. It is anomalous that, given the similarity in concentrations of these classes of compounds in phytoplankton cytosol implying similar fluxes of polyamines and DFAA into the environment as a consequence of viral lysis (Suttle et al. 1990, Cottrell and Suttle 1995) or "sloppy feeding" by grazers (Conover 1966, Lampert 1978, Hasegawa et al. 2001), *in situ* concentrations are so different. Amino acids may "leak" from phytoplankton more readily than polyamines, or release of DFAA by hydrolysis of detrital proteins may account for the apparent differential in sources.

Statistical analysis of our data suggests that the composition and concentration of the polyamine pool is tightly coupled to phytoplankton production, especially by diatoms, while DFAA concentration was controlled by bacterial uptake, as reported previously (Lee and Jϕrgensen 1995). The strong correlation between polyamine uptake and phytoplankton biomass re-emphasizes that phytoplankton are the predominate source of polyamines in the SAB. Due to low *in situ* concentrations, polyamine uptake contributes less to BCD and BND than DFAA uptake, as shown by the weaker correlation between polyamine uptake and bacterial production. Bacterial uptake of polyamines thus appears to be controlled mainly by release from phytoplankton. In contrast, the relatively high concentrations of DFAA are closer to their K_t in seawater (Crawford et al. 1974), resulting in the actual uptake of DFAA approaching Vmax; hence the uptake of DFAA is controlled by the ability of bacteria to transport these compounds. The low *in situ* concentrations of polyamines also suggests rather significant differences in the affinities of bacterial transport systems for polyamines versus amino acids or, alternatively, that there additional sinks for polyamines competing with uptake by bacteria.

Polyamine Contribution to Bacterial C and N Production

We used the turnover rates and *in situ* concentrations we measured to estimate the potential contribution of polyamines to BCD and BND. Low fluxes of polyamines into bacterioplankton suggest that they are less important to bacterial production than amino acids. Our calculations supported this prediction, showing that polyamines contributed a very small proportion to bacterial C and N demand compared to amino acids. Due to low C: N ratios (PUT: 4:2, SPD: 7:3 and SPM: 10:4), the contributions of polyamines to bacterial N demand were more significant, indicating the potential of polyamines to serve as a source of nitrogen for bacterial production. However, as discussed above, our estimates of the contribution of polyamines to bacterial production could be underestimated because we did not correct for respiration and regeneration, while the elevated substrate concentrations we used to measure turnover rates is another potential source of bias.

Unlike C, the fate of assimilated polyamine N has not been fully characterized. We assume that the amine groups of respired polyamines would be remineralized by heterotrophic bacteria and released as ammonia, as shown previously for amino acids (Hollibaugh 1978; Goldman et al. 1987; Goldman and Dennett 1991), or used to produce amino acids from α-ketoacids by a transaminase, followed by incorporation into protein (Bagni et al. 1978; Rastogi and Davies 1990). The correlation of polyamine uptake with ammonium concentration and with bacterial 16S rRNA gene abundance suggests regeneration of polyamine N is important; however, additional studies are required to test this hypothesis.

CONCLUSIONS

Polyamine turnover rates in the SAB are rapid and comparable to those of amino acids, indicating that they are available to bacterioplankton despite their low concentrations (sub-nmol L^{-1}). The extremely low polyamine concentrations limit polyamine uptake and their potential to be significant sources of C and N to bacteria as compared to amino acids. The cycling of polyamines and DFAA varied spatially and were both strongly influenced by phytoplankton abundance and microbial activity; however, polyamine uptake was more closely correlated with phytoplankton biomass while DFAA uptake was more closely related to bacterial production. More polyamine carbon was assimilated than respired in our experiments. The fate of N in polyamines has not been studied; however, the close association between polyamine uptake and ammonium concentration suggests heterotrophic remineralization of amine groups in polyamine compounds.

ACKNOWLEDGEMENTS

We thank the captain and crew of the R/V Savannah for their assistance with sample collection during two cruises, as well as Anna M. Bratcher for assisting with processing the nutrient data presented here. We would also like to thank the crew of the R/V Salty Dawg, especially Jacob Shalack, for assistance with sample collections at GCE-LTER sites, as well as Mary Price and Gracie Townsend for helping with facilities and equipment at UGAMI. The research was funded by the National Science Foundation (NSF OCE 1029742 to J.T.H and OCE 1029607 to X.M.).

REFERENCES

Agustí S, Duarte CM (2013) Phytoplankton lysis predicts dissolved organic carbon release in marine plankton communities. Biogeosciences 10: 1259-1264

Alcázar R, Marco F, Cuevas J, C., Patron M, Ferrando A, Carrasco P, Tiburcio AF, Altabella T (2006) Involvement of polyamines in plant response to abiotic stress. Biotechnol Lett 28: 1867-1876

Azam F, Frenchel T, Field JG, Gray JS, Meyer-Reil LA, Thingstad F (1983) The ecological role of water-column microbes in the sea. Mar. Ecol. Prog. Ser 10: 257-263

Badini L, Pistocchi R, Bagni N (1994) Polyamine transport in the seaweed *Ulva Rigida* (Chlorophyta). Journal of Phycology 30: 599-605

Bagni N, Calzoni GL, Speranza A (1978) Polyamines as sole nitrogen sources for *Helianthus Tuberosus* explants *in vitro*. New Phytol 80: 317-323

Bano N, Hollibaug JT (2000) Diveristy and distribution of DNA sequences with affinity to ammonia-oxidizing bacteria of the beta subdivision of the class Proteobacteria in the Arctic Ocean. Appl. Environ. Microbiol. 66:1960-1969

Berg GM, Glibert PM, Lomas MW, Burford MA (1997) Organic nitrogen uptake and growth by the chrysophyte *Aureococcus anophagefferens* during a brown tide event. Marine Biology 129: 377-387

Bridoux MC, Ingalls AE (2010) Structural identification of long-chain polyamines associated with diatom biosilica in a Southern Ocean sediment core. Geochimica et Cosmochimica Acta 74: 4044-4057

Bronk DA, Glibert PM (1993) Application of a ^{15}N tracer method to the study of dissolved organic nitrogen uptake during spring and summer in Chesaspeake Bay. Marine Biology 115 (3): 501-508

Bronk DA, See JH, Bradley P, Killberg L (2006) DON as a source of bioavailable nitrogen for phytoplankton. Biogeoscience Discuss 3: 1247-1277

Brzezinski MA, Nelson DM (1989) Seasonal changes in the silicon cycle within a Gulf Stream warm-core ring. Deep-Sea Res 36:1009-1030

Brzezinski MA, Phillips DR, Chavez FP, Friederich GE, Dugdale, RC (1997) Silica production in the Monterey, California, upwelling system. Limnology and Oceanography 42(8): 1694-1705

Buchan A, Hadden M, Suzuki MT (2009) Development and application of quantitative-PCR tools for subgroups of the *Roseobacter clade*. Appl Environ Microbiol 75: 7542-7547

Conover RJ (1966) Feeding on large particles by *Calanus hyperboreus*. In: Some Contemporary Studies in Marine Science, H. Barnes, Ed. George Allen and Unwin Ltd., London, pp 187-194

Cottrell MT, Suttle CA (1995) Dynamics of a lytic virus infecting the photosynthetic marine picoflagellate *Micromonas pusilla*. Limnology and Oceanography 40: 730-739

Crawford CC, Hobbie JE, Webb KL (1974) The utilization of dissolved free amino acids by estuarine microorganisms. Ecology 55: 551-563

Denger K, Smits THM, Cook AM (2006) Genome-enabled analysis of utilization of taurine as sole source of carbon or of nitrogen by *Rhodobacter sphaeroides* 2.4. 1. Microbiology 152: 3197-3206

Ducklow HW, Steinberg DK, Buesseler KO (2001) Upper ocean carbon export and the biological pump. Oceanography 14: 50-58

Ferguson RL, Sunda WG (1984) Utilization of amino acids by planktonic marine bacteria: Importance of clean technique and low substrate additions. Limnology and Oceanography 29: 258-274

Fuell C, Elliott KA, Hanfrey CC, Franceschetti M, Michael AJ (2010) Polyamine biosynthetic diversity in plants and algae. Plant Physiology and Biochemistry 48: 513-520

Fuhrman J (1990) Dissolved free amino acids cycling in an estuarine outflow plume. Mar. Ecol. Prog. Ser 66: 197-203

Fuhrman J (1987) Close coupling between release and uptake of dissolved free amino acids in seawater studied by an isotope dilution approach. Mar. Ecol. Prog. Ser 37: 45-52

Goldman JC, Caron DA, Dennett MR (1987) Regulation of gross growth efficiency and ammonium regeneration in bacteria by substrate C:N ratio. Limnology and Oceanography 32: 1239-1252

Goldman JC, Dennett MR (1991) Ammonium regeneration and carbon utilization by marine bacteria grown on mixed substrates. Marine Biology 109: 369-378

Hamana K, Matsuzaki S (1985) Further study on polyamines in primitive unicellular eukaryotic algae. J. Biochem 97: 1311-1315

Hamana K, Matsuzaki S (1992) Polyamines as a chemotaxonomic marker in bacterial systematics. Critical Reviews in Microbiology 18:261-283

Hamana K, Matsuzaki S (1982) Widespread occurrence of norspermidine and norspermine in eukaryotic Algae. J. Biochem 91(4):1321-1328

Hasegawa T, Koike I, Mukai H (2001) Fate of food nitrogen in marine copepods. Marine Ecology Progress Series 210: 167-174

Hobbie JE, Crawford CC, Webb KL (1968) Amino acid flux in an estuary. Science 159: 1463-1464

Hobbie JE, Crawford CC (1969) Respiration corrections for bacterial uptake of dissolved organic compounds in natural waters. Limnology and Oceanography 14: 528-532

Höfle MG (1984) Degradation of putrescine and cadaverine in seawater cultures by marine bacteria. Applied and Environmental Microbiology 47:843-849

Hollibaugh JT (1978) Nitrogen regeneration during the degradation of several amino acids by plankton communities collected near Halifax, Nova Scotia, Canada. Marine Biology 45: 191-201

Hollibaugh JT, Wong PS (1992) Ethanol-extractable substrate pools and the incorporation of thymidine, L-leucine, and other substrates by bacterioplankton. Can. J. Microbiol 38: 605-613

Holmes RM, Aminot A, Kerouel R, Hooker BA, Peterson BJ (1999) A simple and precise method for measuring ammonium in marine and freshwater ecosystems. Can. J. Fish. Aquat. Sci 56: 1801-1808

Igarashi K, Kashiwagi K (1999) Polyamine transport in bacteria and yeast. Biochem. J 344: 633-642

Incharoensakdi A, Jantaro S, Raksajit W, Mäenpää P (2010) Polyamines in cyanobacteria: biosynthesis, transport and abiotic stress. Current Research, Technology and Education Topics in Applied Microbiology and Microbial Biotechnology 23-32

Jantaro S, Mäenpää P, Mulo P, Incharoensakdi A (2003) Content and biosynthesis of polyamines in salt and osmotically stressed cells of *Synechocystis* sp. PCC 6803. FEMS Microbiology Letters 228: 129-135

Jones MN (1984) Nitrate reduction by shaking with cadmium: alternative to cadmium columns. Water Res 18(5): 643-646

Kirchman DL, K'nees E, Hodson R (1985) Leucine incorporation and its potential as a measure of protein synthesis by bacteria in natural aquatic systems. Applied and Environmental Microbiology 49: 599-607

Körös Á, Varga Z, Molnár-Perl I (2008) Simulatneous analysis of amino acids and amines as their o-phthalaldehyde-ethanethiol-9-fluorenylmethyl chloroformate derivatives in cheese by high-performance liquid chromatography. J. Chromatogr. A 1203:146-152

Kröger N, Deutzmann R, Bergsdorf C, Sumper M (2000) Species-specific polyamines from diatoms control silica morphology. PNAS 97: 14133-14138

Kusano T, Yamaguchi K, Berberich T, Takahashi Y (2007) Advances in polyamine research in 2007. J Plant Res 120: 345-350

Lampert W (1978) Release of dissolved organic carbon by grazing zooplankton. Limnology and Oceanography 23: 831-834

Lee C (1992) Controls on organic carbon preservation: The use of stratified water bodies to compare intrinsic rates of decomposition in oxic and anoxic systems. Geochimica et Cosmochimica Acta 56: 3323-3335

Lee C, Jørgensen NOG (1995) Seasonal cycling of putrescine and amino acids in relation to biological production in a stratified coastal salt pond. Biogeochemistry 29:131-157

Legendre P, Legendre L (2012) Volume 24: Numerical Ecology, 3rd Edition. *Elsevier.*

Lin S, Zou T, Gao H, Guo X (2009) The vertical attenuation of irradiance as a function of turbidity: a case of the Huanghai (Yellow) Sea in spring. Acta Oceanologica Sinica 28(5): 66-75

Lu X, Zou L, Clevinger C, Liu Q, Hollibaugh JT, Mou X (2014) Temporal dynamics and depth variations of dissolved free amino acids and polyamines in coastal seawater determined by High-Performance Liquid Chromatography. Marine Chemistry 163: 36-44

Lu Y, Hwang D (2002) Polyamine profile in the paralytic shellfish poison-producing alga *Alexandrium minutum.* Journal of Plankton Research 24 (3): 275-279

Marián FD, García-Jiménez P, Robaina RR (2000) Polyamines in marine macroalgae: Levels of putrescine, spermidine and spermine in the thalli and changes in their concentration during glycerol-induced cell growth in vitro. Physiologia Plantarum 110: 530-534

Moran MA, Belas R, Schell MA, González JM, Sun F, Sun S *et al.* (2007) Ecological genomics of marine roseobacters. Appl Environ Microbiol 73: 4559–4569

Mou X, Sun S, Rayapati P, Moran MA (2010) Genes for transport and metabolism of spermidine in Ruegeria pomeroyi DSS-3 and other marine bacteria. Aquatic Microbial Ecology 58: 311-321

Mou X, Vila-Costa M, Sun S, Zhao W, Sharma S, Moran MA (2011) Metatranscriptomic signature of exogenous polyamines utilization by coastal bacterioplankton. Environmental Microbiology Reports 3: 798–806

Nelson DM, Tréguer P, Brzezinski MA, Leynaert A, Queguiner B (1995) Production and dissolution of biogenic silica in the ocean: revised global estimates, comparison with regional data and relationship to biogenic sedimentation. Global Biogeochemical Cycle 9: 359-372

Nishibori N, Fujihara S, Nishijima T (2006) Changes in intracellular polyamine concentration during growth of *Heterosigma akashiwo* (Raphidophyceae). Fisheries Science 72: 350-355

Nishibori N, Matuyama Y, Uchida T, Moriyama T, Ogita Y, Oda M, Hirota H (2003) Spatial and temporal variations in free polyamine distributions in Uranouchi Inlet, Japan. Marine chemistry 82(3): 307-314

Nishibori N, Nishijima T (2007) Changes in polyamine levels during growth of a red-tide causing phytoplankton *Chattonella antiqua* (Raphidophyceae). European Journal of Phycology 39: 51-55

Nishibori N, Nishii A, Takayama H (2001a) Detection of free polyamine in coastal seawater using ion exchange chromatography. ICES Journal of Marine Science 58: 1201-1207

Nishibori N, Yuasa A, Sakai M, Fujihara S, Nishio S (2001b). Free polyamine concentrations in coastal seawater during phytoplankton bloom. Fisheries Science 67: 79-83

Paasche E (1973) Silicon and the ecology of marine planktonic diatoms. 1. *Thalassiosira pseudonana* (*Cyclotella nana*) grown in chemostats with silicate as the limiting nutrient. Marine Biology 19: 117-126

Rastogi R, Davies PJ (1990) Polyamine metabolism in ripening tomato fruit. Plant Physiol 94: 1449-1455

Simon M, Azam F (1989) Protein content and protein synthesis rates of planktonic Marine bacteria. Mar. Ecol. Prog. Ser. 51: 201-213

Strickland JDH, Parsons TR (1972) A practical handbook of seawater analysis. Fisheries Research Board of Canana. Ottawa, Canada. Minister of Supply and Service Canada.

Strickland JDH, Parsons TR (1977) A practical handbook of seawater analysis. Fisheries Research Board of Canana. Ottawa, Canada. Minister of Supply and Service Canada.

Suttle CA, Chan AM, Cottrell MT (1990) Infection of phytoplankton by viruses and reduction of primary productivity. Nature 347: 467-469

Suttle CA, Chan AM, Fuhrman JA (1991) Dissolved free amino acids in the Sargasso Sea: uptake and respiration rates, turnover times, and concentrations. Mar. Ecol. Prog. Ser. 70: 189-199

Suzuki MT, Taylor LT, Delong EF (2000) Quantitative analysis of small-subunit rRNA genes in mixed microbial populations via 5'-nuclease assays. Appl. Environ. Microbiol 66:1167-1179

Tabor H, Rosenthal, SM, Tabor CW (1958) The biosynthesis of spermidine and spermine from putrescine and methionine. The Journal of Biological Chemistry 233: 907-914

Tabor CW, Tabor H (1966) Transport systems for 1,4-Diaminobutane, Spermidine, and Spermine in *Escherichia coli.* The Journal of Biological Chemistry 241: 3714-3723

Tabor CW, Tabor H (1985) Polyamines in microorganisms. Microbiological Reviews. 49: 81-99.

ter Braak CJF, Smilauer P (2002) CANOCO Reference manual and CanoDraw for Windows User's guild: Software for Canonical Community Ordination (version 4.5). *Ithica: Microcomputer Power*.

Tolar BB, King GM, Hollibaugh JT (2013) An analysis of Thaumarchaeota populations from the northern Gulf of Mexico. Front Microbiol 4(72): 1-36

Table 2.1. Turnover rates, summed concentrations and uptake rates of polyamines (PUT, SPD and SPM) and amino acids (ARG and GLU) in different regions of the SAB and at GCE-LTER sites. The results are presented as mean ± SD of data from samples collected at different stations in the same region. DFAA concentration was the total of 20 dissolved amino acid species, not just ARG plus GLU. Uptake rate was calculated as the measured turnover rate times the sum of measured the in situ substrate concentration (S_n) plus 5 nM added labeled substrate (S_a). PA, polyamines; AA, amino acids; SP, Sapelo Sound; ML, Marsh Landing; AL, Altamaha Sound

Time/Location	Turnover Rate (d^{-1})		Concentration ($nmol\ L^{-1}$)		Uptake Rate ($nmol\ L^{-1}d^{-1}$)	
	PA	AA	PA	DFAA	PA	AA
SAB (Apr 2011)						
Near-shore	0.75±0.62‡	2.3 ±1.4‡	0.70±0.36	75±67	12.3 ± 4.7‡	38.4 ± 15.5‡
Mid-shelf	0.05±0.03	0.28±0.15	0.77±0.64	34±8.9	0.65 ± 0.37	4.7 ±3.0
Shelf-break	0.01±0.01		2.2±1.9	30±37	0.14 ± 0.14	
SAB (Oct 2011)						
Near-shore	0.43 ±0.47‡	0.68 ±0.27‡	1.3±1.8	214±100	5.7 ±1.9‡	18.4 ± 3.1‡
Mid-shelf	0.04±0.04	0.19±0.08	1.4±2.5	479±778	0.74 ± 0.35	6.0 ± 5.5
Shelf-break	0.02 ±0.01	0.05±0.04	0.53±0.69	153±57	0.23 ± 0.11	1.1 ± 1.3
GCE-LTER (Apr 2012)						
SP	1.2±0.8	2.4±1.1	1.9±2.2	160±45	18.8 ± 7.8	47.0 ± 25.0
ML	1.3±0.9	1.8±1.1	0.9±0.5	278±141	28.8 ± 9.0	65.7 ± 25.1
AL	1.9±0.8	1.1±0.5	0.4±0.2	101±61	22.7 ± 8.0	17.1 ± 5.4‡
GCE-LTER (Aug 2011)						
SP	0.7±0.5	1.4 ±0.9	-	-	-	-
ML	0.3±0.2	0.8±0.5	-	-	-	-
AL	1.2±1.3	1.1± 0.7	-	-	-	-

The symbol "‡" indicates the statistical signification (ANOVA and pairwise *t*-test, $p<0.05$) of turnover rates, concentrations and uptake rates of polyamines and amino acids, respectively. The comparison was conducted among different regions of the SAB or at GCE-LTER sites.

- indicates missing data.

Table 2.2. Respiration and assimilation of putrescine carbon (PUT C) in different regions of the SAB and at GCE-LTER sites. The results are presented as mean ± SD of data from samples collected at different stations in the same region

Time/Location	PUT C Respiration (%)	PUT C Assimilation (%)
SAB (Apr 2011)		
Near-shore	24 ± 15	76 ± 15
Mid-shelf	32 ± 23	68 ± 23
Shelf-break	22 ± 12	78 ± 12
SAB (Oct 2011)		
Near-shore	56 ± 7.3	44 ± 7.3
Mid-shelf	60 ± 11	40 ± 11
Shelf-break	38 ± 14	62 ± 14
GCE-LTER (Apr 2012)		
SP	75 ± 4.4	25 ± 4.4
ML	74 ± 11	26 ± 11
AL	60 ±11	40 ± 11
GCE-LTER (Aug 2011)		
ML	33 ± 7.3	67 ± 7.3

Table 2.3. Contributions of polyamines (sum of PUT, SPD and SPM) and amino acids (sum of ARG and GLU) to bacterial C and N demands (BCD and BND, respectively). The results are presented as mean ± SD of samples collected from different stations in the same region. BCD and BND represent bacterial C and N production, respectively, calculated from L-leucine incorporation rates following Simon and Azam (1983). PA C% and AA C% represent percentages of BCD from polyamines and amino acids, respectively. PA N% and AA N% represent percentages of BND from polyamines and amino acids, respectively

Time/Location	BCD ($ng\ L^{-1}d^{-1}$)	PA C%	AA C%	BND ($ng\ L^{-1}d^{-1}$)	PA N%	AA N%
SAB (Apr 2011)						
Near-shore	5029±3114	0.47±0.32	39±27	1006±623	2.4±1.6	105±70
Mid-shelf	1146±1013	0.38±0.45	14±14	229±203	2.4±2.3	39±38
Shelf-break	170±122	1.3±1.2	-	34±24	6.3±5.9	-
SAB (Oct 2011)						
Near-shore	4106±2728	3.1±2.5	24±10	821±546	7.8±6.2	43±16
Mid-shelf	594±197	2.6±4.4	46±61	119±39	6.5±11	129±222
Shelf-break	170±165	0.7±0.4	22±22	25±21	1.8±1.1	60±65
GCE-LTER (Apr 2012)						
SP	4703±1830	1.5±1.9	9.6±5.8	941±366	8.9±11.3	56±34
ML	4375±1592	2.3±1.8	23±8.5	875±318	14±10	137±49
AL	6232±2107	0.7±0.4	2.8±2.6	1246±421	4.1±2.4	16±15

- indicates missing data.

Table 2.4. Comparisons of concentrations and turnover rates of putrescine in natural waters from early studies with results from this study

Environment	Putrescine Concentration (nmol L^{-1})	Putrescine Turnover Rate (d^{-1})	Reference
Eutrophic Stratified Pool	0 - 250	2.4-16.8	Lee and Jørgensen (1995)
Oxic Layer of a Eutrophic Salt Pond	10	2	Lee (1992)
Oxic Layer of a Stratified Trench with Low Production	5	0.032	Lee (1992)
Anoxic Layer of a Stratified Trench with Low Production	15	0.006	Lee (1992)
SAB Near-shore (Apr/Oct)	0.34/0.02	0.24/0.11	This Study
SAB Mid-shelf (as above)	0.34/0	0.03/0.01	
SAB Shelf-break (as above)	0.18/0.26	0.005/0.007	
GCE-LTER Inshore (Apr/Aug)	4.4[a]/-	0.7/0.94	

- Samples were not collected

[a] The concentration was only detected in one sample

Fig. 2.1: PCA of environmental characteristics of SAB samples collected during April (a) and October (b) cruises. *RF* relative fluorescence (Chl a fluorescence), *K* attenuation coefficient, *T* temperature, *S* Salinity, *Oxygen* dissolved oxygen, *Bact 16S* bacterial 16S rRNA gene abundance. *Symbols* represent samples from different water regions on the SAB: *triangles* near-shore; *cross* Gray's Reef (GR); *cycles* mid-shelf; *diamonds* shelf-break

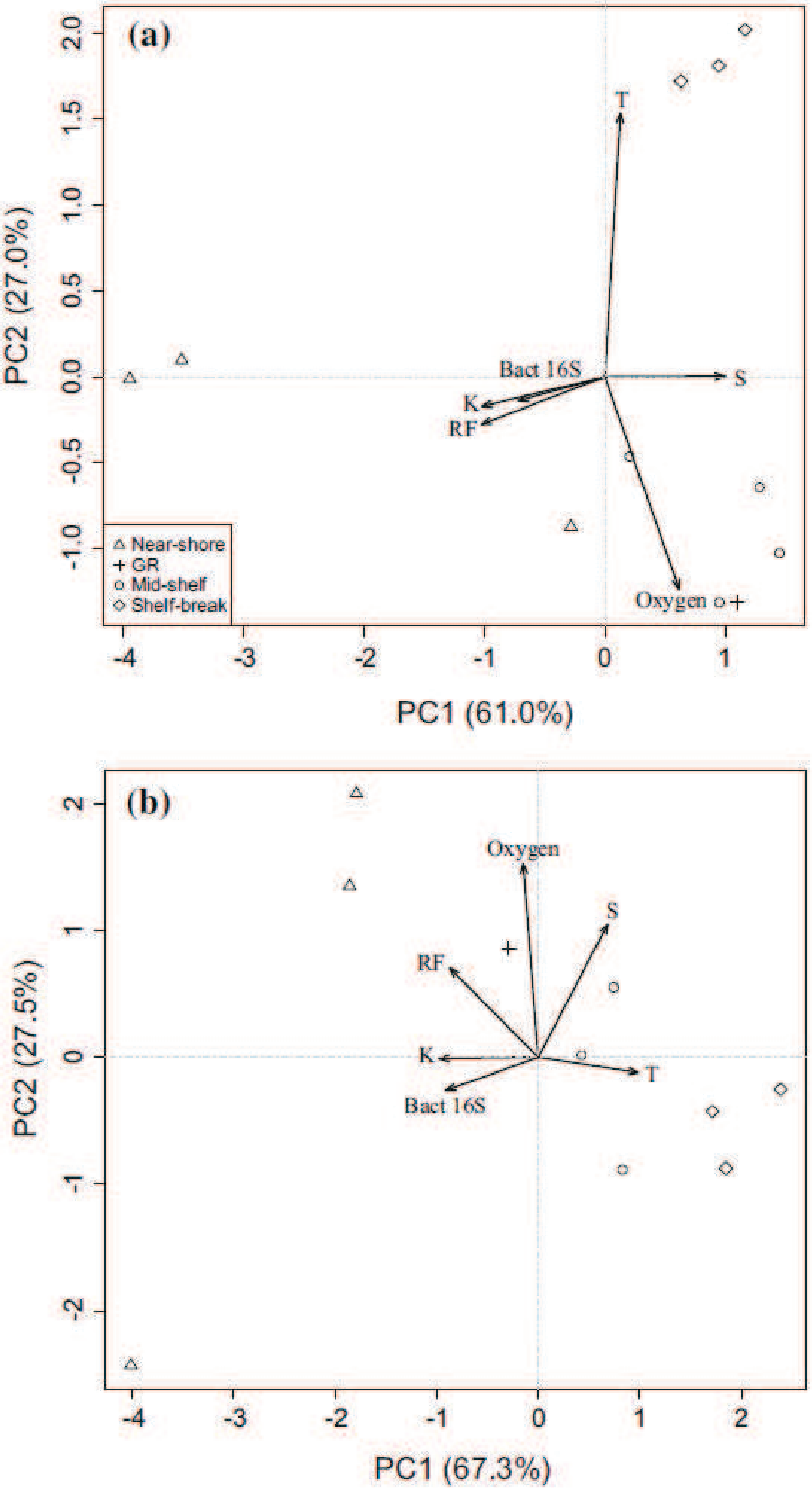
(a)
PC2 (27.0%)
PC1 (61.0%)
T
S
Bact 16S
K
RF
Oxygen
Near-shore
GR
Mid-shelf
Shelf-break
2.0
1.5
1.0
0.5
0.0
-0.5
-1.0
-4
-3
-2
-1
0
1
(b)
PC2 (27.5%)
PC1 (67.3%)
Oxygen
S
RF
K
T
Bact 16S
2
1
0
-1
-2
-4
-3
-2
-1
0
1
2

Fig. 2.2: Turnover rates of polyamines and amino acids in samples collected from the SAB in April 2011 (a, b) and October 2011 (c, d). Numbers on the abscissa identify the station as per Fig. A.1a. *SW* surface water, *MW* mid-water, *BW* bottom water. Stations are allocated to regions of the shelf (near-shore, mid-shelf and shelf-break) based on water quality properties analyzed by PCA. *Error bars* indicate the standard error of triplicate measurements of one sample and *asterisks* indicate the lost data

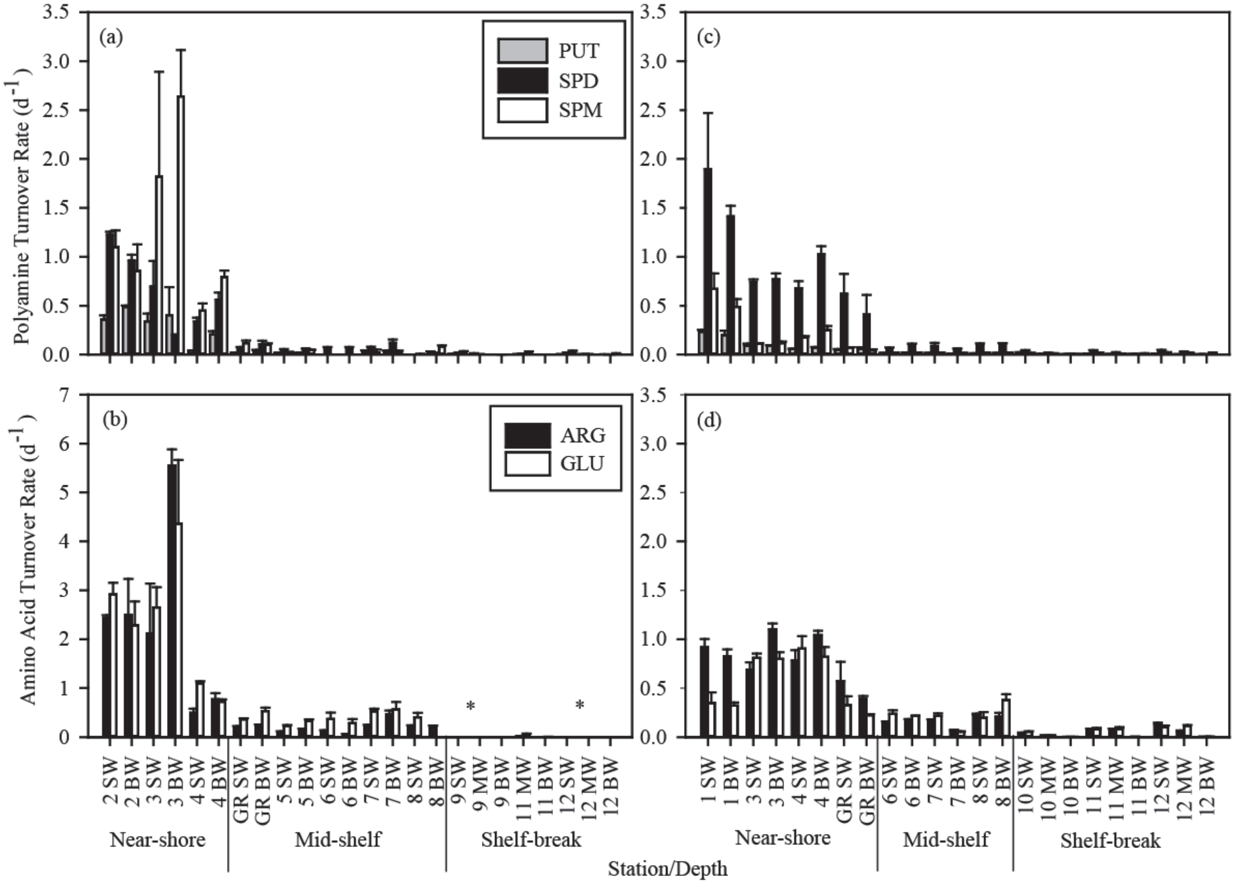

* missing data

Fig. 2.3: Turnover rates of polyamines and amino acids in samples collected from GCE-LTER sites located at the Sapelo Sound (SP - 1, 2 and 3), Marsh Landing (ML) and the Altamaha Sound (AL-7, 8 and 9) in April of 2012 (a, b) and August of 2011 (c, d). *Numbers* on the abscissa identify the station as per Fig. A1.1b. Samples from ML were collected over 24-hour period. *HW* high tide water sample, *LW* low tide water sample. *Error bars* indicate the standard error of triplicate measurements of one sample

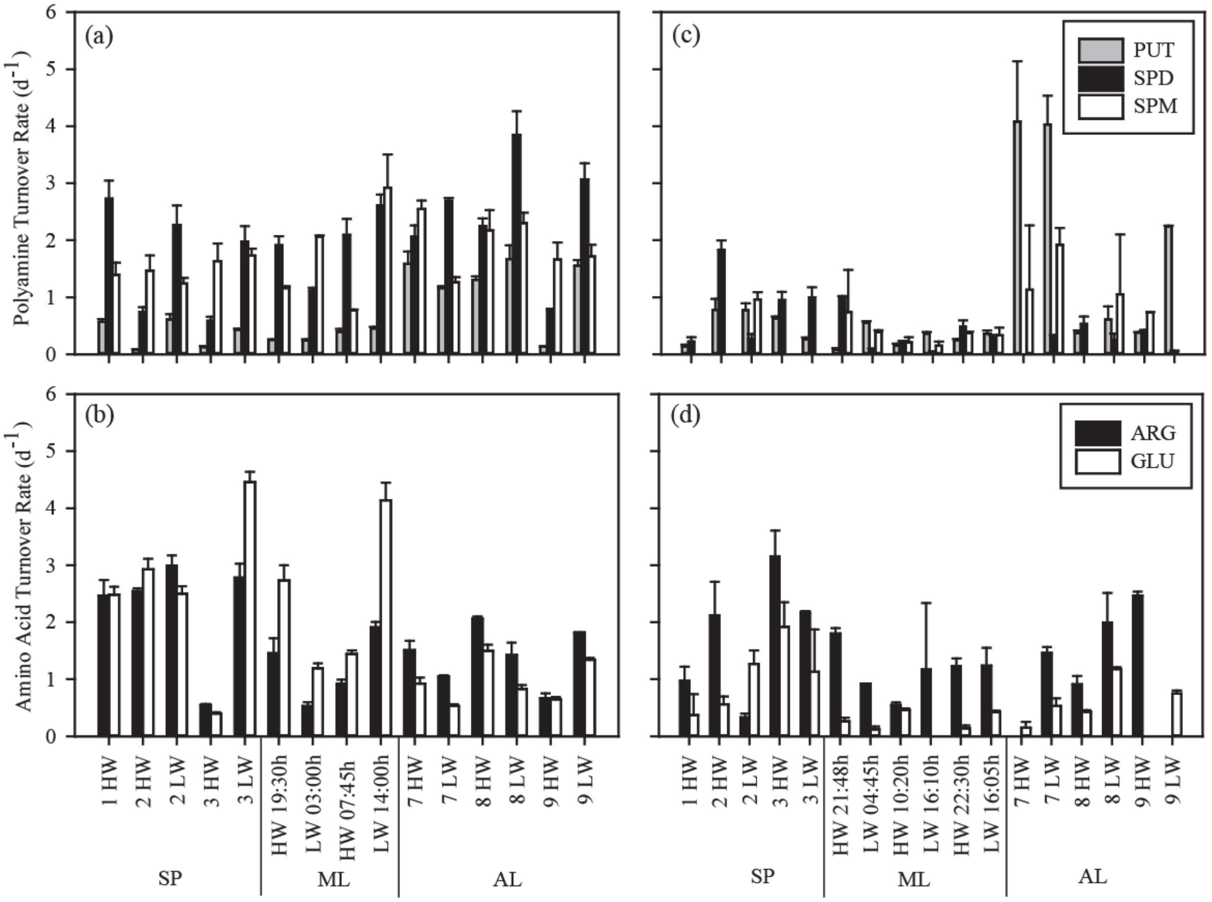
(a)
(b)
(c)
(d)
Polyamine Turnover Rate (d^{-1})
Amino Acid Turnover Rate (d^{-1})
0
1
2
3
4
5
6
PUT
SPD
SPM
ARG
GLU
1 HW
2 HW
2 LW
3 HW
3 LW
HW 19:30h
LW 03:00h
HW 07:45h
LW 14:00h
7 HW
7 LW
8 HW
8 LW
9 HW
9 LW
HW 21:48h
LW 04:45h
HW 10:20h
LW 16:10h
HW 22:30h
LW 16:05h
SP
ML
AL

Fig. 2.4: Concentrations of polyamines and DFAA in samples collected from the SAB in April of 2011 (a, b) and October of 2011 (c, d) as well as from GCE-LTER sites located at the Sapelo Sound (SP-1, 2 and 3), Marsh Landing (ML) and the Altamaha Sound (AL-7, 8 and 9) in April of 2012 (e, f). *Numbers* on the abscissa identify the station as per Fig. A1.1. *Error bars* indicate the standard error of triplicate measurements of one sample and asterisks indicate the lost data

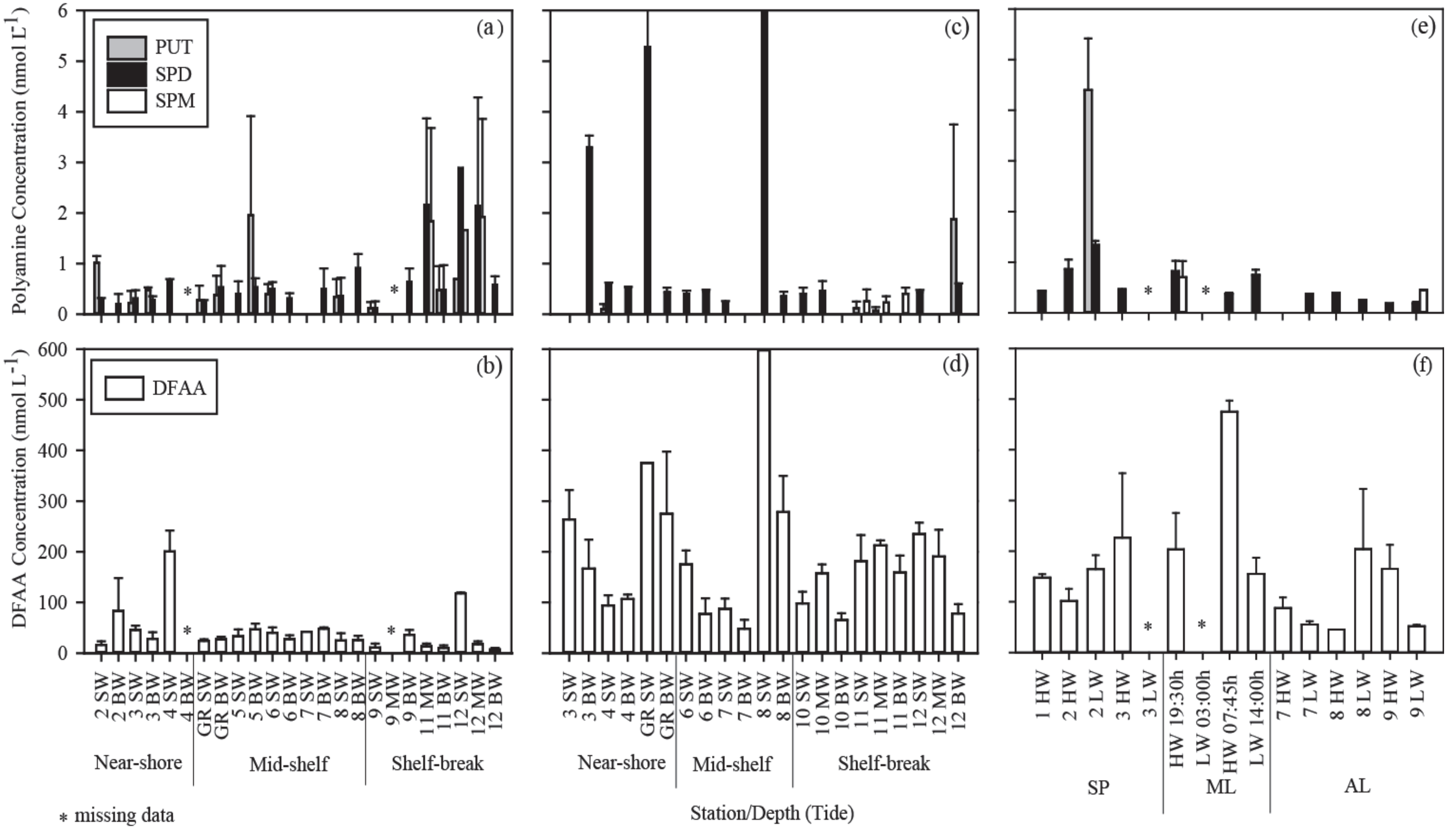
Polyamine Concentration (nmol L-1)
DFAA Concentration (nmol L-1)
0
1
2
3
4
5
6
0
100
200
300
400
500
600
PUT
SPD
SPM
DFAA
(a)
(b)
(c)
(d)
(e)
(f)
*
2 SW
2 BW
3 SW
3 BW
4 SW
4 BW
GR SW
GR BW
5 SW
5 BW
6 SW
6 BW
7 SW
7 BW
8 SW
8 BW
9 SW
9 MW
9 BW
11 MW
11 BW
12 SW
12 MW
12 BW
3 SW
3 BW
4 SW
4 BW
GR SW
GR BW
6 SW
6 BW
7 SW
7 BW
8 SW
8 BW
10 SW
10 MW
10 BW
11 SW
11 MW
11 BW
12 SW
12 MW
12 BW
1 HW
2 HW
2 LW
3 HW
3 LW
HW 19:30h
LW 03:00h
HW 07:45h
LW 14:00h
7 HW
7 LW
8 HW
8 LW
9 HW
9 LW
Near-shore
Mid-shelf
Shelf-break
Near-shore
Mid-shelf
Shelf-break
SP
ML
AL
* missing data
Station/Depth (Tide)

Fig. 2.5: Uptake of polyamines and amino acids in samples collected from the SAB in April of 2011 (a, b) and October of 2011 (c, d) as well as from GCE-LTER sites located at the Sapelo Sound (SP-1, 2 and 3), Marsh Landing (ML) and the Altamaha Sound (AL-7, 8 and 9) in April of 2012 (e, f). *Numbers* on the abscissa identify the station as per Fig. A1.1. *Error bars* indicate the standard error of triplicate measurements of one sample

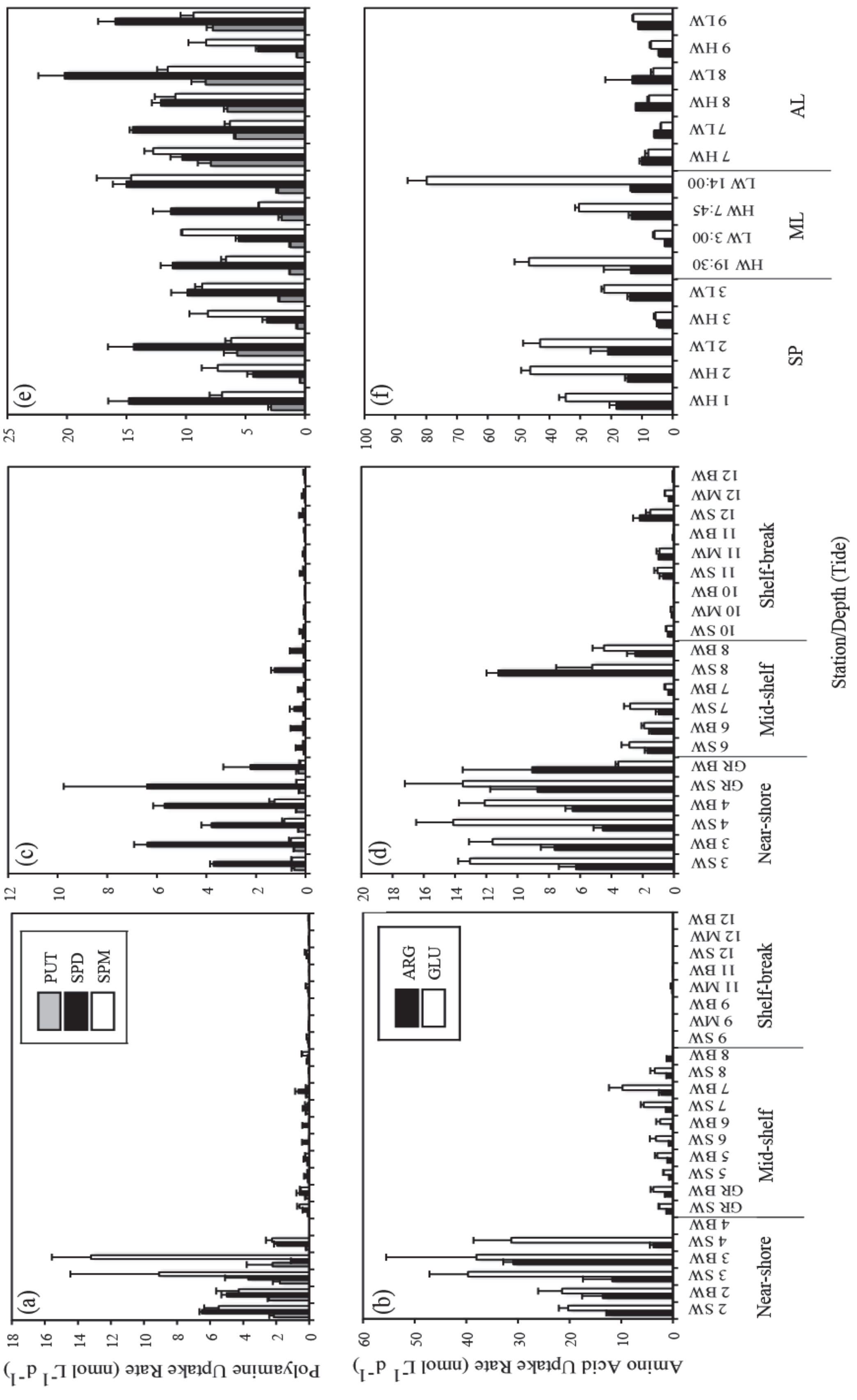

Polyamine Uptake Rate (nmol L-1 d-1)
Amino Acid Uptake Rate (nmol L-1 d-1)
Station/Depth (Tide)
(a)
(b)
(c)
(d)
(e)
(f)
PUT
SPD
SPM
ARG
GLU
Near-shore
Mid-shelf
Shelf-break
SP
ML
AL
0
2
4
6
8
10
12
14
16
18
20
25
30
40
50
60
70
80
90
100
2 SW
2 BW
3 SW
3 BW
4 SW
4 BW
GR SW
GR BW
5 SW
5 BW
6 SW
6 BW
7 SW
7 BW
8 SW
8 BW
9 SW
9 MW
9 BW
10 SW
10 MW
10 BW
11 SW
11 MW
11 BW
12 SW
12 MW
12 BW
1 HW
2 HW
2 LW
3 HW
3 LW
HW 19:30
LW 3:00
HW 7:45
LW 14:00
7 HW
7 LW
8 HW
8 LW
9 HW
9 LW

Fig. 2.6: Redundancy Analysis (RDA) ordination plots of turnover rates (a), concentrations (b) and uptake rates (c) versus environmental conditions for polyamines and amino acids. The length and angle of *arrows* show the contribution of each variable to RDA axes. The projected length of turnover rates, concentrations and uptake rates on a particular environmental variable indicates the correlation between two variables. *PA Conc* summed polyamine concentrations, *DFAA Conc* total concentrations of 20 dissolved free amino acids, *PA uptake* summed polyamine uptake, *AA uptake* summed uptake of ARG and GLU, *LEU* L-leucine incorporation rates, *RF* relative fluorescence, equivalents of chlorophyll a fluorescence, *T* temperature, *S* Salinity, *Bact 16S* bacterial 16S rRNA gene abundance, *BSi* concentrations of biogenic silica

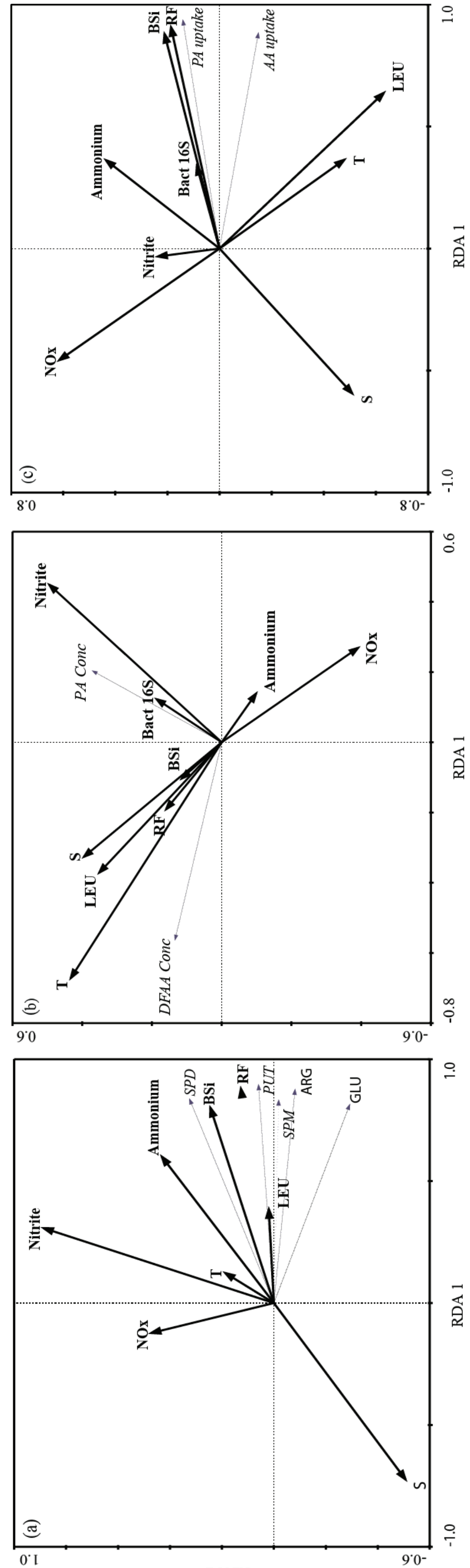
(a)
Nitrite
Ammonium
SPD
BSi
RF
PUT
ARG
GLU
SPM
LEU
T
NOx
S
RDA 1
RDA 2
1.0
-0.6
-1.0
1.0
(b)
Nitrite
PA Conc
Bact 16S
Ammonium
NOx
BSi
RF
S
LEU
DFAA Conc
T
RDA 1
0.6
-0.6
-0.8
0.6
(c)
BSi
RF
PA uptake
AA uptake
LEU
Ammonium
Bact 16S
T
Nitrite
NOx
S
RDA 1
0.8
-0.8
-1.0
1.0

CHAPTER 3

RESPONSE OF POLYAMINE POOLS IN MARINE PHYTOPLANKTON TO NUTRIENT LIMITATION AND VARIATION IN TEMPERATURE AND SALINITY[2]

---

[2] Liu, Q., N. Nishibori, I. Ichiro, and J.T. Hollibaugh. 2016. Marine Ecology Progress Series. 544:93-105. Reprinted here with permission of publisher.

ABSTRACT

Previous field observations suggest that the composition of intracellular polyamine pools in phytoplankton determines the profile of polyamines released to the surrounding environment, thus knowing how these pools vary among species and in response to factors affecting phytoplankton growth provides a basis for understanding fluctuations in dissolved polyamines. Our analyses of the polyamine content of axenic marine phytoplankton cultures show that intracellular polyamine pools are large (100's to 1000's µmol l^{-1} of biovolume) and that putrescine and spermidine are the major compounds present; however, composition varied with species. Norspermidine and norspermine were the dominant compounds found in the diatom *Thalassiosira pseudonana* and the dinoflagellate *Amphidinium carterae*, respectively. We explored the effects of temperature, salinity and nutrient limitation on polyamine pools in *T. pseudonana*, and found that either increasing temperature or decreasing salinity increased polyamine concentrations in cells and in the growth medium. Nutrient (N, P or Si) limitation caused reductions of intracellular polyamine concentrations, but release was enhanced under N or Si limitation. Polyamine ratios in the media were not the same as in intracellular pools, suggesting selective release or uptake of polyamines by phytoplankton. Thus, the composition of the dissolved polyamine pool in seawater can vary significantly, and on short time scales, depending on phytoplankton community composition and environmental factors affecting phytoplankton physiology. Our work provides experimental verification that biological mechanisms support inferences derived from environmental correlations about the factors controlling polyamine distributions in the sea.

INTRODUCTION

Polyamines (PAs) are a group of related aliphatic compounds containing multiple primary or secondary amine functional groups. They are ubiquitous in both prokaryotic and eukaryotic cells. Putrescine (PUT), spermidine (SPD) and spermine (SPM) are 3 widely distributed and relatively abundant PAs that have been studied most thoroughly. The discovery of less common PAs such as diaminopropane (DAP), norspermidine (NSPD) and norspermine (NSPM) in some organisms (Rodriguez-Garay et al. 1989, Hamana & Matsuzaki 1992) has recently attracted attention due to their potential role in newly discovered biochemical pathways (Lee et al. 2009).

PAs are essential for cellular growth, regulating cell division and maintaining normal physiological function (Tabor & Tabor 1985, Kusano et al. 2007). They carry positive charges (2 in PUT, 3 in SPD and 4 in SPM) at physiological pH (7.4), and contribute to stabilizing membranes and nucleic acids by binding to negatively charged groups (Galston & Sawhney 1990, Incharoensakdi et al. 2010, Orsini et al. 2011). A correlation between RNA synthesis and SPD concentration indicates that PAs could regulate RNA synthesis or indirectly affect protein synthesis (Stevens 1970). PA metabolism can change in higher plants in response to abiotic stresses. PUT concentration usually changes as a strategy for protecting cells against osmotic stress, salinity, hypoxia, etc. (Bouchereau et al. 1999, Alcázar et al. 2006, Incharoensakdi et al. 2010).

Eukaryotes normally synthesize PUT directly from L-ornithine by ornithine decarboxylase or from arginine by a combination of arginine decarboxylase and agmatine ureohydrolase (Tabor & Tabor 1985). PUT is the precursor of SPD, and subsequent metabolism produces SPM or thermospermine by the addition of aminopropyl groups from decarboxylated

S-adenosyl methionine (Fuell et al. 2010). Oxidation of SPD or SPM to DAP by a spermine synthase orthologue can produce the tetraamine NSPM with an intermediate triamine NSPD (Bagga et al. 1991). The biosynthesis of PAs in eukaryotic phytoplankton is primarily controlled by ornithine decarboxylase activity (Theiss et al. 2002), while the arginine decarboxylase controlled pathway dominates in prokaryotic cyanobacteria (Incharoensakdi et al. 2010). Two enzymes related to PA synthesis (ornithine decarboxylase, EC 4.1.1.17, and spermidine synthase, EC 2.5.1.16) have been identified in the genome sequence of the diatom *Thalassiosira pseudonana* (Armbrust et al. 2004).

PA distributions in the ocean are usually correlated with phytoplankton biomass and bacterial production (Lee 1992, Lee & Jørgensen 1995, Lu et al. 2014, Liu et al. 2015). PUT and SPD are ubiquitous and relatively abundant (low nmol l^{-1}), with other PAs present either at lower levels (e.g. SPM, pmol l^{-1}) or only detected occasionally (e.g. NSPD, NSPM, diaminopropane and cadaverine , Nishibori et al. 2001a, b, 2003, Liu et al. 2015). Based on our previous work (Liu et al. 2015), we hypothesized that the PA composition of seawater is determined by the balance between release of PAs from phytoplankton and uptake by bacterioplankton. As the source of PAs, phytoplankton might play a more important role than bacterioplankton in determining PA profiles in the environment because species-specific differences in the composition of intracellular PA pools could affect the composition of PAs released into the environment. Moreover, environmental factors such as temperature, salinity, and nutrient status might affect the composition of intracellular PA pools and thus PA release from algal cells, resulting in spatial and temporal changes of PA profiles.

We studied the variability of PA profiles in representative phytoplankton to address this question. The species we selected represent groups that are commonly found in seawater and cover a spectrum of phylogeny and cell sizes (see Table 1). Diatoms have a wide geographic distribution and are often important in coastal algal blooms. The diatom *T. pseudonana* is commonly used for physiological studies and its genome has been sequenced (Armbrust et al. 2004). Thus, we chose to use *T. pseudonana* for a detailed study of intracellular PA pools and PA release in response to different environmental conditions. A PA uptake experiment was also performed to evaluate the ability of *T. pseudonana* to remove PAs from the medium and to determine if PA uptake was affected by environmental conditions or nutritional status.

MATERIALS AND METHODS

Profiles of Extractable PAs

The diatoms *Thalassiosira pseudonana* (CCMP1335) and *Chaetoceros* sp. (CCMP199), the cyanobacterium *Synechococcus* sp. (CCMP1334) and the dinoflagellate *Amphidinium carterae* Hulburt (CCMP1314) were purchased from the National Center for Marine Algae and Microbiota (NCMA). These axenic, pure cultures were inoculated into 100 ml of culture media (f/2 for diatoms and f/2-Si for the cyanobacterium and the dinoflagellate; salinity=35) in 300- ml glass Erlenmeyer flasks and were grown at 18 °C under a cool-white fluorescent light intensity of 100 μmol photons m^{-2} s^{-1} in a 14 h light: 10 h dark cycle. After a period of adaptation to the laboratory environment (~2 or 3 transfers), a portion of the stock culture of each species was transferred into 100 ml of fresh medium at an initial density of 10^4 cells ml^{-1} for diatoms and *A. carterae* and10^5 cells ml^{-1} for *Synechococcus* sp. All experiments were conducted using batch cultures with triplicates. Culture sterility was checked frequently with an epi-illuminated fluorescence microscope (DM-RXA, Leica) after staining with 4', 6-diamidino-2-phenylindole (DAPI; Porter & Feig 1980). Growth rates and changes in cell volumes of the diatoms and the dinoflagellate were determined by counting them daily using a Z2 Coulter® Particle Count and Size Analyzer (Beckman), while *Synechococcus sp.* was measured and quantified by epi-illuminated fluorescence microscopy with DAPI stain. Samples of diatom and *Synechococcus sp.* cultures (~5×10^7 cells) were collected at the end of exponential growth and harvested by centrifugation at 3000 × *g* for 10 min. The cell pellet was washed with sterile artificial seawater, centrifuged again, then dispersed into 2 ml of ice-cold 6% perchloric acid (PCA) (Lu & Hwang 2002). A total of 60 ml of the *A. carterae culture* was collected and adjusted to pH 8.4. The cells were precipitated by addition of $KAl(SO_4)_2$ (0.3 mol l^{-1}) to a final concentration of 1 mmol l^{-1} then centrifuged at 1500 × *g* for 10 min (Haxo et al. 1976). The pellet was dispersed in 2 ml 6% PCA, sonicated for 30 min and centrifuged at 10,000 × *g* for 10 min. The supernatant was collected and stored at -80 °C until analysis. We considered PAs in the supernatant to be free PAs extracted from the cells, versus combined PAs that are covalently bonded in macromolecules such as silafins. However, it is likely that under physiological conditions a large fraction of the extractable PAs are not dissolved in the cytosol, but rather are bonded ionically to negatively charged groups in the cell, such as the phosphate backbone of nucleic acids. The concentration of PAs in the intracellular pools of phytoplankton is expressed as µmol l^{-1} of biovolume and was calculated by dividing the amount of PAs extracted from a sample by the total biovolume of cells in that sample (calculated from abundance and measurements of cell dimensions or of equivalent spherical diameter as determined by the Coulter Counter).

Extractable and Extracellular PA Contents during Growth of T. pseudonana

A total of 300 ml of f/2 media in 500 ml Erlenmeyer flasks was inoculated with *T. pseudonana* to an initial density of 10^4 cells ml^{-1}. The experiment was conducted in triplicate batch cultures under the same culture conditions as above. Samples (20 ml) were withdrawn each day and processed as above until the growth rate declined. A total of 9 ml of culture medium (supernatant from the first centrifugation) was placed into a 15 ml Teflon tube then 1 ml 60 % PCA was added to attain a final concentration of 6 % PCA. The samples were frozen at -80 °C for later measurement of PA concentrations in the culture medium. The concentration of extractable PA is expressed as amol cell^{-1}, calculated from the amount of PAs extracted from the cell pellet divided by the number of cells in the pellet.

Extractable and Extracellular PA Contents of T. pseudonana at Different Temperatures and Salinities

Triplicate 100 ml cultures initially containing 10^4 *T. pseudonana* cells ml^{-1} were incubated at 18 and 24 °C. Cells were harvested as above from duplicate 20 ml samples of each culture at the end of the exponential growth phase. Salinity manipulation experiments used cultures grown in modified artificial seawater media (ESAW: $[NO_3]$ = 549 µmol l^{-1}; $[PO_4]$ = 25.6 µmol l^{-1}; and $[SiO_3]$ = 106 µmol l^{-1}, described on the Canadian Center for the Culture of Microorganisms website, http://www3.botany.ubc.ca/cccm/NEPCC/esaw.html; Harrison et al. 1980) prepared at salinities of 15, 25, 35 and 45 by adding corresponding additional amounts of the salts (NaCl, $MgCl_2.6H_2O$ and Na_2SO_4) used in this medium. The pH was adjusted to 8.2. *T. pseudonana* cells were grown and transferred 3 times (~12 d in total) under the experimental conditions (temperature and salinity) tested before the experiment began. Cell pellets and supernatants were collected at the end of the exponential growth phase and processed as above.

Extractable and Extracellular PA Contents of T. pseudonana Grown under N, P or Si Limitation

Nutrient limitation was attained by decreasing the relative concentration of the target nutrient in the medium while keeping the concentrations of the other nutrients the same as that of the original ESAW formulation. A semi-continuous culture approach was applied, in which half of the culture was replaced daily by new medium once growth of the initial culture had reached the end of the exponential phase (Kilham 1978). Nitrogen-limited cultures were grown in ESAW prepared with 0, 10, 20 and 50 μmol l^{-1} $NaNO_3$ and inoculated with N-starved *T. pseudonana* cells at an initial density of 10^4 cells ml^{-1}. Cell pellets and supernatant were collected and processed as above after 5 doubling cycles. Similar experiments were conducted for P- and Si-limited cultures using ESAW prepared with different phosphate (0, 0.5, 1 and 2 μmol l^{-1}) and silicate (0, 5, 20 and 50 μmol l^{-1}) concentrations, respectively. The Si-limited cultures were grown in 250 ml Nalgene polycarbonate bottles (Thermo Scientific).

PA Measurement

The acidified samples were injected into a high-performance liquid chromatography (HPLC) system equipped with a 2.6 mm id × 50 mm cation exchange column (Hitachi No. 2619F, 5 μm particle size) maintained at 75 ºC. PAs were eluted using 2 buffers: Buffer A consisted of 0.045 mol l^{-1} sodium citrate, 0.061 mol l^{-1} citric acid, and 0.064 mol l^{-1} NaCl (pH = 4); and Buffer B contained 0.2 mol l^{-1} sodium citrate, 2.0 mol l^{-1} NaCl (pH = 7). The gradient program was as follows: start at 50% B for 6 min and change to 85% B for 6 min, change to 90% B for 3 min and then change to 100% B for 50 min; with a flow rate 0.25 ml min^{-1}. After reaction with *o* - phthaldialdehyde (OPA) reagent (0.8 g OPA in10 ml ethanol, 15.0 g boric acid, 8.0 g sodium hydroxide, 2.0 ml of 2-mercaptoethanol in 1 l of OPA reagent), PAs were detected on a fluorescence spectrometer at excitation and emission wavelengths of 340 and 435 nm.

PA Uptake by T. pseudonana

ESAW was prepared with salinities of 22 and 32 as above. These media were amended with sodium nitrate to final concentrations of 20 or 50 µmol l^{-1}. *T. pseudonana* cells were grown under these conditions as semi-continuous cultures for 5 generations, and then 20 ml of culture was inoculated into 20 ml of fresh medium of the same composition. Radiolabeled PUT ([2, 3-^{14}C]-putrescine, 100 mCi $mmol^{-1}$ and [1, 4-^{14}C]-putrescine, 110 mCi $mmol^{-1}$; American Radiolabeled Chemicals) were mixed in equimolar proportions and added to 40 ml of culture to a final concentration of 50 nmol l^{-1} (~0.2 µCi $tube^{-1}$). Cultures were incubated for 24 h under a 14 h light: 10 h dark cycle. Either 6 or 8 ml of culture was collected at 1, 6, 12, 19 and 24 h, and filtered through 0.45 µm pore size Millipore filters (type HA) held on a model 1225 Sampling Manifold (Millipore). Each filter was rinsed to remove unincorporated substrate, and then placed in a 7 ml scintillation vial. Scintillation cocktail was added prior to counting on a Tri-carb® 2910TR Liquid Scintillation Analyzer (PerkinElmer).

Statistical Analysis

Student's *t* test and an analysis of variance (ANOVA) were used to test statistical significance of differences between treatments. Data were logarithm-transformed where necessary to achieve normality. Correlations between 2 variables were analyzed as Pearson product-moment correlations and the correlation coefficient (r) was calculated. Statistical significance was evaluated at a 95% confidence interval.

RESULTS

PA Profiles in Phytoplankton

The species we tested, which represented 3 widely different taxonomic groups, contained significant, but distinct, extractable PA profiles at the late exponential phase. Total extractable PA concentrations ranged from 168 to 1176 µmol l^{-1} (Table 3.1). *Thalassiosira pseudonana* (CCMP1335) had the most diverse PA pool, which was dominated by NSPD and PUT, followed by SPD, DAP and NSPM. The other diatom (*Chaetoceros* sp. CCMP199) only contained PUT and SPD, at concentrations similar to those in *T. pseudonana* (Table 3.1). The concentration of extractable PAs in the cyanobacterium *Synechococcus* sp. (CCMP1334) was similar to that in the diatoms; however, SPD was the major PA, followed by PUT and NSPD. The dinoflagellate *Amphidinium carterae* (CCMP1314) contained the largest PA pool of the species we studied; NSPM was the only PA detected in the cell (Table 3.1). SPM was not detected in the cells of any of these phytoplankton cultures.

Composition and Concentration of Extractable and Extracellular PA during the Growth of T. pseudonana

Extractable PA concentrations and the PA profile changed as *T. pseudonana* cultures grew (Fig. 3.1a, b). Extractable PAs increased monotonically from 2.1 ± 0.4 amol $cell^{-1}$ during the lag phase to 31 ± 3 amol $cell^{-1}$ during the late stationary phase. The greatest increase (8 ± 3 amol $cell^{-1}$ d^{-1}) occurred during the late stationary phase (Fig. 3.1a). NSPD was the predominant PA present in the extractable PA pool at all stages of cell growth, accounting for 100 % of the extractable pool during the lag phase and 54 % at the late stationary phase. PUT, SPD and NSPM were detected during exponential growth in similar concentrations (< 2 amol $cell^{-1}$).

However, the PUT concentration increased to 8.7 ± 2.1 amol cell^{-1} during the late stationary phase, when concentrations of SPD and NSPM were 2.6 ± 0.6 and 2.9 ± 0.7 amol cell^{-1}, respectively (Fig. 3.1b). NSPD was the only PA detected in the medium of *T. pseudonana* cultures (Fig. 3.1c), in contrast to the more complex profile of the extractable PA pool. The concentration of NSPD in the medium did not change significantly during growth (1-way ANOVA, $p = 0.7$), being 2.3 nmol l^{-1} on average (Fig. 3.1c).

Effects of Temperature and Salinity on PA Profiles of T. pseudonana

Temperature had a significant effect on extractable PA pools of *T. pseudonana* cultures (Fig. 3.2a) (at 18 °C, 20 ± 1 amol cell^{-1}; 24 °C, 45 ± 7 amol cell^{-1}; *t*-test, $p < 0.002$). Concentrations of all individual PAs increased significantly with temperature (*t*-test, $p < 0.005$) except NSPM (*t*- test, $p = 0.3$). Differences in the relative increase of individual PA concentrations resulted in changes in PA profiles. PUT increased most dramatically, from 4.2±0.3 amol cell^{-1} at 18 °C to 19.1±2.5 amol cell^{-1} at 24 °C and became the dominant PA in cells grown at 24 °C (Fig. 3.2a). The concentration and composition of extracellular PAs were also different under the 2 temperature treatments (Fig. 3.2b). Significantly higher concentrations of PA were found in the medium at 24 °C (5.7 ± 1.8 nmol l^{-1}) than that at 18 °C (2.2 ± 0.5 nmol L^{-1}). NSPD was detected in the medium under both growth temperatures, but NSPM was only detected at 24 °C (Fig. 3.2b). We found a significant correlation between extracellular and extractable PA concentrations ($r = 0.7$, $p = 0.01$; Fig. 3.2c).

The salinity (S) of the culture medium also influenced the extractable PA content of *T. pseudonana* (at $S = 15$: 36 ± 5 amol cell^{-1}, $S = 25$: 18 ± 1 amol cell^{-1}, $S = 35$: 12 ± 1 amol cell^{-1} and $S = 45$: 8 ± 1 amol cell^{-1}; 1-way ANOVA, $p < 0.05$; Fig. 3.2d), and there was an inverse correlation between the size of the extractable PA pool (log-transformed) and salinity ($r = 0.95$, $p < 0.001$; Fig. 3.3). As salinity decreased, all extractable PA pools increased except NSPM, which was low and variable at all salinities (range 0.3 to 2.7 amol $cell^{-1}$). The NSPD pool increased significantly from $S = 45$ (5.7 ± 0.7 amol $cell^{-1}$) to $S = 25$ (12 ± 1 amol $cell^{-1}$, 1-way ANOVA, $p < 0.05$), then remained constant as salinity decreased to 15. We found that mesohaline conditions ($S = 15$) resulted in accumulation of PUT and SPD with pools of 19.2 ± 6.5 and 5.6 ± 1.8 amol $cell^{-1}$, respectively significantly larger than those measured at higher salinities (1-way ANOVA and Tukey's HSD test, $p < 0.05$). PUT became the dominant PA at $S = 15$ (Fig. 3.2d). Extracellular PA concentrations also changed with salinity (1-way ANOVA, $p < 0.001$; Fig. 3.2e) and were correlated with extractable PA pools ($r = 0.8$, $p < 0.001$; Fig. 3.2f). NSPD was found in the medium at all salinities, and its concentration did not change significantly (~6 nmol l^{-1}, 1-way ANOVA, $p > 0.05$). NSPM was only detected at salinities of 25 and 35, at very low concentrations (< 0.6 nmol l^{-1}). PUT was present in the medium at $S = 15$ (8.2 ± 0.5 nmol l^{-1}; Fig. 3.2e), coincident with the increase in extractable PUT concentration shown in Fig. 3.2d.

Effect of Nutrient Availability on PA Profiles of T. pseudonana

The availability of N, P or Si in the culture medium affected the concentration of extractable PA in *T. pseudonana* (Fig. 3.4). Final cell density increased with increasing initial nutrient concentration (Fig. 3.4), indicating that the nutrient tested (N, P or Si) was limiting growth in the treatment. Extractable PA pools of *T. pseudonana* increased as initial nitrate concentrations increased ($r = 0.96$, $p = 0.03$; Fig. 3.4a). Polyamine pools in cells from cultures with no added nitrate were ~1 amol $cell^{-1}$, and contained only NSPD and NSPM. PUT and SPD were detected in nitrate-amended cultures, but their pools were consistently low (≤ 0.5 amol $cell^{-}$

^{1}, 1-way ANOVA, $p > 0.05$; Fig. 3.4b). NSPD varied similarly to total PA in that its extractable concentrations correlated with initial nitrate concentrations ($r = 0.97$, $p = 0.03$), while the extractable pool of NSPM did not change in response to differences in N supplied (1-way ANOVA, $p > 0.05$; Fig. 3.4b). PAs could only be detected in the medium of cultures with low nitrate amendments (0 and 10 μmol l^{-1}), and the extracellular PA concentration was significantly greater in these N-starved cultures (4.5 nmol L^{-1}) than in cultures receiving greater N amendments (1.6 nmol l^{-1}, Fig. 3.4c). SPD was the only PA detected (Fig. 3.4c).

The extractable PA pool of P-limited cultures also increased with increasing initial P concentrations ($r = 0.9$, $p < 0.001$; Fig. 3.4d). PUT and NSPD were the major PAs detected and their pool size correlated significantly with initial P additions ($r = 0.9$, $p < 0.001$). SPD pools increased as the initial [PO_4] increased from 0 to 1 μmol l^{-1}, and then remained constant (~2 amol cell^{-1}). NSPM was only detected in P-amended cultures, and the pool size was similar under all treatments (~ 0.5 amol cell^{-1}, 1-way ANOVA, $p > 0.05$; Fig. 3.4e). Extracellular PAs were detected in P-amended culture medium and NSPD was the only PA found. Concentrations of extracellular PA ranged from 1.7 to 3.6 nmol l^{-1} and correlated positively with initial P concentrations ($r = 0.9$, $p < 0.05$; Fig. 3.4f).

Total extractable PA pools changed significantly (1-way ANOVA, $p < 0.001$) with increasing initial concentrations of silicate, but the response was very different from that seen with N or P limitation (Fig. 3.4g). Total extractable PA increased from 36 ± 1 amol cell^{-1} in Si-starved cultures to 42 ± 3 amol cell^{-1} in cultures with 5 μmol l^{-1} initial silicate concentration, then declined to 19 ± 1 amol cell^{-1} as the initial SiO_3 concentration increased to 50 μmol l^{-1} (Fig. 3.4g). Extractable pools of PUT, SPD and NSPD all followed a similar trend to the total extractable PA pool and varied under different SiO_3 concentrations (1-way ANOVA, $p < 0.001$,

Fig. 3.4h). Again, NSPM was only detected in Si-amended cultures and the concentration did not change with the amendment size (~1 amol cell^{-1}; 1-way ANOVA, $p = 0.2$; Fig. 3.4h). Samples for analysis of PAs in media of cultures grown with 5 µmol l^{-1} added SiO_3 were lost before they could be processed. NSPD was the only PA detected in the remaining samples and its extracellular concentration was similar (~7 nmol l^{-1}) in cultures with different initial Si concentrations (1-way ANOVA, $p > 0.05$, Fig. 3.4i).

Extractable PA Pool vs. Specific Growth Rate in T. pseudonana

Our studies showed that the size of the extractable PA pool in *T. pseudonana* cells covaried with specific growth rate (μ) (Fig. 3.5). When the growth of *T. pseudonana* was not limited by Si, concentrations of total extractable PAs and of PUT, SPD and NSPD were all positively correlated with μ (Fig. 3.5a-d, $p < 0.05$); however, the correlations were inverse when growth was limited by Si (Fig. 3.5e-h, $p < 0.05$). The NSPM pool did not change as a function of μ ($p > 0.5$). The specific growth rates of *T. pseudonana* under limitations of N, P and Si were determined from exponential growth before starting the semi-continuous culture.

PUT Uptake by T. pseudonana

Our data demonstrate that *T. pseudonana* can take up PUT from the culture medium (Fig. 3.6). Cultures of *T. pseudonana* took up ^{14}C supplied as PUT from the medium at the fastest rate (2.3 ± 0.1 amol cell^{-1} h^{-1}, 1-way ANOVA, $p < 0.0001$) under $S = 22$ and $[NO_3^-] = 50$ µmol L^{-1} (Table 3.2). We also found that *T. pseudonana* cells assimilated PUT at different rates when grown under different salinities and nitrate concentrations (2-way ANOVA, $p < 0.0001$, Fig. 3.6b and Table 3.2). PUT was taken up by *T. pseudonana* cells at a higher rate under lower salinity (p

< 0.0001) or higher initial [NO_3^-] ($p < 0.05$, Table 3.2) and there was no significant interaction between salinity and nitrate concentration ($p > 0.05$).

DISCUSSION

Extractable PA Profiles in Phytoplankton

The composition of extractable PA pools differed greatly among the 4 phytoplankton species we tested, even though *Thalassiosira pseuodonana* and *Chaetoceros* sp. are both centric diatoms, suggesting that PA composition profiles are species-specific in phytoplankton. The frequent detection of PUT, SPD, NSPD and NSPM is similar to the results of previous studies of PA profiles in phytoplankton (Hamana & Matsuzaki 1982, 1985, Nishibori & Nishio 1997, Lu & Hwang 2002, Nishibori & Nishijima 2004). We found that the cyanobacterium *Synechococcus* sp. contained an extractable PA concentration that was comparable to that of diatoms (100s of μmol l^{-1} of biovolume), despite the large difference in the size of these cells (Table 3.1). The dinoflagellate *Amphidinium carterae* contained the highest concentration of extractable PA (1000s of μmol l^{-1}) among the phytoplankton species that we studied, indicating the potential of dinoflagellates to contribute significantly to the dissolved PA pool of the ocean. The PAs we found in these species included most of the PAs commonly detected in the ocean (Nishibori et al. 2001a, b, 2003, Nishibori & Nishijima 2004, Lu et al. 2014, Liu et al. 2015), suggesting that variability of PA concentrations in seawater could be a consequence of varying composition in phytoplankton communities.

PA Profiles during Growth of T. pseudonana

Our study showed that PA concentration and composition changed at different points during the growth of *T. pseudonana*; however, the steady increase in PA concentration we detected differed from the trend seen in other groups of phytoplankton (dinoflagellates, Chlorophyceae and Raphidophyceae), where PA concentrations were reported to decrease as cells lost viability (Kotzabasis & Senger 1994, Lu & Hwang 2002, Theiss et al. 2002, Nishibori & Nishijima 2004, Nishibori et al. 2006). This difference might be attributed to the unique function of PAs in the synthesis of the nano-silicate structure of the diatom cell wall and in the role of silicate in diatom cell division (Kröger et al. 2000, Sumper & Lehmann 2006, Sumper & Brunner 2008). The failure to detect extractable PUT and SPD in diatoms during the early stages of lag phase growth could be due to the conjugation of PAs into silafins (proteins involved in silica precipitation), or into long-chain polyamines (LCPAs) in the cell wall (Sumper et al. 2005, Bridoux & Ingalls 2010). When cells began to die at the end of the stationary phase, PAs (especially PUT) may accumulate intracellularly as a result of low rates of silicate precipitation, or as a result of dissolution of the cell wall and catabolism of cell wall structures, including silafins and LCPAs.

Effect of Environmental Factors on Extractable PA Pools of T. pseudonana

Temperature and salinity are 2 important environmental factors in the microbial ecology of the coastal environment. Growth rates of phytoplankton are influenced by both of these factors (Eppley 1972, Balzano et al. 2011). The strong correlation between extractable PA concentrations and growth rates of *T. pseudonana* suggests that PA pools in the cell are directly affected by growth (Fig. 3.5). Thus, temperature and salinity may control the intracellular PA pool indirectly by affecting the growth rate. Moreover, PA biosynthesis in *T. pseudonana* cells is assumed to use the ornithine decarboxylase -mediated pathway (Armbrust et al. 2004). Ornithine is also the precursor of proline, an osmolyte synthesized by the cell, and Liu & Hellebust (1976) found that proline was synthesized in the diatom *Cyclotella cryptica* as salinity increased to >30. Thus, our observation that concentrations of extractable PAs in *T. pseudonana* decreased as salinity increased could be a consequence of suppressed PA synthesis via the ornithine decarboxylase-mediated pathway in favor of osmolyte production. The significant increase in the concentration of extractable PAs under heat stress could also be a consequence of a high demand for PAs in order to stabilize DNA against heat denaturation (Balasundaram et al. 1996, Valdés-Santiago & Ruiz-Herrera 2014).

Nutrient availability is known to influence the chemical composition of phytoplankton (Harrison et al. 1990, Johanssen & Granéli 1999). Specifically, N or P limitation was found to reduce the cell quota of that element in phytoplankton (Johanssen & Granéli 1999). Silica is important to the growth of diatoms because of its role in cell wall structure (Kröger et al. 2000, Sumper & Kröger 2004, Bridoux & Ingalls 2010). Since PAs have a high N content (≥ 2), it is perhaps not surprising that their intracellular concentrations vary with nitrogen availability (Altman & Levin 1993, Minocha et al. 2000). PUT and SPD were not detected in N-starved cells of *T. pseudonana,* suggesting complete inhibition of PUT biosynthesis when N is not available. Phosphorus might not affect the PA content of phytoplankton as directly as nitrogen; however, P-limitation may affect phytoplankton N metabolism indirectly. Studies with higher plants have shown that NO_3 uptake decreased by 70 %, and that uptake of NO_3 and NH_4 together decreased by >80 % under P limitation (Schjørring 1986, Rufty et al. 1990). The relatively large pool of

PAs, especially PUT and SPD, found under P-limitation versus N-limitation suggests that N availability controls the PA pool.

Gröger et al. (2008) used solid-state ^{29}Si NMR spectroscopy to suggest that the transport of Si into *T. pseudonana* was facilitated by rapid binding to PAs and the formation of partially polymerized silica, and that new girdle bands and valves were then formed during cell division. Thus, silicate supply can be expected to have an inverse effect on PA concentrations in the cell. The large pool of PAs observed under Si starvation suggests that Si limitation does not inhibit PA synthesis, but rather that subsequent removal of PA depends on the ongoing formation of cell wall components and is inhibited when growth and cell division cease. Higher initial silicate concentrations supported more growth and enhanced silicate precipitation with the accompanying production of LCPA and proteins. The coincidence of decreased PA content and increased silicate quota in diatoms is consistent with the need for PAs in forming the cell wall structure.

Extracellular PAs from T. pseudonana

Since PAs were not supplied in the original culture medium, PAs detected in the medium during growth of *T. pseudonana* must have been a result of PA released from cells. However, PAs dissolved in the medium were not present at the same concentration ratios as found in the intracellular pool, indicating selective release or uptake of PAs by phytoplankton. We found that *T. pseudonana* can take up PUT added to the medium (Fig. 3.6b), suggesting that the PA concentration measured in the medium may be the net of PA release minus uptake by *T. pseudonana* in these axenic cultures. Selective release of PA may provide another way that the composition of intracellular and extracellular PA pools could diverge. However, the correlation between extracellular and extractable PA concentrations under most of the conditions that we studied suggests passive permeation or diffusion of PAs through the cell membrane of *T. pseudonana* into the medium, similar to the fluxes of urea or amino acids (Bjørnsen 1988). The composition of extracellular PAs thus appears to be regulated by the composition and concentrations of intracellular PAs, differences in the permeability of the cell membrane to individual PAs and uptake by *T. pseudonana*. Uptake by bacterioplankton would further modify the concentrations and composition of dissolved PAs detected in the environment.

The extracellular PA concentration responded differently from extractable pools in response to N-versus Si-limitation. Extracellular PAs were most abundant in *T. pseudonana* cultures with lower N amendments compared to those in cultures with initial [NO_3] over the range tested (≤50 µmol l^{-1}). The relatively high concentration of PA in the medium of N-deficient cultures could be driven by the release of PA from N-stressed cells when re-acquisition of extracellular PAs was limited by a low growth rate. As N-limitation declined, PA release may be counteracted by uptake from the medium (Bjørnsen 1988). Silicate limitation has been shown to cause amino acid release by diatoms (Admiraal et al. 1984), possibly as a result of inhibition of cell division (Hammer & Brockmann 1983). PAs were detected in media of Si-limited cultures and their concentrations were large and similar between treatments (Fig. 3.4i). It is also noteworthy that the identity of the PA released to the medium differed with the limiting nutrient: SPD was released during N-limited growth while NSPD was released during P- or Si-limited growth (Fig. 3.4c, 3.4f, 3.4i). SPD is a minor component of the extractable pool of *T. pseudonana* during N-limited growth, whereas NSPD is a major component of the extractable pools under P- or Si-limited growth (Fig. 3.4b, 3.4e, 3.4h).

Ecological Significance

The widespread occurrence of PAs in the ocean has been documented, and their distribution varies spatially and temporally. Based on the results presented here and from previous work, the distribution of PAs in the ocean can be assumed to be influenced by the abundance and composition of phytoplankton (Lee 1992, Lee & Jørgensen 1995, Liu et al. 2015), since different phytoplankton species contain distinct PA profiles (Hamana & Matsuzaki 1982, 1985, Nishibori et al. 2001a, Nishibori et al. 2003). However, we found that the release of PAs by phytoplankton appears to be selective, possibly as a result of net exchange between cells and the medium. Regardless of the mechanism, the relationship between internal and external PA pools is not straightforward and is controlled by environmental conditions as well as by phytoplankton community composition. Our studies of the diatom *T. pseudonana* showed that the concentrations of PA in the medium of healthy, exponentially growing cultures was very low (<10 nmol l^{-1}) and was consistent with the concentrations found in seawater (Nishibori et al. 2001a, b, 2003, Liu et al. 2015). This suggests that the elevated PA concentrations reported in some studies (Lee 1992, Lee & Jørgensen 1995) resulted from losses from unhealthy cells, or possibly as a consequence of damage and loss of cell membrane integrity due to grazing by zooplankton (Conover 1966, Dagg 1974) or viral lysis (Wilhelm & Suttle 1999), with uptake by bacterioplankton (Lee 1992, Lee & Jørgensen 1995, Liu et al. 2015) further complicating the dynamics of dissolved PA.

ACKNOWLEDGEMENTS

We thank Dr. Ming-Yi Sun for providing laboratory spaces for algal culture and Dr. Brian Hopkinson and Ms. Chen Shen for supplying artificial seawater medium ESAW and access to the Z2 Coulter® Particle Count and Size Analyzer. I would like to also thank the publisher Inter-Research Science Center to publish this manuscript in the Journal of Marine Ecology Progress Series (544: 93–105, 2016) and my co-authors Dr. Naoyoshi Nishibori, Dr. Ichiro Imai and Dr. James T. Hollibaugh, who have contributed their efforts to this study. This paper is dedicated to Cindy Lee and Manfred Höfle, pioneers in environmental polyaminology. The research was funded by the National Science Foundation (NSF OCE 10-29742 to J.T.H.).

REFERENCES

Admiraal W, Laane RWPM, Peletier H (1984) Participation of diatoms in the amino-acid cycle of coastal waters - uptake and excretion in cultures. Marine Ecology Progress Series 15:303-306

Alcázar R, Marco F, Cuevas J, Patron M, Ferrando A, Carrasco P, Tiburcio A, Altabella T (2006) Involvement of polyamines in plant response to abiotic stress. Biotechnol Lett 28:1867-1876

Altman A, Levin N (1993) Interactions of polyamines and nitrogen nutrition in plants. Physiologia Plantarum 89:653-658

Armbrust EV, Berges JA, Bowler C, Green BR, Martinez D, Putnam NH, Zhou S, Allen AE, Apt KE, Bechner M, Brzezinski MA, Chaal BK, Chiovitti A, Davis AK, Demarest MS, Detter JC, Glavina T, Goodstein D, Hadi MZ, Hellsten U, Hildebrand M, Jenkins BD, Jurka J, Kapitonov VV, Kroger N, Lau WW, Lane TW, Larimer FW, Lippmeier JC, Lucas S, Medina M, Montsant A, Obornik M, Parker MS, Palenik B, Pazour GJ, Richardson PM, Rynearson TA, Saito MA, Schwartz DC, Thamatrakoln K, Valentin K, Vardi A, Wilkerson FP, Rokhsar DS (2004) The genome of the diatom Thalassiosira pseudonana: ecology, evolution, and metabolism. Science 306:79-86

Bagga S, Dharma A, Phillips GC, Kuehn GD (1991) Evidence for the occurrence of polyamine oxidase in the dicotyledonous plant *Medicago sativa* L. (alfalfa). Plant Cell Rep 10:550-554

Balasundaram D, Tabor CW, Tabor H (1996) Sensitivity of polyamine-deficient *Saccharomyces cerevisiae* to elevated temperatures. J Bacteriol 178:2721-2724

Balzano S, Sarno D, Kooistra WHCF (2011) Effects of salinity on the grwoth rate and morphology of ten *Skeletonema* strains. Journal of plankton research 33:937-945

Bjørnsen PK (1988) Phytoplankton exudation of organic matter: Why do healthy cells do it? Limnol Oceanogr 33:151-154

Bouchereau A, Aziz A, Larher F, Martin-Tanguy J (1999) Polyamines and environmental challenges: recent development. Plant Science 140:103-125

Bridoux MC, Ingalls AE (2010) Structural identification of long-chain polyamines associated with diatom biosilica in a Southern Ocean sediment core. Geochimica Et Cosmochimica Acta 74:4044-4057

Conover RJ (1966) Feeding on large particles by *Calanus hyperboreus*. IN: Some Contemporary Studies in Marine Science. H. Barnes. London, George Allen and Unwin Ltd.,**:** 187-194.

Dagg MJ (1974) Loss of prey body contents during feeding by an aquatic predator. Ecology 55:903-906

Eppley WR (1972) Temperature and phytoplankton growth in the sea. Fishery Bulletin 70:1063-1085

Fuell C, Elliott AK, Hanfrey CC, Franceschetti M, Michael AJ (2010) Polyamine biosynthesis diversity in plants and algae. Plant Physiology and Biochemistry 48:513-520

Galston AW, Sawhney RK (1990) Polyamines in plant physiology. Plant Physiol 94:406-410

Gröger C, Sumper M, Brunner E (2008) Silicon uptake and metabolism of the marine diatom Thalassiosira pseudonana: Solid-state 29Si NMR and fluorescence microscopic studies. J Struct Biol 161:55-63

Hamana K, Matsuzaki S (1982) Widespread occurrence of norspermidine and norspermine in eukaryotic algae. Journal of biochemistry 91:1321-1328

Hamana K, Matsuzaki S (1985) Further study on polyamines in primitive unicellular eukaryotic algae. Journal of biochemistry 97:1311-1315

Hamana K, Matsuzaki S (1992) Polyamines as a chemotaxonomic marker in bacterial systematics. Crit Rev Microbiol 18:261-283

Hammer KD, Brockmann UH (1983) Rhythmic release of dissolved free amino-acids from partly synchronized *Thalassiosira-Rotula* under nearly natural conditions. Marine Biology 74:305-312

Harrison PJ, Waters RE, Taylor FJR (1980) A broad spectrum artificial medium for coastal and open ocean phytoplankton. Journal of Phycology 51:255-263

Harrison PJ, Thompson PA, Calderwood GS (1990) Effects of nutrient and light limitation on the biochemical composition of phytoplankton. Journal of Applied Phycology 2:45-56

Haxo FT, Kycia JH, Somers GF, Bennett A, Siegelman HW (1976) Peridinin-chlorophyll *a* proteins of the dinoflagellate *Amphidinium carterae* (Plymouth 450). Plant physiology 57:297-303

Incharoensakdi A, Jantaro S, Raksajit W, Maenpaa (2010) Polyamines in cyanobacteria: biosynthesis, transport and abiotic stress response. In: Méndez-Vilas A (ed) Current Research, Technology and Education Topics in Applied Microbiology and Microbial Biotechnology. Formatex Research Center, Badajoz, p 23-32

Johansson N, Granéli E (1999) Influence of different nutrient conditions on cell density, chemical composition and toxicity of *Prymnesium parvum* (Haptophyta) in semi-continuous cultures. Journal of Experimental Marine Biology and Ecology 239:243-258

Kilham SS (1978) Nutrient kinetics of freshwater planktonic algae using batch and semicontinuous methods. Mitteilungen Internationale Vereinigung fur Theoretische und Angewandte Limnologie 21:147-157

Kotzabasis K, Senger H (1994) Free, conjugated and bound polyamines during the cell cycle in synchronized cultures of *Scenedesmus obliquus*. Zeitschrift fur Naturforschung C, Journal of biosciences 49:181-185

Kröger N, Deutzmann R, Bergsdorf C, Sumper M (2000) Species-specific polyamines from diatoms control silica morphology. Proceedings of the National Academy of Sciences of the United States of America 97:14133-14138

Kusano T, Yamaguchi K, Berberich T, Takahashi Y (2007) Advances in polyamine research in 2007. J Plant Res 120:345-350

Lee C (1992) Controls on organic carbon preservation: The use of stratified water bodies to compare intrinsic rates of decomposition in oxic and anoxic systems. Geochimica et Cosmochimica Acta 56:3323-3335

Lee C, Jørgensen NOG (1995) Seasonal cycling of putrescine and amino-acids in relation to biological production in a stratified coastal salt pond. Biogeochemistry 29:131-157

Lee J, Sperandio V, Frantz DE, Longgood J, Camilli A, Phillips MA, Michael AJ (2009) Genomics, proteomics, and bioinformatics: An alternative polyamine biosynthetic pathway is widespread in bacteria and essential for biofilm formation in *Vibrio cholerae*. The journal of Biological Chemistry 284:9899-9907

Liu MS, Hellebust JA (1976) Effects of salinity and osmolarity of the medium on amino acid metabolism in *Cyclotella cryptica*. Canadian Journal of Botany 54:938-948

Liu Q, Lu X, Tolar BB, Mou X, Hollibaugh JT (2015) Concentrations, turnover rates and fluxes of polyamines in coastal waters of the South Atlantic Bight. Biogeochemistry. 123:117-133

Lu XX, Zou L, Clevinger C, Liu Q, Hollibaugh JT, Mou XZ (2014) Temporal dynamics and depth variations of dissolved free amino acids and polyamines in coastal seawater determined by high-performance liquid chromatography. Marine Chemistry 163:36-44

Lu YH, Hwang DF (2002) Polyamine profile in the paralytic shellfish poison-producing alga *Alexandrium minutum*. Journal of Plankton Research 24:275-279

Minocha R, Long S, Magill AH, Aber J, McDowell WH (2000) Foliar free polyamine and inorganic ion content in relation to soil and soil solution chemistry in two fertilized forest stands at the Harvard Forest, Massachusetts. Plant and Soil 222:119-137

Nishibori N, Fujihara S, Nishijima T (2006) Changes in intracellular polyamine concentration during growth of *Heterosigma akashiwo* (Raphidophyceae). Fisheries Science 72:350-355

Nishibori N, Matuyama Y, Uchida T, Moriyama T, Ogita Y, Oda M, Hirota H (2003) Spatial and temporal variations in free polyamine distributions in Uranouchi Inlet, Japan. Marine Chemistry 82:307-314

Nishibori N, Nishii A, Takayama H (2001b) Detection of free polyamine in coastal seawater using ion exchange chromatography. Ices Journal of Marine Science 58:1201-1207

Nishibori N, Nishijima T (2004) Changes in polyamine levels during growth of a red-tide causing phytoplankton *Chattonella antiqua* (Raphidophyceae). Eur J Phycol 39:51-55

Nishibori N, Nishio S (1997) Occurrence of polyamines in the broom forming toxic dinoflagellate *Alexandrium tamarense*. Fisheries Science 63:319-320

Nishibori N, Yuasa A, Sakai M, Fujihara S, Nishio S (2001a) Free polyamine concentrations in coastal seawater during phytoplankton bloom. Fisheries Science 67:79-83

Orsini F, Accorsi M, Gianquinto G, Dinelli G, Antognoni F, Carrasco KBR, Martinez EA, Alnayef M, Marotti I, Bosi S, Biondi S (2011) Beyond the ionic and osmotic response to salinity in Chenopodium quinoa: functional elements of successful halophytism. Functional Plant Biology 38:818-831

Porter KG, Feig YS (1980) The use of dapi for identifying and counting aquatic microflora. Limnology and Oceanography 25:943-948

Rodriguez-Garay B, Phillips GC, Kuehn GD (1989) Detection of norspermidine and norspermine in *Medicago sativa* L. (Alfalfa). Plant physiology 89:525-529

Rufty TW, Mackown CT, Israel DW (1990) Phosphorus stress effects on assimilation of nitrate. Plant physiology 94:328-333

Schjørring JK (1986) Nitrate and ammonium absorption by plants growing at a sufficient or insufficient level of phosphorus in nutrient solutions. Plant and Soil 91:313-318

Stevens L (1970) The biochemical role of naturally occurring polyamines in nucleic acid synthesis. Biological reviews of the Cambridge Philosophical Society 45:1-27

Sumper M, Brunner E (2008) Silica biomineralisation in diatoms: The model organism *Thalassiosira pseudonana*. Chembiochem 9:1187-1194

Sumper M, Brunner E, Lehmann G (2005) Biomineralization in diatoms: Characterization of novel polyamines assoicated with silica. FEBS Letters 579:3765-3769

Sumper M, Kröger N (2004) Silica formation in diatoms: the function of long-chain polyamines and silaffins. Journal of Materials Chemistry 14:2059-2065

Sumper M, Lehmann G (2006) Silica pattern formation in diatoms: species-specific polyamine biosynthesis. Chembiochem 7:1419-1427

Tabor CW, Tabor H (1985) Polyamines in microorganisms. Microbiological reviews 49:81-99

Theiss C, Bohley P, Voigt J (2002) Regulation by polyamines of ornithine decarboxylase activity and cell division in the unicellular green alga *Chlamydomonas reinhardtii*. Plant physiology 128:1470-1479

Valdes-Santiago L, Ruiz-Herrera J (2014) Stress and polyamine metabolism in fungi. Front Chem 1:42

Wilhelm SW, Suttle CA (1999) Viruses and nutrient cycles in the sea. BioScience 49: 781–788.

Table 3.1. Extractable polyamine (PA) concentrations in 4 phytoplankton species. DAP: diaminopropane; PUT: putrescine; SPD: spermidine; NSPD: norspermidine; NSPM: norspermine. Extractable PA concentration values are given as means ± SE.

Phytoplankton species	Class	Cell volume (μm^3)	Extractable PA concentration (μmol l^{-1})					
			DAP	PUT	SPD	NSPD	NSPM	Total
Thalassiosira pseudonana (CCMP1335)	Bacillariophyceae	50	36±1	141±16	40±5	188±11	32±5	437±26
Chaetoceros sp. (CCMP199)	Bacillariophyceae	48	–	133±11	41±3	–	–	174±14
Synechococcus sp. (CCMP1334)	Cyanophyceae	0.5		40±22	120±20	8±6	–	168±40
Amphidinium carterae Hulburt (CCMP1314)	Dinophyceae	427	–	–	–	–	1176±95	1176±95

Table 3.2. Uptake rate of ^{14}C supplied as putrescine by *Thalassiosira pseudonana* cells.

Rates of uptake were determined from triplicate 8 ml samples taken 1 and 6 h after the addition of ^{14}C - putrescine. Values are means ± SE.

Treatment	Uptake rate of ^{14}C supplied as putrescine (amol cell^{-1} h^{-1})		
	$[NO_3^-]$=20 µmol l^{-1}	$[NO_3^-]$=50 µmol l^{-1}	Mean of row
Salinity=22	2.1±0.2	2.3±0.1	2.2±0.1
Salinity=32	0.8±0.02	1.0±0.05	0.9±0.1
Mean of column	1.5±0.3	1.7±0.3	

Fig. 3.1: Changes in (a) cell densities and extractable polyamine (PA) pools of *Thalassiosira pseudonana,* (b) concentrations of individual extractable PAs (PUT: putrescine; SPD: spermidine; NSPD: norspermidine; NSPM: norspermine), and (c) PA concentrations in the medium at different growth stages. Concentrations of PUT, SPD and NSPM below the detection limit are not shown. Error bars: standard error of 6 replicates (duplicate analyses from triplicate cultures). Lag phase: Days 1 and 2; exponential phase: Days 3 and 4; stationary phase: Days 5; late stationary phase: Days 6 to 7

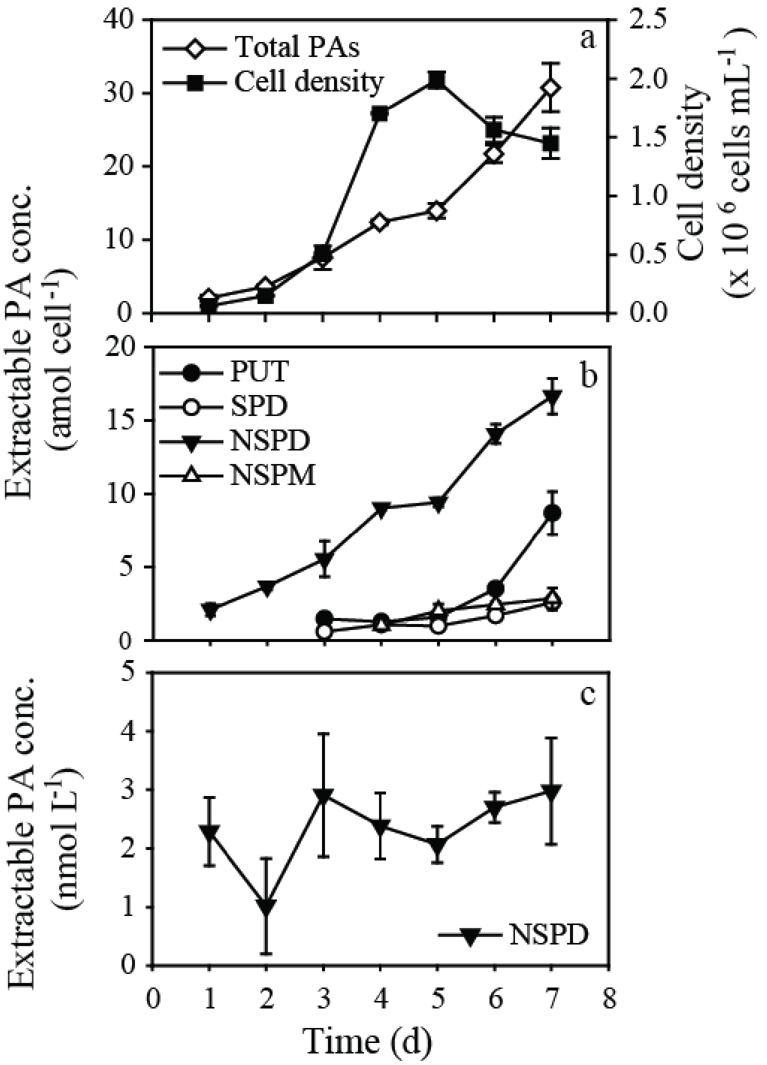

Total PAs
Cell density
a
Extractable PA conc.
(amol cell-1)
Cell density
(x 10 6 cells mL-1)
40
30
20
10
0
2.5
2.0
1.5
1.0
0.5
0.0
b
PUT
SPD
NSPD
NSPM
20
15
10
5
0
c
Extractable PA conc.
(nmol L-1)
NSPD
5
4
3
2
1
0
0
1
2
3
4
5
6
7
8
Time (d)

Fig. 3.2: Concentrations of (a) extractable polyamines (PAs) (DAP: diaminopropane; PUT: putrescine; SPD: spermidine; NSPD: norspermidine; NSPM: norspermine), (b) extracellular PAs during the growth of *Thalassiosira pseudonana* at 18 and 24°C. Panels (d) and (e) show the same variables as (a) and (b), respectively, but under conditions of different salinity (15, 25, 35 and 45). Concentrations of PAs below the detection limit are not shown. Error bars: standard error of 6 replicates (duplicate analyses from triplicate cultures). Concentrations of extracellular and extractable PAs are positively correlated with (c) temperature ($r = 0.7$, $p = 0.01$) or (f) salinity ($r = 0.8$, $p < 0.001$)

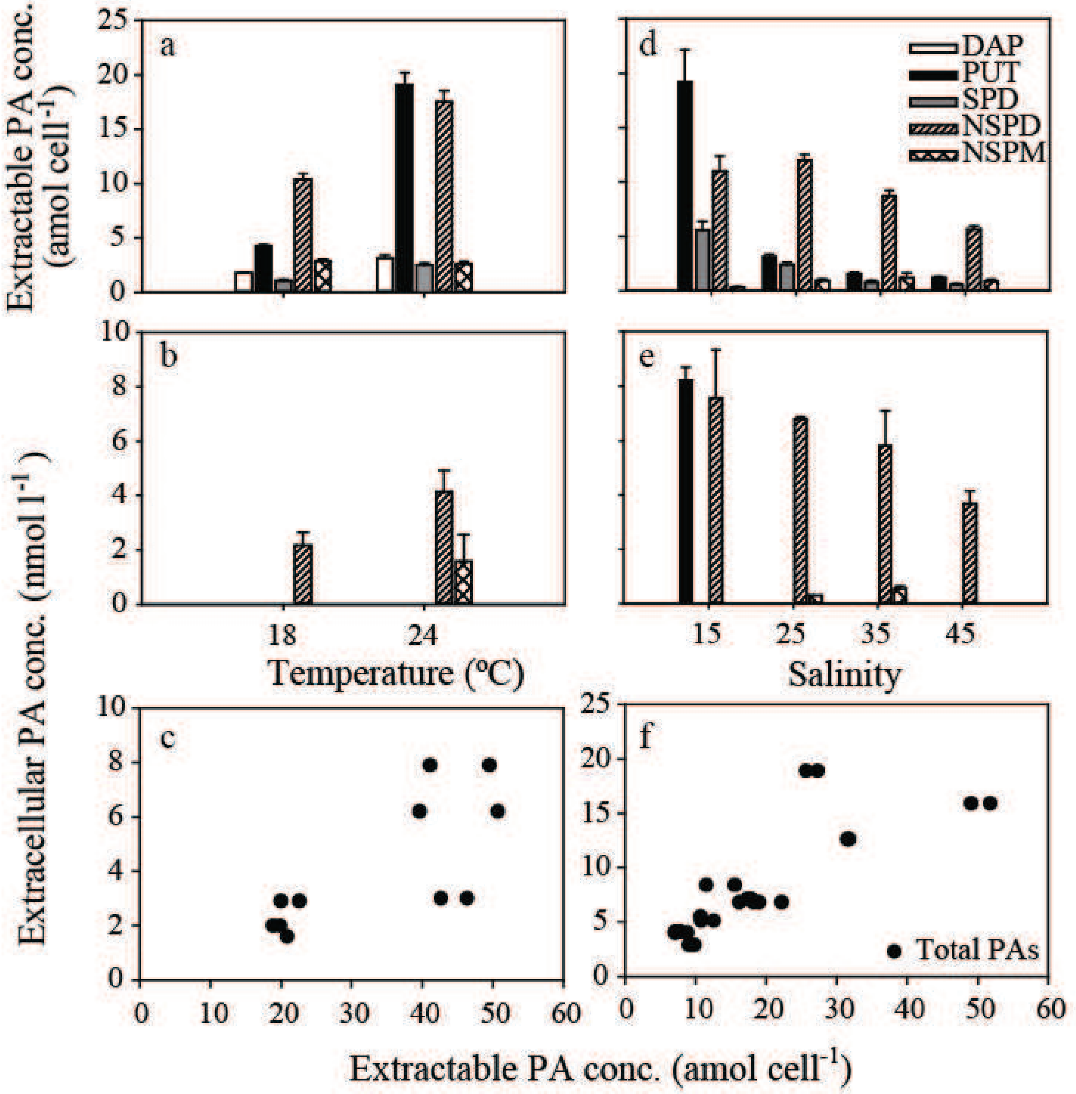
Extractable PA conc. (amol cell^{-1})
Extracellular PA conc. (nmol l^{-1})
a
b
c
d
e
f
DAP
PUT
SPD
NSPD
NSPM
0
5
10
15
20
25
0
2
4
6
8
10
18
24
Temperature (ºC)
15
25
35
45
Salinity
0
10
20
30
40
50
60
Total PAs
Extractable PA conc. (amol cell^{-1})

Fig. 3.3: Correlation between log-transformed extractable polyamine (PA) concentrations and salinity (r = 0.95, $p < 0.001$). Error bars: standard error of 6 replicates (duplicate analyses from triplicate cultures)

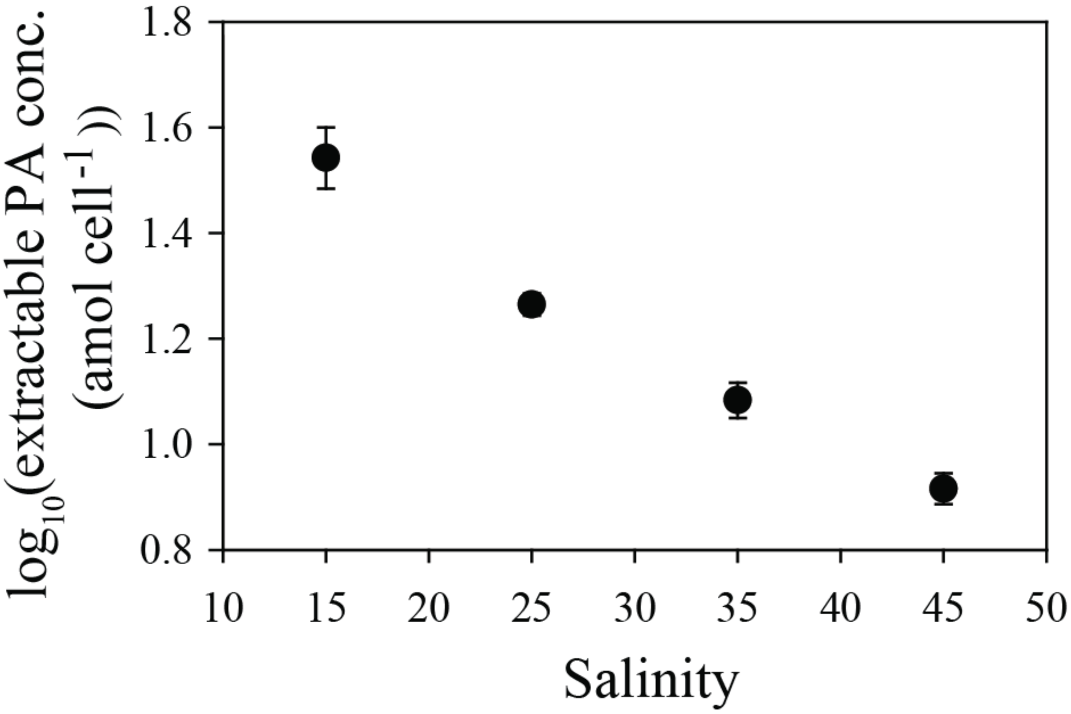

log$_{10}$(extractable PA conc. (amol cell^{-1}))
1.8
1.6
1.4
1.2
1.0
0.8
10
15
20
25
30
35
40
45
50
Salinity

Fig. 3.4: (a) Cell densities and extractable polyamine (PA) concentrations, (b) individual extractable PA concentrations and (c) extracellular PA concentrations during the growth of *Thalassiosira pseudonana* under different initial nitrate concentrations (0, 10, 20 and 50 µmol l^{-1}). Panels (d–f) and (g–i) show the same variables as (a–c), but for growth under different concentrations of phosphate (0, 0.5, 1 and 2 µmol l^{-1}) or silicate (0, 5, 20 and 50 µmol l^{-1}), respectively. Concentrations of PAs below the detection limit were not shown. Asterisk in (i) indicate no data available due to lost samples. Error bars: standard error of 6 replicates (duplicate analyses from triplicate cultures). PUT: putrescine; SPD: spermidine; NSPD: norspermidine; NSPM: norspermine

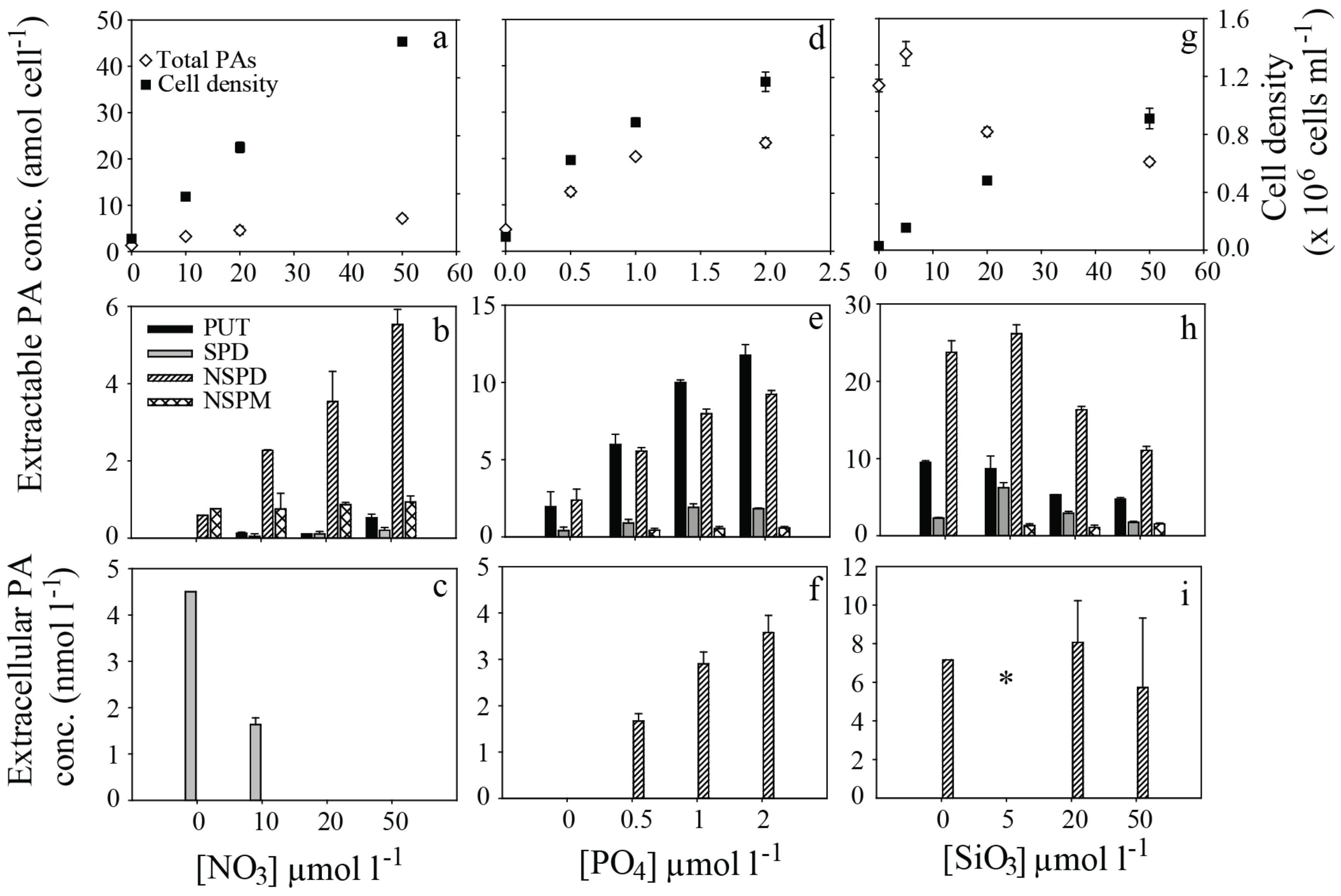
Extractable PA conc. (amol cell^{-1})
Extracellular PA conc. (nmol l^{-1})
Cell density (x 10^6 cells ml^{-1})
a
d
g
b
e
h
c
f
i
◇ Total PAs
■ Cell density
PUT
SPD
NSPD
NSPM
0
10
20
30
40
50
0
10
20
30
40
50
60
0.0
0.5
1.0
1.5
2.0
2.5
0.0
0.4
0.8
1.2
1.6
0
2
4
6
0
5
10
15
0
10
20
30
0
1
2
3
4
5
0
2
4
6
8
10
12
0
10
20
50
0
0.5
1
2
0
5
20
50
*
[NO$_3$] µmol l^{-1}
[PO$_4$] µmol l^{-1}
[SiO$_3$] µmol l^{-1}

Fig. 3.5: Correlations between concentrations of (a) total extractable polyamines (PAs), (b) putrescine (PUT), (c) spermidine (SPD), and (d) norspermidine (NSPD) with specific growth rates (μ; d^{-1}) of *Thalassiosira pseudonana* under different growth conditions ($p < 0.05$). Panels (e–h) show correlations between concentrations of total extractable PAs, PUT, SPD, and NSPD with μ of *T. pseudonana* grown under silicate limitation ($p < 0.05$)

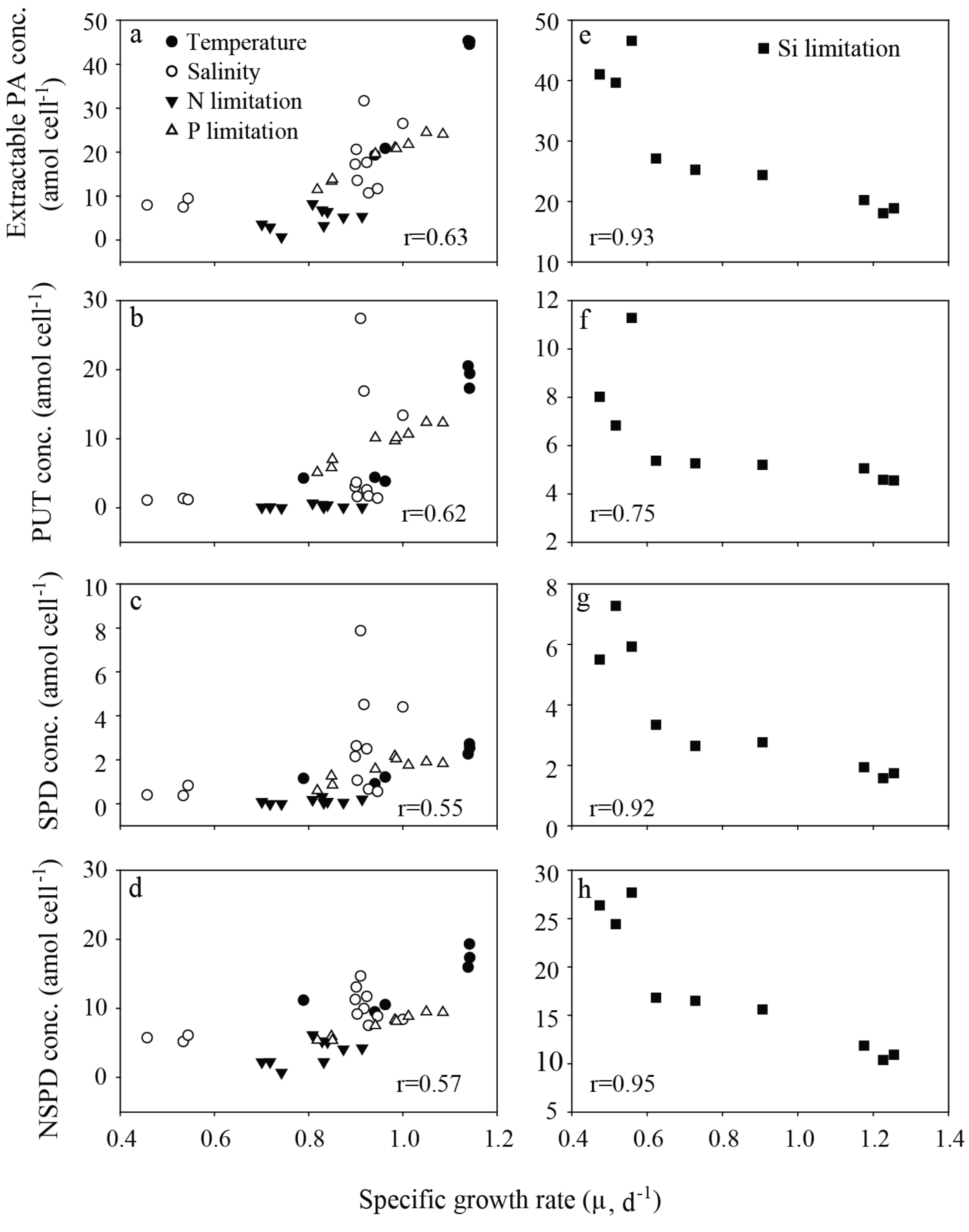
Extractable PA conc. (amol cell^{-1})
PUT conc. (amol cell^{-1})
SPD conc. (amol cell^{-1})
NSPD conc. (amol cell^{-1})
a
● Temperature
○ Salinity
▼ N limitation
△ P limitation
r=0.63
b
r=0.62
c
r=0.55
d
r=0.57
e
■ Si limitation
r=0.93
f
r=0.75
g
r=0.92
h
r=0.95
0.4
0.6
0.8
1.0
1.2
1.4
Specific growth rate (μ, d^{-1})

Fig. 3.6: Time courses of (a) *Thalassiosira pseudonana* abundance and (b) uptake of ^{14}C supplied as ^{14}C-putrescine by *T. pseudonana* cells grown under different culture conditions (filled circles: S = 22, [NO_3^-] = 20 µmol l^{-1}; open circles: S = 22, [NO_3^-] = 50 µmol l^{-1}; filled triangles: S = 32, [NO_3^-] = 20 µmol l^{-1}; open triangles: S = 32, [NO_3^-] = 50 µmol l^{-1}); S = salinity. Light and dark periods are separated by vertical dashed lines. The concentration of ^{14}C from putrescine in the cell (amol cell^{-1}) was calculated by dividing disintegrations per minute (DPM) taken up by cells by the specific activity of ^{14}C putrescine and the number of cells in the sample. Error bars: standard error of 3 replicates

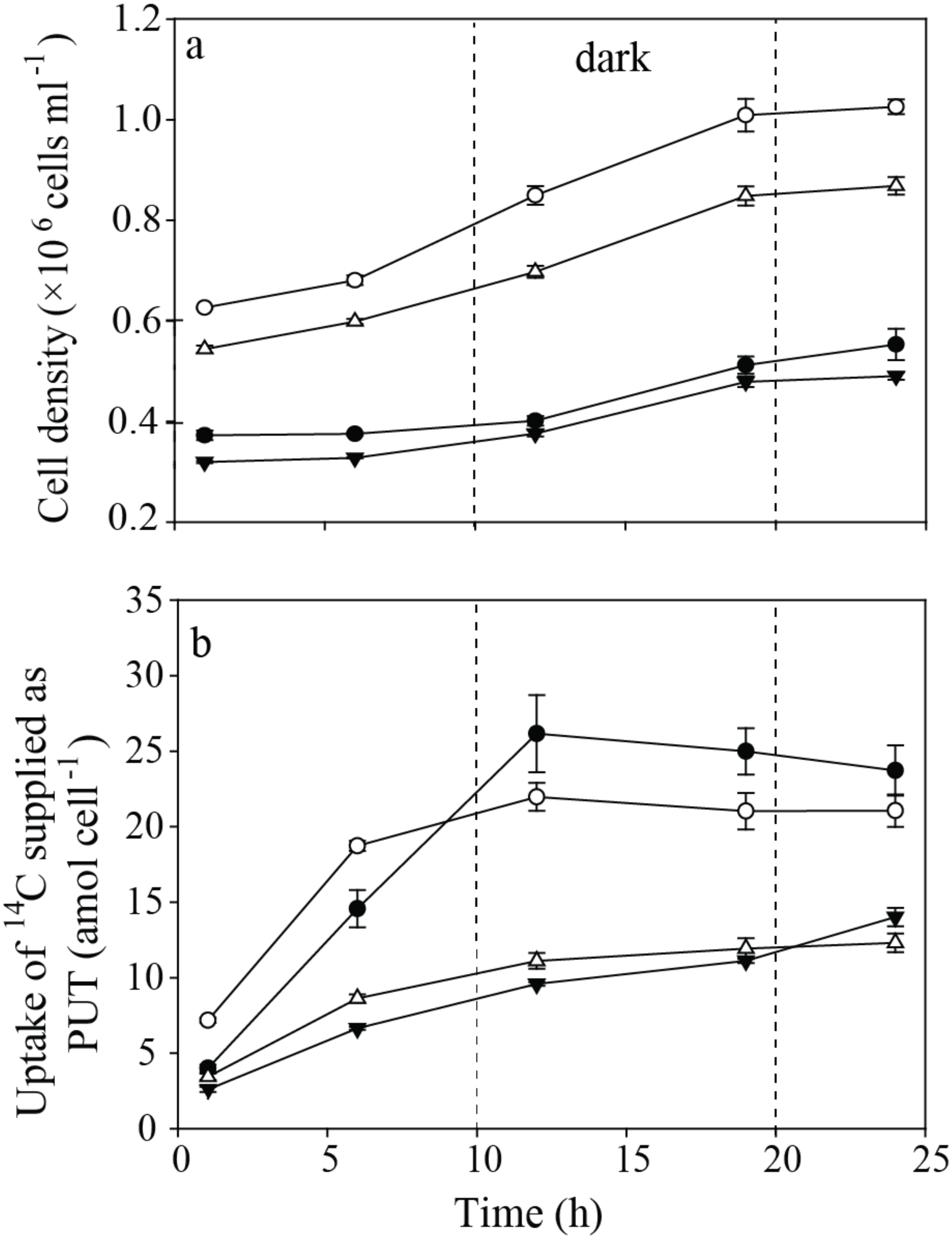
a
dark
Cell density (×10⁶ cells ml⁻¹)
1.2
1.0
0.8
0.6
0.4
0.2
b
Uptake of ¹⁴C supplied as PUT (amol cell⁻¹)
35
30
25
20
15
10
5
0
0
5
10
15
20
25
Time (h)

CHAPTER 4

SEASONAL VARIABILITY OF AMMONIA-OXIDIZING ARCHAEA AND AMMONIA-OXIDATION RATES AT THE SOUTH ATLANTIC BIGHT[3]

---

[3] Liu, Q., B.B. Tolar, M.J. Ross, J.B. Cheek, C.M. Sweeney, N.J. Wallsgrove, B.N. Popp, and J.T. Hollibaugh. To be submitted to *Limnology and Oceanography*.

ABSTRACT

Previous work in nearshore waters of the Georgia USA coast has demonstrated midsummer peaks of Thaumarchaeota abundance accompanied by spikes in nitrite concentration. These studies were performed at one location so that the extent of the bloom is unknown, nor has it been conclusively demonstrated that the bloom develops in nearshore waters. We used qPCR to quantify 16S rRNA genes from Thaumarchaeota, Bacteria and *Nitrospina*, a putative nitrite-oxidizing genus; and *amoA* genes from Archaea and Betaproteobacteria, in samples collected on 6 cruises from April to November on transects of the South Atlantic Bight (SAB), from inshore waters to the Gulf Stream. Nitrification rates were measured at selected stations using $^{15}NH_4^+$. Thaumarchaeota abundance increased in nearshore waters starting in July and peaking in August ($>10^7$ copies L^{-1}). The bloom did not extend out onto the mid-shelf, where Thaumarchaeota abundances ranged from 10^3 to 10^5 copies L^{-1}. Thaumarchaeota were also abundant ($>10^6$ copies L^{-1}) on all 6 cruises in oxygen deficient waters at 75–200 m at the shelf-break. This population is phylogenetically distinct from the nearshore population. Ammonia oxidation rates were highest at inshore stations and were near the limit of detection at mid-shelf stations. Betaproteobacteria *amoA* genes were present in relatively low numbers (undetectable to 10^4 copies L^{-1}) throughout the study area. Ammonia oxidation rates correlated with the abundance of Thaumarchaeota, but not with the abundance of ammonia-oxidzing Betaproteobacteria. The abundance of *Nitrospina* 16S rRNA genes was correlated with Thaumarchaeota abundance. The overall pattern of nitrification in the SAB is highest activity mid-summer at inshore stations, dropping dramatically at the transition from the turbid, nearshore water mass to the mid-shelf.

INTRODUCTION

Ammonia oxidation is the rate-limiting first step of nitrification and supplies one of the substrates, nitrite, to denitrification or anaerobic ammonium oxidation (anammox) (Kuypers et al. 2005, Francis et al. 2007, Jetten et al. 2009). Ammonia oxidation is thus of global significance to nitrogen geochemistry. Ammonia-oxidizing organisms (AOO) include members of the Beta- and Gammaproteobacteria (Ammonia-Oxidizing Bacteria or AOB) and Archaea (Ammonia-Oxidizing Archaea or AOA). AOA have recently (Brochier-Armanet et al. 2008) been proposed as a new phylum of the Archaea, the Thaumarchaeota.

Previous studies of Thaumarchaeota populations in Georgia coastal waters revealed a regular midsummer peak of abundance coinciding with a peak in nitrite (Hollibaugh et al. 2014, Tolar 2014). These studies were conducted at one location (Marsh Landing) at the mouth of the Duplin River, a tidal creek draining an extensive area of salt marsh inshore of Sapelo Island, GA. This inshore station is located adjacent to, and exchanges water with, Doboy Sound and thence the South Atlantic Bight. The South Atlantic Bight (SAB) is characterized by a broad, shallow (<50 m) continental shelf that extends along the southeast coast of the United States from approximately Jacksonville FL to Wilmington NC and from the nearshore across the shelf to the edge of the Gulf Stream (Atkinson and Menzel 1985). Water properties in the inshore and nearshore zones of the SAB are influenced by river flow and tidal exchange with salt marshes and estuaries, while shelf-break and slope waters are influenced by the Gulf Stream. The water column is well-mixed by tidal currents (3 m tidal amplitude at the apex of the SAB) at inshore, nearshore and mid-shelf stations; but stratified over deeper water at the shelf-break, with a thermocline between 50 and 100 m.

Thaumarchaeota were first detected in samples from Marsh Landing during studies of seasonal variation in bacterioplankton metatranscriptomes (Gifford et al. 2011, 2013). A mid-summer peak ($>10^7$ copies L^{-1}) of Thaumarchaeota 16S rRNA and Archaea *amoA* genes was detected in a quarterly sampling at this site (Hollibaugh et al. 2011, 2014). Because these studies focused on one location in a dynamic coastal environment, they could not distinguish between *in situ* growth of the Thaumarchaeota population versus local dynamics coupled to broader scale patterns that include advection or mixing from a population outside the study area, or resuspension of populations associated with sediment. To address the first of these questions, we extended our survey of Thaumarchaeota populations to the continental shelf and shelf-break waters of the SAB. We sampled at approximately monthly intervals from April to November to determine if the seasonal dynamics of Thaumarchaeota populations in the SAB reflected, or drove, the dynamics we recorded at Marsh Landing. Although covariance of nitrite concentrations and Thaumarchaeota abundance at Marsh Landing strongly indicate that this population oxidizes ammonia, we have not routinely measured ammonia oxidation rates. Thus, we measured ammonia oxidation rates directly on these cruises, using ^{15}N-labeled ammonium, with the goal of determining whether rates coincided with the distribution of Thaumarchaeota in the SAB. In addition to recording the abundance of Thaumarchaeota, we also recorded the abundances of Betaproteobacteria AOB to evaluate their contribution to ammonia oxidation in the SAB. Finally, we measured the abundance of the *Nitrospina*, an important marine member of the guild of nitrite-oxidizing bacteria, to evaluate coupling between ammonia- and nitrite-oxidation in these waters.

METHODS

Sampling Site

Samples were collected on 6 cruises of the R/V Savannah across the SAB (2-6 April, 15-18 May, 15-19 July, 4-7 Aug, 23-30 Sep and 3-7 Nov of 2014); station locations are shown in Appendix Figure B.1. Surface and bottom water samples were collected at inshore and shelf stations. We collected samples from 10 m, 75 m, 200 m and 450 m at shelf-break station C10. Station locations and depths sampled are given in Appendix Table B.1. Seawater samples were collected using 12 L Niskin bottles mounted on a CTD rosette. Profiles of environmental variables (temperature, salinity, dissolved oxygen, relative fluorescence) were taken by sensors mounted on the CTD during hydrocasts to collect water samples. Approximately 1L of water was filtered through 0.22 μm pore size Durapore filters (Millipore), the filters were placed in Whirl-Pak bags, 2 mL of lysis buffer (0.75 mol L^{-1} sucrose, 40 mmol L^{-1} EDTA, 50 mmol L^{-1} Tris; pH = 8.3) was added, then the filters were frozen on dry ice and stored frozen at -80 ^{o}C until they were processed. DNA was extracted from filters using sodium dodecyl sulfate/lysozyme and proteinase K then purified by phenol-chloroform extraction as described previously (Bano and Hollibaugh 2000, Tolar et al. 2013). Approximately 150 mL of the filtrate was frozen at -20 °C for nutrient (NO_2, NO_x, NH_4 and urea) analysis. Ammonium was measured using a fluorometric method described in Holmes et al. (1999). Nitrate plus nitrite (NO_x) was analyzed by reducing nitrate to nitrite with cadmium (Jones 1984), and nitrite was determined following Strickland and Parsons (1972). Urea was measured following a procedure adapted from Mulvenna and Savidge (1992) and Revilla et al. (2005). A total of ~ 1L seawater was filtered through a 47 mm Whatman GF/C glass filter paper to collect chlorophyll a during all cruises except May. Two or three drops (~0.1-0.2 mL) of magnesium carbonate (0.01g mL^{-1})

were added at the end of the filtration to avoid the production of phaeophytin. Filters were wrapped by alumni foil and stored at -20 °C. Chlorophyll a was extracted by 90% of acetone and measured by spectrophotometer as described in Strickland and Parsons (1972).

Quantitative PCR

All quantitative PCR analyses were performed on a C1000 Touch^{TM} Thermal cycler (Bio-rad). Quantitative PCR reactions were run in triplicate with a dilution series of standards made from environmental amplicons as described in Kalanetra et al. (2009) and Tolar et al. (2013). We determined the abundance (copies L^{-1}) of Thaumarchaeota and Bacteria 16S rRNA genes (*rrs*), Archaea and Betaproteobacteria *amoA* genes; and *Nitrospina* 16S rRNA genes. The primers and probes used and the qPCR efficiency for each primer are given in Table B.2. Thaumarchaeota and Bacteria *rrs* were detected using TaqMan primers and probes and all other genes were quantified using SYBRgreen (Bio-rad). The relative abundance of Thaumarchaeota (percent of prokaryotes) was calculated based on gene abundance (copies per liter, calculated from copies per reaction, volume filtered for each sample, extract volume and the volume of template used in each reaction) assuming one *rrs* or *amoA* gene per Thaumarchaeota genome (IMG database) and 1.8 *rrs* per bacterial genome (Biers et al. 2009).

Phylogenetic Analysis

We generated clone libraries of Thaumarchaeota *rrs* and Archaea *amoA* amplicons from DNA samples collected from surface water samples collected at inshore (SAPES, DOBES and ALTES), nearshore (C1) and middle-shelf (C4) stations, as well as from samples taken at 10 and 200 m at the shelf-break station (C10) on the July cruise. We chose July to coincide with the onset of growth of the inshore Thaumarchaeota population. Thaumarchaeota *rrs* (~900 bp) and Archaea *amoA* (~635 bp) fragments were amplified using the primers in Table B.2. Three PCRs were pooled to minimize PCR bias and electrophoresed on a 1% agarose gel. The processes of gel extraction and cloning followed the protocol described previously (Kalanetra et al. 2009, Tolar et al. 2013). Clones were randomly selected from each library and sequenced with the plasmid primer M13F (-21) (Genewiz, Inc.).

The vector contamination and Euryarchaeota *rrs* sequences were identified by BLAST (Zhang et al., 2000) and removed from the dataset. Sequences were trimmed and aligned against reference sequences and edited to remove uninformative positions using Geneious 8.1.7. Operational taxonomic units (OTUs) were determined with cutoff of 0.01 for Thaumarchaeota *rrs* and cutoff of 0.02 for Archaea *amoA*. Diversity (Shannon) and richness (Chao) indices were calculated using equations (1) and (2), respectively.

$$\mathrm{H}' = -\sum_{i=1}^{R} pi \ln pi \qquad (1)$$

$$S_{Chao1} = S_{obs} + \frac{\mathrm{n}_1\,(\mathrm{n}_1 - 1)}{2\,(\mathrm{n}_2 + 1)} \qquad (2)$$

where, p_i=the proportion of clones belonging to each type of OTU in one location, S_{obs} = the observed number of species, n_1= the number of OTUs with only one sequence and n_2 = the number of OTUs with only two sequences. Phylogenetic trees of Thaumarchaeota *rrs* and Archaea *amoA* were constructed using MR BAYES implemented in Geneious 8.1.7.

Ammonia Oxidation (AO) Rates

AO rates were measured in 24 h incubations at in situ temperature in the dark using ^{15}N-labeled ammonium (>99 atom-percent $^{15}NH_4Cl$; Cambridge Isotope Laboratories, Tewksbury, MA) added to a final concentration of 50 nmol L^{-1}. Incubations were terminated by freezing at -20 °C. Controls were frozen immediately after the addition of $^{15}NH_4Cl$. The produced $^{15}NO_x$ was measured using the "denitrifier method" (Sigman et al. 2001) as described previously (Popp et al. 1995, Dore et al. 1998, Beman et al. 2012). Briefly, $^{15}N_2O$ produced from NO_2^- and NO_3^- by incubation with the denitrifier *Pseudomonas aureofaciens* cultures was transferred from a reaction vial, cryofocused, separated from other gases using a 0.32-mm i.d. × 25-m × 5 µm CP-PoraBOND Q capillary column (Agilent Technologies, Santa Clara, CA) at room temperature, and introduced into a Finnigan MAT-252 isotope ratio mass spectrometer (Thermo Fisher Scientific, Waltham, MA). $^{15}N_2O$ concentrations and $\delta^{15}N$ were determined to calculate the AO rates with modified equation described previously (Ward et al. 1989, Beman et al. 2011, Beman et al. 2012)

$$^{15}R_{ox} = \frac{(n_t - noNO_X{}^{-}) \times [NO_3{}^{-} + \mathrm{NO_2}{}^{-}]}{(n\mathrm{NH_4}{}^{+} - no\mathrm{NH_4}{}^{+}) \times t}$$

Where n_t is the at% of ^{15}N in the NO_x^- (NO_3^-+NO_2^-) pool measured at time t, $noNO_x^-$ is the measured at% ^{15}N of unlabeled NO_x^- , $noNH_4^+$ is the initial at% of ^{15}N of NH_4^+ and nNH_4^+ is at% of ^{15}N of NH_4^+ at time t.

Statistical Analysis

Model II linear regression method using major axis (MA) regression was calculated to determine the relationship between abundances of targeted genes using R (Legendre and

Legendre 2012). Parametric 95% confidence intervals were computed for the slopes and intercepts. The non-parametric Spearman's rank correlation was used to calculate correlation coefficients (R) between two variables. Statistical significance was evaluated at a 95% confidence interval. Redundancy analysis (RDA) was used to determine the environmental impact on the seasonal distribution of Thaumarchaeota in the SAB with 999 Monte-Carlo permutations using the software package CANOCO (4.5; ter Braak and Smilauer 2002). The variables were log-transformed before the statistical analysis.

RESULTS

Environmental Conditions in the SAB

The water column was well mixed at inshore stations and on the continental shelf during the months sampled, but stations on the shelf-break (C8-10) experienced stratification with a surface mixed layer down to ~100 m (Table B.3). Temperature, salinity, dissolved oxygen and relative fluorescence measured in surface waters changed seasonally along transects of the SAB (Fig. 4.1 and Table B.3). Temperature increased from April (16 ^{o}C) to August (30 ^{o}C), and then decreased in fall (Fig. 4.1 and Table B.3). Freshwater inflow from the Altamaha River lowered salinity in inshore waters, especially during April (21 ± 4). Salinity was lowest at station ALTES at the mouth of the Altamaha River throughout the sampling period (range 13-30). The concentration of dissolved oxygen on the continental shelf was relatively low between May and September (ranging from 4-7 mg L^{-1}). Relative fluorescence, a proxy of chlorophyll a, was highest at inshore stations (Fig. 4.1 and Table B.3). Although these waters also have high concentrations of colored dissolved organic carbon (CDOM), we found a significant correlation between relative fluorescence and extracted chlorophyll a concentration in the subset of samples

($n = 280$, $R = 0.91$, $p < 0.05$), indicating that relative fluorescence measured by the fluorometer on the CTD reflected the abundance of phytoplankton biomass. Concentrations of NH_4^+, NO_2^- and NO_3^- were relatively higher at inshore stations, especially during summer (July to September), and much lower or undetectable in surface waters of further offshore (< 0.6 µmol L^{-1}; Table B.4). The average concentration of urea in the SAB were < 0.5 µmol L^{-1} (Table B.4).

Seasonal Distributions of Nitrifying Organisms

The abundances of Thaurmarchaeota *rrs* and Archaea *amoA* genes varied spatially and seasonally across the SAB (Fig. 4.2a-b and Table B.4). The well-mixed coastal waters contained the similar Thaumarchaeota population between surface and bottom waters (Table B.4). Abundances of Thaumarchaeota *rrs* and Archaea *amoA* co-varied in the SAB during all cruises ($R^2 = 0.74$, $p < 0.001$; Fig. 4.3a). Generally, Thaumarchaeota *rrs* and Archaea *amoA* genes were most abundant in inshore waters (10^5-10^8 copies L^{-1}) and decreased to the mid-shelf, where the abundances were low and less variable (10^3-10^5 copies L^{-1}; Fig. 4.2 and Table B.4). Thaumarchaeota *rrs* and Archaea *amoA* gene abundances in surface waters of shelf-break stations were similar to the concentrations at mid-shelf stations except during April and November, when Thaumarchaeota abundances were relatively high and similar to concentrations measured at inshore stations (> 10^5 copies L^{-1}; Table B.4).

Seasonal patterns of Thaumarchaeota abundance differed among inshore, nearshore and shelf-break stations (Fig. 4.2a-b and Table B.4). Thaumarchaeota populations at inshore stations increased from April (*rrs*: $3.1 \pm 1.1 \times 10^5$ copies L^{-1} and *amoA*: $5.8 \pm 4.6 \times 10^4$ copies L^{-1}) to August (*rrs*: $5.5 \pm 4.0 \times 10^7$ copies L^{-1} and *amoA*: $2.6 \pm 2.5 \times 10^7$ copies L^{-1}), and then decreased to November (*rrs*: $2.9 \pm 0.8 \times 10^6$ copies L^{-1} and *amoA*: $6.1 \pm 3.8 \times 10^5$ copies L^{-1}; Table B.5).

Thaumarchaeota abundance in nearshore waters also increased seasonally, but peaked in September (*rrs:* 5.1 ± 5.6 × 10^6 copies L^{-1} and *amoA*: 1.3 ± 2.1 × 10^6 copies L^{-1}; Table B.5). In contrast to the summer peak of Thaumarchaeota abundance at stations close to shore, the abundance of both genes in surface waters at shelf-break stations decreased from spring (*rrs*: 1.2 ± 1.7 × 10^5 copies L^{-1} and *amoA*: 1.5 ± 1.9 × 10^5 copies L^{-1}) to summer (*rrs*: 4.4 ± 3.4 × 10^3 copies L^{-1} and *amoA*: 3.1 ± 3.7 × 10^3 copies L^{-1}) and then increased back to 2.7 ± 0.3 × 10^5 copies L^{-1} and 3.2 ± 0.3×10^5 copies L^{-1} in November, respectively (Table B.4). At mid-shelf stations, Thaumarchaeota abundances did not show a seasonal pattern and varied ≤ 10-fold of magnitude (*rrs*: 1.8 ± 2.2 × 10^4 copies L^{-1} in April to 1.9 ± 1.1 × 10^5 copies L^{-1} in November; *amoA*: 3.0 ± 1.4 × 10^3 copies L^{-1} in April to 2.3 ± 4.3 × 10^4 copies L^{-1} in May).

The abundance of Betaproteobacteria *amoA* ranged from 10^2 to10^5 copies L^{-1} in the SAB, decreasing from inshore to shelf-break surface waters (Fig. 4.2c and Table B.4). It did not show a strong seasonal pattern, and was 0.1-10% of the Archaea *amoA* abundance. The abundance of *Nitrospina* sp. 16S rRNA gene was highest in inshore waters (10^4 to 10^6 copies L^{-1}) and showed no strong seasonal pattern in the SAB (Fig. 4.2d and Table B.4). We found a significant correlation between *Nitrospina* and Thaumarchaeota 16S rRNA gene abundances across all samples collected ($R^2 = 0.68$, $p < 0.001$; Fig. 4.3b).

Vertical Distribution of Thaumarchaeota at Shelf-break Stations

The water column was stratified at shelf-break station C10 on all cruises. Temperature decreased from > 25°C at 10 m to < 10°C at 400 m, while salinity varied within a narrow range (34.5-36.5). Relative fluorescence, displayed a maximum at ~ 100 m (Fig. 4.4). Dissolved oxygen decreased below the surface mixed layer; however, the oxygen concentration in deep waters (> 200 m) was ~ 4 mg L^{-1}, still greater than 2 mg L^{-1}, which is considered as hypoxic level (Diaz and Rosenberg 2008).

Thaumarchaeota *rrs* and Archaea *amoA* gene abundance varied with depth and showed different profiles at Station C10 (Fig. 4.4). The abundance of Archaea *amoA* in the surface water ranged from 1.5×10^3 to 3.5×10^5 copies L^{-1} and increased to reach a peak at 75-200 m (1.5×10^6 to 1.9×10^7 copies L^{-1}) through the year. Archaea *amoA* gene abundance declined sharply below 200 m, to between 1.4×10^4 to 2.2×10^5 copies L^{-1} (Fig. 4.4). Thaumarchaeota *rrs* also exhibited an increase in abundances from the surface (6.1×10^2 to 3.0×10^5 copies L^{-1}) to 75-200 m (7.7×10^6 to 1.4×10^7 copies L^{-1}); however, *rrs* abundance was relatively constant below 200 m (Fig. 4.4). As a consequence, the ratio of Archaea *amoA* to Thaumarchaeota *rrs* decreased from 1.5 ± 1.1 (mean ± SD) in the surface waters to 0.01 ± 0.004 at ~ 400 m. The maximum abundances of Thaumarchaeota *rrs* and Archaea *amoA* below the surface of C10 was less variable among sampling months, < 10^1-fold, in comparison to 10^2- to 10^3-fold changes at inshore stations (Fig. 4.4). The peak of Archaea *amoA* abundance at Station C10 generally coincided with the relative fluorescence maxima and was above the oxycline during all months sampled except April (Fig. 4.4). The NO_2 maximum at station C10 was at the same depth as the maximum of Archaea *amoA* abundance during May, July and September (Fig. 4.4). The abundance of Betaproteobacteria *amoA* ranged from below the limit of detection to 10^4 copies L^{-1} and did not show a consistent profile between cruises (Fig. 4.4). The abundance of Archaea *amoA* was 10- to 10^5-fold higher than Betaproteobacteria *amoA*. The contribution of Thaumarchaeota to total prokaryotes (summed abundances of Thaumarchaeota and Bacteria) increased from surface to the bottom water at the shelf-break, with a maximum of 15% at 400 m during November, in comparison to < 0.2% in surface waters on the continental shelf of the SAB during all months sampled.

AO Rates in the SAB

Ammonia oxidation rates were greatest at inshore stations, similar to the distribution of Archaea *amoA* gene across transects of the SAB (Fig. 4.5a). The maximum AO rate, 842 nmol L^{-1} d^{-1}, was measured in bottom water at inshore station ALTES during September (Table B.4). Although the maximum of Thaumarchaeota abundance occurred in August at inshore stations, AO rates at this time were < 10 nmol L^{-1} d^{-1}. This low rate, 1% to 10% of rates measured in July and September at the same regions (Fig. 4.5a and Table B.4), was unexpected because measurements made for another study at Marsh Landing on the Duplin river (adjacent to station DOBES) during August in 2011 and 2012 ranged from 100-400 nmol L^{-1} d^{-1}. AO rates at inshore stations in November were lowest (0.3-6.9 nmol L^{-1} d^{-1}; Table B.4). AO rates at nearshore and mid-shelf stations were extremely low (non-detectable to 0.3 nmol L^{-1} d^{-1}) during all months sampled, except at nearshore stations A1 (surface: 104 nmol L^{-1} d^{-1}, bottom: 132 nmol L^{-1} d^{-1}) and C1 (bottom: 4.9 nmol L^{-1} d^{-1}) during September, which were comparable to the ammonia oxidation rates at adjacent inshore stations (Table B.4).

AO rates varied with depth at shelf-break Station C10 and displayed seasonal variation. Maximum rates were detected at 75 m during May, July and September and at 200 m during April and November (Fig. 4.5b). Ammonia oxidation rates at 75 m ranged from 0.6 nmol L^{-1} d^{-1} in April to 12.4 nmol L^{-1} d^{-1} in September. Below 75 m, ammonia oxidation was relatively slow except at 200 m in November (7.2 nmol L^{-1} d^{-1}). Ammonia oxidation was detected down to 400 m in April, May and July, but the rates were < 0.5 nmol L^{-1} d^{-1} (Fig. 4.5b).

AO rates were strongly correlated with [NO_2^-] (Spearman's rank correlation, R = 0.54, p < 0.001; Fig. 4.6a) and [NH_4^+] (R = 0.4, p < 0.001; Fig.4.6b). Figure 4.6c shows that AO rates were very low (undetectable to 2 nmol L^{-1} d^{-1}) as the abundance of Archaea *amoA* gene was below 10^5 copies L^{-1} in the water column, but these two variables were still correlated ($R = 0.55$, $p < 0.001$; Fig. 4.6c).

Phylogenetic Composition of Thaumarchaeota Populations in the SAB

We retrieved a total of 253 Archaea *amoA* sequences (586 bp) from 7 clone libraries (surface water of SAPES, DOBES, ALTES, C1, C4, C10 and from 200 m at Station C10) constructed from samples collected on the July cruise. These libraries contained from 8 to 27 OTUs defined at 98% nucleotide identity, with a total of 89 OTUs at all stations. Twenty OTUs were shared among all stations. The diversity and richness of Archaea *amoA* genes were highest at inshore stations DOBES and ALTES and at 200 m at Station C10 (Table B.5). Most of the Archaea *amoA* gene sequences from inshore (SAPES, 91%; DOBES, 77.5%; ALTES, 81%) and nearshore (C1, 71%) stations fell into the group 'Water /Sediment', in which most of sequences from SAPES (71%) and C1 (42%) were most closely related to '*Candidatus* Nitrosopumilus maritimus' strain SCM1 (> 98% identity; Fig. 4.7a). Most of sequences retrieved from C4 (86%) and 10 m at Station C10 (61%) fell into the 'Water Column' clade, along with 29% of the sequences retrieved from Station C1 and 22.5% of the sequences retrieved from DOBES. Fewer than 10% of the sequences retrieved from SAPES and ALTES belonged to the 'Water Column' group. Two OTUs from Station ALTES (14% of sequences retrieved from that station) clustered with the Soil clade. Eighty nine percent of the OTUs recovered from 200 m at Station C10 were unique to that depth and 18 of 27 OTUs, ~ 65% of the sequences recovered from that library, fell into Group B, an open ocean, deep water ecotype (Fig. 4.7c; Francis et al. 2005). Three OTUs recovered from 10 m at Station C10 (8% of the sequences recovered from that sample) and 1 OTU from mid-shelf Station C4 (3% of total clones from C4) also fell into Group B. The remaining OTUs recovered from 200 m at Station C10 fell into Group A, the open ocean, shallow water ecotype (Fig. 4.7b; Francis et al. 2005), along with 3 OTUs from 10 m at Station C10 (21% of sequences recovered).

A large proportion of the Archaea *rrs* sequences recovered in samples from continental shelf stations were most closely related to Euryarchaeota (64-96%); thus, only 1 to 3 OTUs (defined at 99% nucleotide identity) and 1-14 Thaumarchaeota *rrs* sequences (474 bp) were recovered per sample (Table B.5). Only 20% of the Archaea *rrs* sequences retrieved from 200 m at Station C10 were Euryarchaeota, and a total of 25 OTUs were recovered from 40 Thaumarchaeota *rrs* sequences (Table B.5). Thaumarchaeota *rrs* sequences retrieved from SAPES, DOBES (9 of 10 sequences), C1 and C4 were most closely related to *N. maritimus* strain SCM1 and to reference sequences from coastal waters (> 98% identity of 16S rRNA gene sequence; Fig. 4.8). Two OTUs from 200 m at Station C10 clustered with the coastal strains at > 95% identity and two OTUs clustered at > 93% identity with the open ocean surface water isolate '*Candidatus* Nitrosopelagicus brevis' strain CN25 (> 93%; Fig. 4.8). Ninety percent of the sequences recovered from 200 m and both Thaumarchaeota sequences recovered from 10 m at Station C10 were grouped with environmental reference sequences from deep water (> 200 m; Fig. 4.8). The diversity and richness of Thaumarchaeota *rrs* in surface water samples were low due to the high content of Euryarchaeota sequences in these samples (Table B.5).

Environmental Controls on Distributions of Thaumarchaeota

The phylogenic analysis of Archaea *amoA* we conducted suggested that Thaumarchaeota sequences from surface waters of the SAB were most closely related to coastal or sediment reference sequences. To explore this relationship further, we analyzed the relationship between environmental factors and spatial and seasonal distributions of Thaumarchaeota *rrs* and Archaea *amoA* genes abundances in the SAB in two separate RDA analyses, one targeting the gene abundances in surface waters and the other focusing on gene abundances at depth at shelf-break stations (Fig. 4.9). The RDA biplot (Fig. 4.9a) shows the relationship between abundances of Thaumarchaeota genes and physiochemical variables in surface waters, in which 71% of the variability in composition was explained by RDA axis 1 and only 1% was explained by RDA axis 2. The analysis showed that fluorescence, S, T and concentrations of nitrite and urea contributed significantly ($n = 88$, $p < 0.05$) to the distribution of Thaumarchaeota *rrs* and Archaea *amoA* abundances during all cruises (Fig. 4.9a and Table B.6), and fluorescence explains most (53%, Table B.6) of the variance of the canonical eigenvalues. Temperature and salinity were positively and inversely correlated with Thaumarchaeota *rrs* and Archaea *amoA* abundances, respectively, and Thaumarchaeota distribution was not associated with DO. The concentration of urea in surface waters was low ($< 0.5\ \mu\text{mol L}^{-1}$), but Thaumarchaeota gene abundances were positively associated with urea (Fig. 4.9a and Table B.6). The light attenuation K calculated following Lin et al. (2009) and Liu et al. (2015) co-varied with fluorescence ($R = 0.58$, $p < 0.01$), but did not significantly contribute to the RDA axes ($p = 0.1$; Fig. 4.9a).

In the Thaumarchaeota –environment relationship at depths of shelf-break stations, RDA axis 1 explained most of the variability (76%), while RDA axis 2 explained 9% (Fig. 4.9b and Table B.6). Depth contributed to 47% of the variance on both RDA axes ($p = 0.002$). Temperature and Bacteria 16S rRNA gene abundance contributed significantly to RDA axis 2 ($p < 0.05$; Fig.4.9b and Table B.6).

DISCUSSION

Distributions of Thaumarchaeota rrs and Archaea amoA in the SAB

We observed a mid-summer peak of Thaumarchaeota abundance at SAB inshore and nearshore stations during this study (Fig. 4.2) that was consistent with seasonality observed in a long-term sampling program at Marsh Landing (Hollibaugh et al. 2011, 2014, unpublished data). We did not observe a mid-summer peak in Thaumarchaeota abundance at mid-shelf stations. Phylogenetic analysis (Fig. 4.7, 4.8) showed that inshore and nearshore populations consisted of the same ecotypes, suggesting similar environmental conditions or mixing exchange between these two water masses, resulting in a uniform distribution of Thaumarchaeota ecotypes. Archaea *amoA* gene sequences from mid-shelf and shelf-break stations were distinct from the major genotypes found at inshore/nearshore waters (< 87% similarity), indicating that these two populations of ammonia-oxidizing Archaea contain different species (Pester et al. 2012, Bouskill et al. 2012, Mincer et al. 2007). Most of the Thaumarchaeota *rrs* and Archaea *amoA* gene sequences recovered from inshore stations (SAPES, DOBES and ALTES) and near-shore station C1 were closely related (> 98% similar to '*Ca* Nitrosopumilus maritimus' strain SCM1; Könneke et al. 2005) and ≥ 93% similar to coastal isolates PS0 and HCA1 (Qin et al. 2014). The mid-summer peak of Thaumarchaeota abundance we observed in 2014 is consistent with a longer term record obtained from sampling at Marsh Landing (Hollibaugh et al. 2014), suggesting a regular seasonal cycle of Thaumarchaeota abundance in inshore and nearshore waters of the SAB. However, the mid-summer peak in Thaumarchaeota abundance contrasts with the mid-winter maximum of Thaumarchaeota reported for coastal waters of the North Sea (Wuchter et al. 2006, Herfort et al. 2007, Pitcher et al. 2011), coastal NW Mediterranean Sea (Galand et al. 2010) and polar oceans (Murray et al. 1998, Church et al. 2003). Phytoplankton have been suggested to compete with Thaumarchaeota for NH_4^+ in the North Sea and inhibit the growth of Thaumarchaeota during the spring and summer when the phytoplankton bloom; however, co-occurrences of Thaumarchaeota and phytoplankton have been noted in a few studies (Wells et al. 2006, Talor et al. 2013) as well as in this study (Fig. 4.9a), suggesting that competition with phytoplankton is not the direct cause of the seasonal decline in Thaumarchaeota abundance. Light, which also affects phytoplankton growth, has been shown to inhibit Thaumarchaeota growth (Merbt et al. 2012, Qin et al. 2014); thus the summer disappearance of Thaumarchaeota from the euphotic zone at high latitudes could be a response to the strong seasonal increase in irradiance there. Mid-winter maxima of Thaumarchaeota abundance at lower latitudes (Galand et al. 2010) may be the result of enhanced vertical mixing during winter, as suggested in Mincer et al. (2007). The well-mixed inshore and nearshore waters of the SAB are turbid due to sediment suspension and have high attenuation coefficients due to CDOM from river discharge (Fig. B.2). Light penetration into the water column is limited and thus light may not inhibit Thaumarchaeota growth in these areas. The distributions of Thaumarchaeota and of ammonia oxidation rates we observed are consistent with the extent of nearshore turbidity seen in a satellite photo of the region (Fig. B.2). Water clarity increases over the mid-shelf where Thaumarchaeota populations were greatly reduced and no mid-summer peak in abundance or ammonia oxidation rates were observed. Although Betaproteobacteria *amoA* gene was outnumbered by Archaea *amoA*, their spatial pattern was similar to that of Archaea *amoA*, decreasing from inshore to mid-shelf. Since ammonia-oxidizing Bacteria are associated with high ammonium concentration, the decrease of Betaproteobacteria *amoA* gene could be a result of low ammonia concentration (Martens-Habbena et al. 2009), but light inhibition could also be the key factor determining the distribution of ammonia-oxidizing Bacteria (Merbt et al. 2012).

Ammonia availability has also been suggested to control the distribution of Thaumarchaeota (Urakowa et al. 2011, Martens-Habbena et al. 2009, Horak et al. 2013). Ammonium concentrations measured in the SAB ranged from the limit of detection (~50 nmol L^{-1}) to 6.4 µmol L^{-1}, with higher concentrations in inshore waters (Table B.4). Concentrations at the limit of detection (< 50 nmol L^{-1}) may not be low enough to limit Thaumarchaeota growth (substrate threshold ≤ 10 nmol L^{-1}; Martens-Habbena et al. 2009). We did not detect a significant contribution of ammonium concentration to the Thaumarchaeota-environment relationship in the RDA analysis; however, the summer bloom of Thaumarchaeota coincided with relatively high ammonium concentrations (0.35-5.5 µmol L^{-1}) at inshore stations. Urea has been suggested as an alternate source of reduced nitrogen for ammonia-oxidizing Archaea (Alonso-Sáez et al. 2012, Lu et al. 2012). The RDA analysis showed that urea significantly contributed to Thaumarchaeota-environment relationship in surface waters of the SAB, suggesting a potential role for urea in nitrification in the SAB. However, we did not quantify urease genes or measure oxidation of ^{15}N supplied as urea in this study.

The vertical distributions of Thaumarchaeota *rrs* and Archaea *amoA* in the water column at shelf-break Station C10 were similar to previous observations in other regions (Santoro et al. 2010, Beman et al. 2012, Tolar et al. 2013), with Thaumarchaeota abundance peaking at or below the bottom of the euphotic zone. However, the apparent decrease in the abundance of Archaea *amoA* genes below the euphotic zone relative to constant abundance of Thaumarchaeota *rrs* resulted in a shift in the ratio of *amoA* to *rrs*, with values as low as 0.01 at depth, in contrast to the 1:1 ratio expected from the copy numbers in Thaumarchaeota genomes. The low ratio of

Archaea *amoA* to Thaumarchaeota *rrs* in deep waters is likely a consequence of bias of the Wuchter et al. (2006) qPCR primers we used against deep water clade B *amoA* (Beman et al. 2008, Santoro et al. 2010, Tolar et al. 2013).

Betaproteobacteria *amoA* gene abundance was lower than Archaea *amoA* in the water column of the SAB, especially during the summer peak of Thaumarchaeota abundance at inshore and nearshore stations. Furthermore, ammonia oxidation rates correlated with Thaumarchaeota, but not with AOB *amoA* gene abundance. Thus, the rapid ammonia oxidation and accumulation of nitrite at inshore/nearshore stations and at the bottom euphotic zone of the shelf-break may be attributed to ammonia-oxidizing Archaea.

Ammonia Oxidation Rate

Ammonia oxidation rate was correlated with Archaea *amoA* gene abundance in this study (R = 0.55); however, the rate was only elevated (> 2 nmol $L^{-1}d^{-1}$) when Archaea *amoA* gene abundance was > 10^5 copies L^{-1} (Fig. 4.6c). Even though Thaumarchaeota were abundant at both inshore and nearshore stations during summer, AO rates were extremely low or undetectable at nearshore stations. The correlations between AO rates with ammonium (R = 0.4) and nitrite (R = 0.54) concentrations suggests regulation of AO rates by ammonium availability (Martens-Habbena et al. 2009, Newell et al. 2013, Horak et al. 2013). The ammonium concentrations measured in nearshore and mid-shelf waters was in the range (0.04-1.36 µmol L^{-1}) that were much lower than those measured at inshore stations (0.35-5.5 µmol L^{-1}); thus, the availability of ammonium could be a key factor driving AO rates in nearshore/mid-shelf waters.

Previous measurements of ammonia oxidation in surface waters of the shelf-break stations of the SAB during April and October 2011 were less than 0.2 nmol L^{-1} d^{-1} (Tolar 2014);

thus, in this study, $^{15}NH_4$ oxidation in surface waters of the shelf-break was assumed similarly to that in surface waters of mid-shelf and not measured. Ammonia oxidation rates measured between 75-200 m at shelf-break Station C10 were relatively high compared to those measured in surface waters or the deeper waters but were much lower than rates measured at inshore during summer, although the abundances of Archaea *amoA* genes were similar in these two water masses. Low nutrient availability ($[NH_4^+]$ was < 0.15 μmol L^{-1}) may limit ammonia oxidation rates at the depth. Moreover, Thaumarchaeota ecotypes from different environments have been reported to have different growth rates and cell-specific AO rates (Wuchter et al. 2006, Martens-Habbena et al. 2009, Santoro et al. 2010, Santoro and Casciotti et al. 2011, Lehtovirta-Morley et al. 2011, Qin et al. 2014). Smith et al. (2014) found that ammonia oxidation rates in Monterey Bay surface waters correlated with the abundance of water column clade A (WCA), while the deep water samples dominated by deep water clade B (WCB) had consistently low ammonia oxidation rates. We found two distinct Thaumarchaeota ecotypes in inshore versus shelf-break waters, respectively. The former was mainly composed of *N. maritimus* strain SCM1-like *amoA* sequences and the latter may contain a mix of open ocean shallow ecotype Cluster A and deep ecotype Cluster B based on the compositions of clone libraries in 10 m and 200 m (Francis et al. 2005, Beman et al. 2008). Thus, the greater per cell ammonia oxidation rates of *N. maritimus* strain SCM1 than the open ocean strains (Martens-Habbena et al. 2009, Santoro and Casciotti et al. 2011) could explain the higher ammonia oxidation rates in inshore waters.

Phylogenetic Composition of Thaumarchaeota

Thaumarchaeota genotypes were partitioned by habitat in the SAB. Clone libraries of the inshore and nearshore samples shared few OTUs with samples from the shelf-break deep water sample and genotypes from each region were closely related to reference sequences from sites with similar oceanographic characteristics (Fig. 4.7, 4.8). However, a mix of inshore and open ocean clades was found in surface waters from mid-shelf and shelf-break stations suggesting that advection and mixing affect the distribution of Thaumarchaeota in this region. The dominance of *N. maritimus* strain SCM1 *amoA* in inshore (e.g. SAPES) and nearshore (C1) waters corresponded to the metatranscriptomic evidence from Marsh Landing (Hollibaugh et al. 2011). Sequences most closely related to the low salinity adapted species *Candidatus* "Nitrosoarchaeum limnia" strain SFB1 were encountered most frequently at Stations ALTES and DOBES, stations more strongly influenced by freshwater input from the Altamaha River.

As a consequence of abundance of Euryarchaeota *rrs* in our samples, the richness and diversity of Thaumarchaeota in the SAB can be only inferred from Archaea *amoA* gene. Our analysis showed that the Thaumarchaeota populations sampled at inshore station DOBES and from 200 m at shelf-break station C10 contained the highest richness and greatest diversity, and the rarefaction curves for these samples indicated that diversity was under-sampled at both of these locations (Fig. B.3). Interestingly, the sample collected from SAPES was much less diverse than other two inshore stations and the clone libraries from this station seemed to be saturated (Fig. B.3). OTUs from SAPES clustered with isolates or environmental sequences from the water column while OTUs from DOBES and ALTES were more closely related to those retrieved from sediment. Biller et al. (2012) found that sequences from coastal sediments had the greatest number of OTUs, while fewer OTUs were found in the water column. Therefore, sediment suspension may be a more important source of the Thaumarchaeota in samples from ALTES or DOBES and result in high diversity and richness of Thaumarchaeota there than at Stations SAPES.

CONCLUSIONS

Thaumarchaeota are widespread in waters of the SAB, but elevated abundance of Archaea16S rRNA and *amoA* genes was constrained to nearshore sites of the SAB in summer. Thaumarchaeota appear to be the dominant ammonia oxidizing organisms in the SAB. Temperature, salinity and urea appear to contribute to the distribution of Thaumarchaeota population and nitrite, as a product of ammonia oxidation, also showed a positive correlation with Thaumarchaeota abundance. In addition, we found a strongly positive correlation between phytoplankton and Thaumarchaeota abundance, suggesting that competition with phytoplankton for ammonia may not limit Thaumarchaeota growth, either as a consequence of high ammonia availability or uptake of oxidized forms of inorganic N by phytoplankton in the SAB. Moreover, the potentially different responses of diverse Thaumarchaeota ecotypes to environmental and biological factors make it difficult to explain the dynamics of Thaumarchaeota in the water column. The ammonia oxidation rates measured in the SAB were determined by both Thaumarchaeota abundances and ammonium concentrations, and the latter is the major factor driving the ammonia oxidation.

ACKNOWLEDGEMENTS

We thank the captain and crew of R/V Savannah for assisting in sample collection. I would also like to thank Drs.Daniela Di Iorio, Yeping Yuan and Yuntao Wang for helping with sample collections, especially Dr. Yeping Yuan for suggestions and assistance with creation of figures using MATLAB, as well as Dr. John Schalles from Creighton University, Omaha for providing satellite graphs of the SAB. The research was funded by the National Science Foundation (NSF OCE 13-35838 to JTH).

REFERENCES

Alonso-Saez L, Waller AS, Mende DR, Bakker K, Farnelid H, Yager PL, et al. (2012) Role for urea in nitrification by polar marine Archaea. *Proc Natl Acad Sci U S A* **109**: 17989-17994.

Atkinson, LP, Menzel, DW (1985) Introduction: Oceanography of the Southeast United States Continental Shelf, in Oceanography of the Southeastern U.S. Continental Shelf (eds L. P. Atkinson, D.W. Menzel and K.A.Bush), American Geophysical Union, Washington, D.C.. doi:10.1029/CO002p0001

Bano N, and Hollibaugh JT (2000) Diversity and distribution of DNA sequences with affinity to ammonia-oxidizing bacteria of the beta subdivision of the class Proteobacteria in the Arctic Ocean. *Appl Environ Microbiol* **66**: 1960-1969.

Beman JM, Chow CE, King AL, Feng YY, Fuhrman JA, Andersson A, Bates NR, Popp BN, Hutchins DA (2011) Global declines in oceanic nitrification rates as a consequence of ocean acidification. *P Natl Acad Sci USA* 108:208-213

Beman JM, Popp BN, Alford SE (2012) Quantification of ammonia oxidation rates and ammonia-oxidizing archaea and bacteria at high resolution in the Gulf of California and eastern tropical North Pacific Ocean. *Limnology and Oceanography* **57**: 711-726.

Beman JM, Popp BN, Francis CA (2008) Molecular and biogeochemical evidence for ammonia oxidation by marine Crenarchaeota in the Gulf of California. *ISME J* **2**: 429-441.

Biers EJ, Sun S, Howard EC (2009) Prokaryotic genomes and diversity in surface ocean waters: interrogating the global ocean sampling metagenome. *Appl Environ Microbiol* **75**: 2221-2229.

Biller SJ, Mosier AC, Wells GF, Francis CA (2012) Global biodiversity of aquatic ammonia-oxidizing Archaea is partitioned by habitat. *Front Microbiol* **3**: 252. DOI=10.3389/fmicb.2012.00252

Bouskill NJ, Eveillard D, Chien D, Jayakumar A, Ward BB (2012) Environmental factors determining ammonia-oxidizing organism distribution and diversity in marine environments. *Environ Microbiol* 14:714-729

Brochier-Armanet C, Boussau B, Gribaldo S, Forterre P (2008) Mesophilic Crenarchaeota: proposal for a third archaeal phylum, the Thaumarchaeota. *Nat Rev Microbiol* 6:245-252

Church MJ, DeLong EF, Ducklow HW, Karner MB, Preston CM, Karl DM (2003) Abundance and distribution of planktonic Archaea and Bacteria in the waters west of the Antarctic Peninsula. *Limnology and Oceanography* **48**: 1893-1902.

DeLong EF (1992) Archaea in coastal marine environments. *Proc Natl Acad Sci U S A* 89: 5685-5689.

Diaz RJ, Rosenberg R (2008) Spreading dead zones and consequences for marine ecosystems. *Science* 321:926-929

Dore JE, Popp BN, Karl DM, Sansone FJ (1998) A large source of atmospheric nitrous oxide from subtropical North Pacific surface waters. *Nature* 396:63-66

Francis CA, Beman JM, Kuypers MM (2007) New processes and players in the nitrogen cycle: the microbial ecology of anaerobic and archaeal ammonia oxidation. *ISME J* 1:19-27

Francis CA, Roberts KJ, Beman JM, Santoro AE, Oakley BB (2005) Ubiquity and diversity of ammonia-oxidizing archaea in water columns and sediments of the ocean. *Proc Natl Acad Sci U S A* **102**: 14683-14688.

Galand PE, Gutiérrez-Provecho C, Massana R, Gasol JM, Casamayor EO (2010) Inter-annual recurrence of archaeal assemblages in the coastal NW Mediterranean Sea (Blanes Bay Microbial Observatory). *Limnology and Oceanography* **55**: 2117-2125.

Gifford SM, Sharma S, Booth M, Moran MA (2013). Expression patterns reveal niche diversification in a marine microbial assemblage. *ISME* J **7**: 281-298.

Gifford SM, Sharma S, Rinta-Kanto JM, Moran MA (2011). Quantitative analysis of a deeply sequenced marine microbial metatranscriptome. *ISME* J **5**: 461-472.

Herfort L, Schouten S, Abbas B, Veldhuis MJ, Coolen MJ, Wuchter C, et al. (2007) Variations in spatial and temporal distribution of Archaea in the North Sea in relation to environmental variables. *FEMS Microbiol Ecol* **62**: 242-257.

Hollibaugh JT, Gifford SM, Moran MA, Ross MJ, Sharma S, Tolar BB (2014) Seasonal variation in the metatranscriptomes of a Thaumarchaeota population from SE USA coastal waters. *ISME J* **8**: 685-698.

Hollibaugh JT, Gifford S, Sharma S, Bano N, Moran MA (2011) Metatranscriptomic analysis of ammonia-oxidizing organisms in an estuarine bacterioplankton assemblage. *ISME J* **5**: 866-878.

Holmes RM, Aminot A, Kerouel R, Hooker BA, Peterson BJ (1999) A simple and precise method for measuring ammonium in marine and freshwater ecosystem. *Can J Fish Aquat Sci* **56**: 1801-1808.

Horak RE, Qin W, Schauer AJ, Armbrust EV, Ingalls AE, Moffett JW, et al. (2013) Ammonia oxidation kinetics and temperature sensitivity of a natural marine community dominated by Archaea. *ISME J* **7**: 2023-2033.

Hornek R, Pommerening-Roser A, Koops HP, Farnleitner AH, Kreuzinger N, Kirschner A, et al. (2006) Primers containing univeral bases reduce multiple amoA gene specific DGGE band patterns when analysing the diversity of beta-ammonia oxidizers in the environment. *J Microbial Methods* **66**: 147-155.

Huelsenbeck JP, Ronquist F (2001). MRBAYES: Bayesian inference of phylogenetic trees. *Bioinformatics*. **17** (8):754-755

Jetten MS, Niftrik L, Strous M, Kartal B, Keltjens JT, Op den Camp HJ (2009) Biochemistry and molecular biology of anammox bacteria. *Crit Rev Biochem Mol Biol* 44:65-84

Jones MN (1984) Nitrate reduction by shaking with cadmium - alternative to cadmium columns. *Water Research* **18**: 643-646.

Kalanetra KM, Bano N, Hollibaugh JT (2009) Ammonia-oxidizing Archaea in the Arctic Ocean and Antarctic coastal waters. *Environ Microbiol* **11**: 2434-2445.

Könneke M, Bernhard AE, de la Torre JR, Walker CB, Waterbury JB, Stahl DA (2005) Isolation of an autotrophic ammonia-oxidizing marine archaeon. *Nature* **437**: 543-546.

Kuypers MM, Lavik G, Woebken D, Schmid M, Fuchs BM, Amann R, et al. (2005) Massive nitrogen loss from the Benguela upwelling system through anaerobic ammonium oxidation. *Proc Natl Acad Sci U S A* **102**: 6478-6483.

Lehtovirta-Morley LE, Stoecker K, Vilcinskas A, Prosser JI, Nicol GW (2011) Cultivation of an obligate acidophilic ammonia oxidizer from a nitrifying acid soil. *Proc Natl Acad Sci U S A* **108**: 15892-15897.

Legendre P, Legendre L (2012) Volume 24: Numerical Ecology, 3rd Edition. *Elsevier.*

Lin S, Zou T, Gao H, Guo X (2009) The vertical attenuation of irradiance as a function of turbidity: a case of the Huanghai (Yellow) Sea in spring. Acta Oceanologica Sinica **28(5)**: 66-75

Liu Q, Lu X, Tolar BB, Mou X, Hollibaugh JT (2015) Concentrations, turnover rates and fluxes of polyamines in coastal waters of the South Atlantic Bight. *Biogeochemistry* **123**: 117-133.

Lu L, Han W, Zhang J, Wu Y, Wang B, Lin X, et al. (2012) Nitrification of archaeal ammonia oxidizers in acid soils is supported by hydrolysis of urea. *ISME J* **6**: 1978-1984.

Martens-Habbena W, Berube PM, Urakawa H, de la Torre JR, Stahl DA (2009) Ammonia oxidation kinetics determine niche separation of nitrifying Archaea and Bacteria. *Nature* **461**: 976-979.

Merbt SN, Stahl DA, Casamayor EO, Marti E, Nicol GW, Prosser JI (2012) Differential photoinhibition of bacterial and archaeal ammonia oxidation. *FEMS Microbiol Lett* **327**: 41-46.

Mincer TJ, Church MJ, Taylor LT, Preston C, Karl DM, DeLong EF (2007) Quantitative distribution of presumptive archaeal and bacterial nitrifiers in Monterey Bay and the North Pacific Subtropical Gyre. *Environ Microbiol* **9**: 1162-1175.

Mulvenna PF, Savidge G (1992) A modified manual method for the determination of urea in seawater using diacetylmonoxime reagent. *Estuarine Coastal and Shelf Science* **34**: 429-438.

Murray AE, Preston CM, Massana R, Taylor LT, Blakis A, Wu K, DeLong EF (1998) Seasonal and spatial variability of bacterial and archaeal assemblages in the coastal waters near Anvers Island, Antarctica. *Appl Environ Microbiol* **64**: 2585-2595.

Newell SE, Babbin AR, Jayakumar A, Ward, BB (2011) Ammonia oxidation rates and nitrification in the Arabian Sea. *Global Biogeochemical Cycles* **25**: n/a-n/a.

Newell SE, Fawcett SE, Ward BB (2013) Depth distribution of ammonia oxidation rates and ammonia-oxidizer community composition in the Sargasso Sea. *Limnology and Oceanography* **58**: 1491-1500.

Pester M, Rattei T, Flechl S, Grongroft A, Richter A, Overmann J, et al. (2012) amoA-based consensus phylogeny of ammonia-oxidizing archaea and deep sequencing of amoA genes from soils of four different geographic regions. *Environ Microbiol* **14**: 525-539.

Pitcher A, Wuchter C, Siedenberg K, Schouten S, Sinninghe Damsté JS (2011) Crenarchaeol tracks winter blooms of ammonia-oxidizing Thaumarchaeota in the coastal North Sea. *Limnology and Oceanography* **56**: 2308-2318.

Popp BN, Sansone FJ, Rust TM, Merritt DA (1995) Determination of Concentration and Carbon Isotopic Composition of Dissolved Methane in Sediments and Nearshore Waters. *Anal Chem* 67:405-411

Qin W, Amin SA, Martens-Habbena W, Walker CB, Urakawa H, Devol AH, et al. (2014) Marine ammonia-oxidizing archaeal isolates display obligate mixotrophy and wide ecotypic variation. *Proc Natl Acad Sci U S A* **111**: 12504-12509.

Revilla M, Alexander J, Glibert PM (2005) Urea analysis in coastal waters: comparison of enzymatic and direct methods. Limnology and Oceanography-Methods **3**: 290-299.

Rotthauwe JH, Witzel KP, Liesack W (1997) The ammonia monooxygenase structural gene amoA as a functional marker: Molecular fine-scale analysis of natural ammonia-oxidizing populations. *Applied and Environmental Microbiology* **63**: 4704-4712.

Santoro AE, Casciotti KL (2011) Enrichment and characterization of ammonia-oxidizing archaea from the open ocean: phylogeny, physiology and stable isotope fractionation. *ISME J* **5**: 1796-1808.

Santoro AE, Casciotti KL, Francis CA (2010) Activity, abundance and diversity of nitrifying archaea and bacteria in the central California Current. *Environ Microbiol* **12**: 1989-2006.

Sigman DM, Casciotti KL, Andreani M, Barford C, Galanter M, Bohlke JK (2001) A bacterial method for the nitrogen isotopic analysis of nitrate in seawater and freshwater. *Anal Chem* **73**: 4145-4153.

Smith JM, Casciotti KL, Chavez FP, Francis CA (2014) Differential contributions of archaeal ammonia oxidizer ecotypes to nitrification in coastal surface waters. *ISME J* **8**: 1704-1714.

Strickland JDH, Parsons TR (1972) A practical handbook of seawater analysis. *Fisheries Research Board of Canada, Minister of Supply and Service Canada, Ottawa*.

Suzuki MT, Taylor LT, DeLong EF (2000) Quantitative analysis of small-subunit rRNA genes in mixed microbial populations via 5'-nuclease assays. *Appl Environ Microbiol* **66**: 4605-4614.

ter Braak CJF, Smilauer P (2002) CANOCO Reference manual and CanoDraw for Windows User's guild: Software for Canonical Community Ordination (version 4.5). *Ithica: Microcomputer Power.*

Tolar BB (2014). The influence of environmental factors including reactive oxygen species on the spatial and temporal distribution of marine Thaumarchaeota (Doctoral dissertation).

Tolar BB, King GM, Hollibaugh JT (2013) An analysis of Thaumarchaeota populations from the northern gulf of Mexico. *Front Microbiol* **4**: 72. doi: 10.3389/fmicb.2013.00072

Urakawa H, Martens-Habbena W, Stahl DA (2011) Physiology and genomics of ammonia-oxidizing archaea. In: Ward BB, Arp DJ, Klotz MG (eds) Nitrification.ASM Press, Washington (DC), pp 117–155

Ward BB, Kilpatrick KA, Renger EH, Eppley RW (1989) Biological nitrogen cycling in the nitracline. *Limnology and Oceanography* 34:493-513

Wells lE, Cordray M, Bowerman S, Miller LA, Vincent WF, Deming JW (2006) Archaea in particle-rich waters of the Beaufort Shelf and Franklin Bay, Canadian Arctic: Clues to an allochthonous origin? *Limnology and Oceanography* **51**: 47-59.

Wuchter C, Abbas B, Coolen MJ, Herfort L, van Bleijswijk J, Timmers P, et al. (2006) Archaeal nitrification in the ocean. *Proc Natl Acad Sci U S A* **103**: 12317-12322.

Zhang Z, Schwartz S, Wagner L, Miller W (2000) A greedy algorithm for aligning DNA sequences. *J Comput Biol* **7**: 203-214.

Fig. 4.1: Seasonal and spatial variability of: a) temperature (°C), b) salinity, c) dissolved oxygen concentration (DO, mg L^{-1}) and d) relative fluorescence (µg L^{-1}); in surface waters on the continental shelf of the South Atlantic Bight. Dots indicate the sampling stations with reference to Appendix Figure B.1. Figures in each column represent environmental variables from the same sampling month. The means and ranges of each variable were listed in Table B.3.

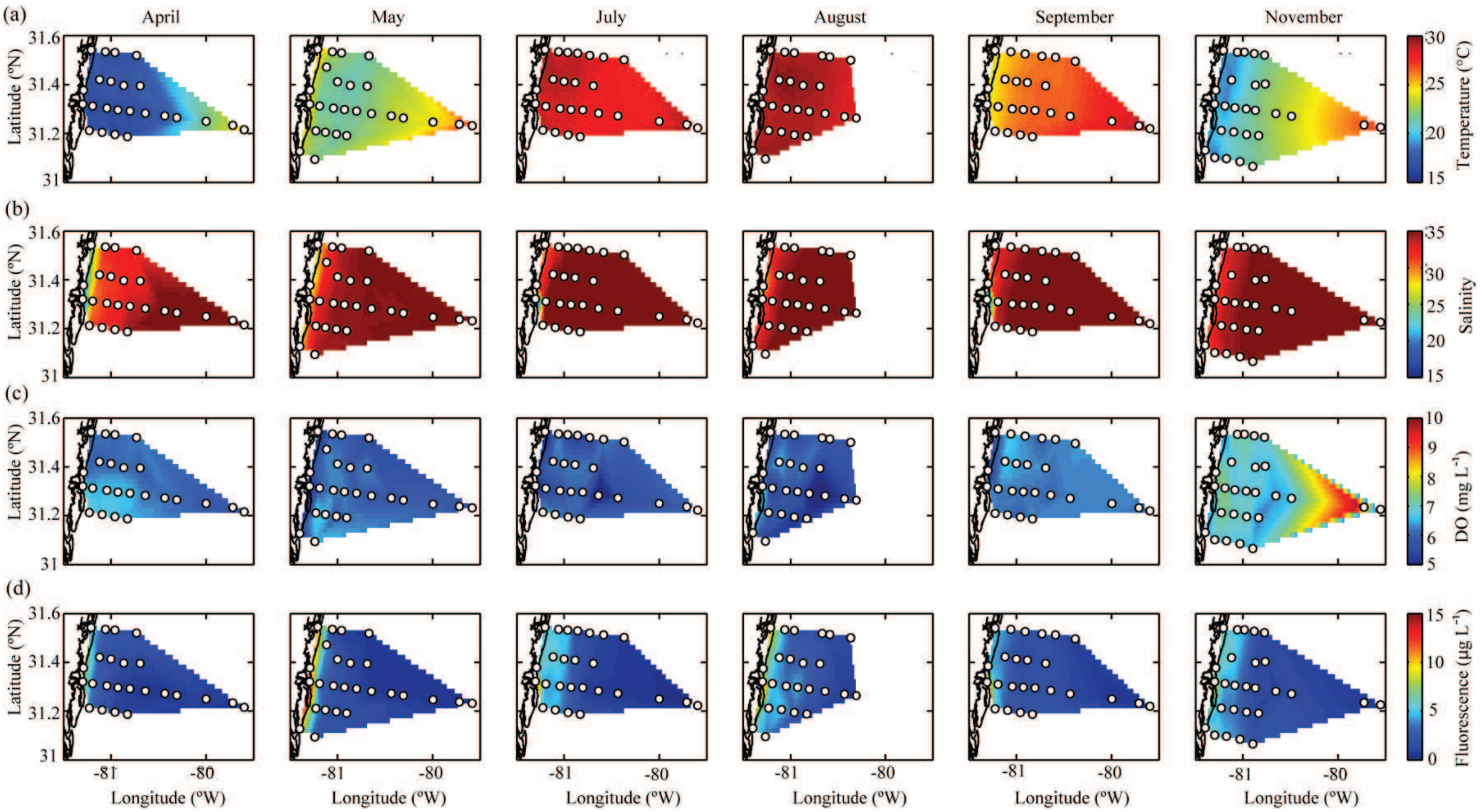
(a)
April
May
July
August
September
November
Temperature (°C)
30
25
20
15
(b)
Salinity
35
30
25
20
15
(c)
DO (mg L^{-1})
10
9
8
7
6
5
(d)
Fluorescence (µg L^{-1})
15
10
5
0
Latitude (°N)
31.6
31.4
31.2
31
Longitude (°W)
-81
-80

Fig. 4.2: Seasonal and spatial distributions of: a) Archaea *amoA*, b) Thaumarchaeota *rrs*, c) Betaproteobacteria *amoA* and d) *Nitrospina* sp.16S rRNA genes (copies L^{-1}); in surface waters on the continental shelf of the South Atlantic Bight. Dots indicate the sampling stations referenced to Appendix Figure B.1. Figures in each column represent environmental variables from the same sampling month. The means and ranges of each variable were listed in Table B.4.

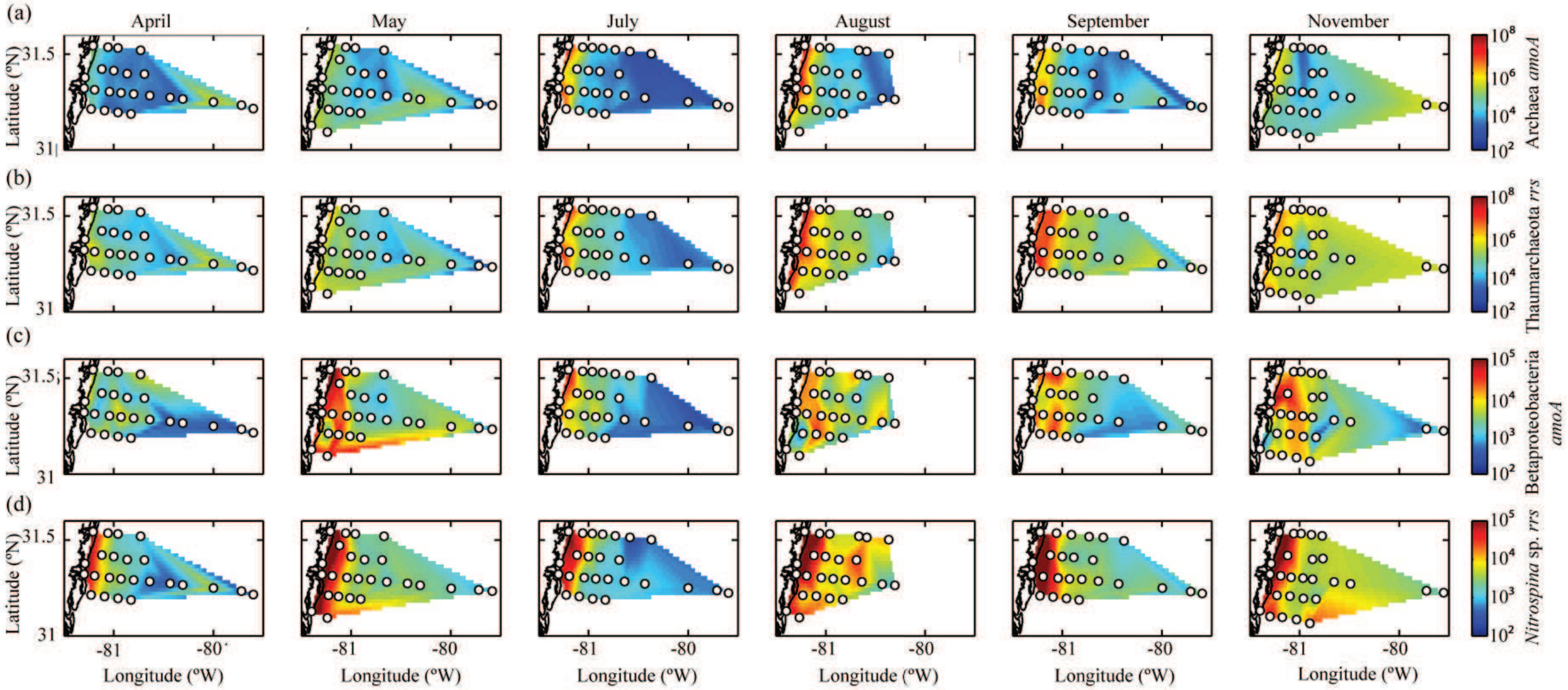
(a)
(b)
(c)
(d)
April
May
July
August
September
November
Latitude (°N)
31.5
31
-81
-80
Longitude (°W)
Archaea *amoA*
Thaumarchaeota *rrs*
Betaproteobacteria *amoA*
Nitrospina sp. *rrs*
10^8
10^6
10^5
10^4
10^3
10^2

Fig. 4.3: Relationships between a) Archaea *amoA* and Thaumarchaeota *rrs* genes abundances, and b) *Nitrospina* sp. 16S rRNA and Thaumarchaeota *rrs* genes abundances in the South Atlantic Bight. Lines are model II regressions (Legendre and Legendre 2012) of all data.

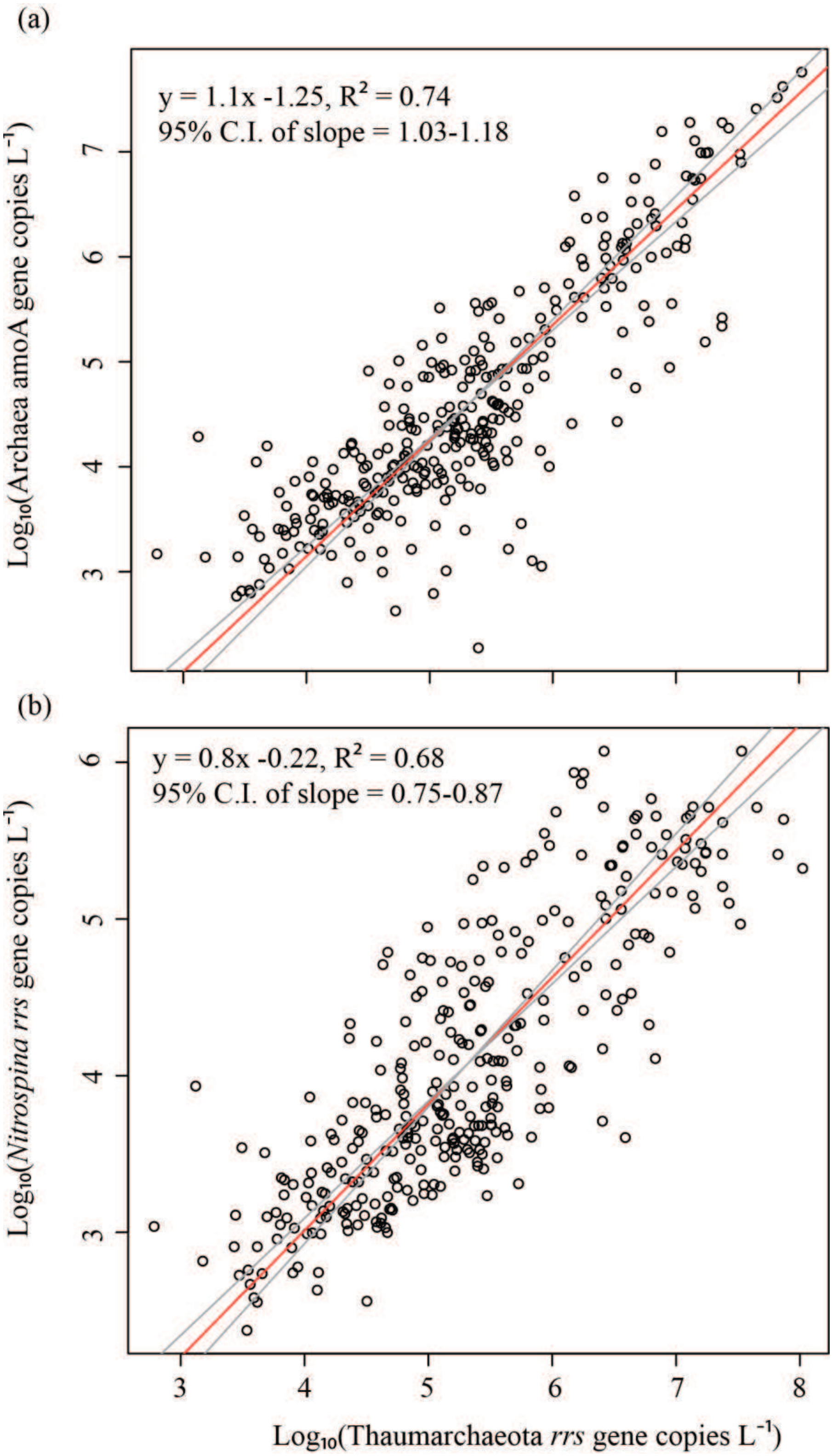
(a)
y = 1.1x -1.25, R² = 0.74
95% C.I. of slope = 1.03-1.18
Log10(Archaea amoA gene copies L-1)
3
4
5
6
7
(b)
y = 0.8x -0.22, R² = 0.68
95% C.I. of slope = 0.75-0.87
Log10(Nitrospina rrs gene copies L-1)
3
4
5
6
3
4
5
6
7
8
Log10(Thaumarchaeota rrs gene copies L-1)

Fig. 4.4: Vertical profiles of Archaea *amoA* (AOA), Thaumarchaeota *rrs* (T*rrs*), Betaproteobacteria *amoA* (AOB), *Nitrospina* sp. 16S rRNA (N*rrs*), environmental variables (temperature, salinity, fluorescence and dissolved oxygen) and nutrients (NO_2^-, NH_4^+ and NO_3^-) at the shelf-break Station C10 of the South Atlantic Bight in a) April, b) May, c) July, d) September and e) November.

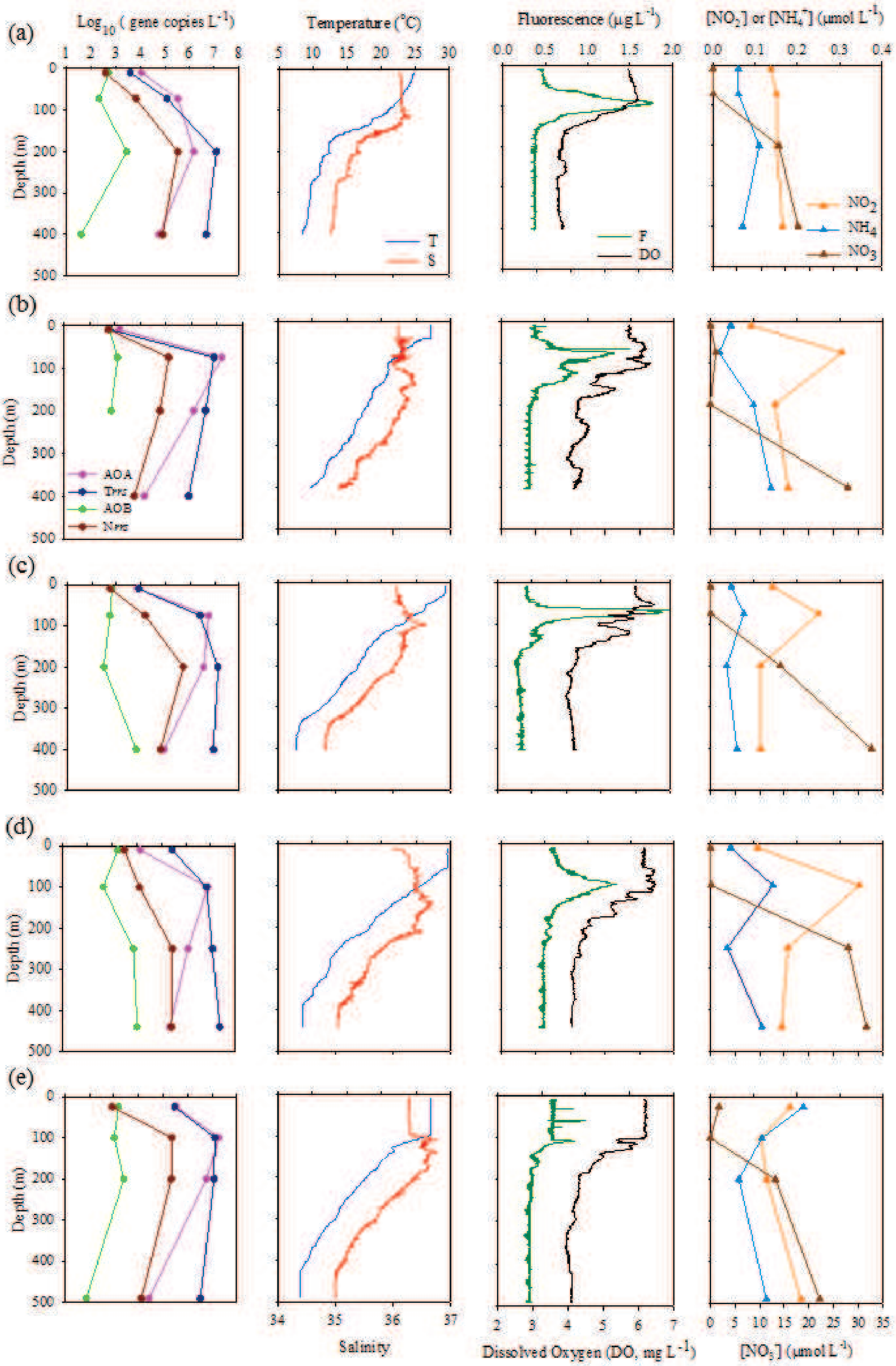
(a)
(b)
(c)
(d)
(e)
Log$_{10}$ (gene copies L^{-1})
1 2 3 4 5 6 7 8
Temperature (°C)
5 10 15 20 25 30
Fluorescence (μg L^{-1})
0.0 0.5 1.0 1.5 2.0
[NO$_2^-$] or [NH$_4^+$] (μmol L^{-1})
0.0 0.1 0.2 0.3 0.4
Depth (m)
0 100 200 300 400 500
T
S
F
DO
NO$_2$
NH$_4$
NO$_3$
AOA
Thrc
AOB
Nsrc
34 35 36 37
Salinity
2 3 4 5 6 7
Dissolved Oxygen (DO, mg L^{-1})
0 5 10 15 20 25 30 35
[NO$_3^-$] (μmol L^{-1})

Fig. 4.5: Ammonia oxidation rates measured (a) on the continental shelf, and (b) at 75 m, 200 m and 400 m of the shelf-break Station C10 of the South Atlantic Bight. Error bar in (a) indicates the standard deviation of ammonia oxidation rates measured in both surface and bottom waters of the stations in the same regions

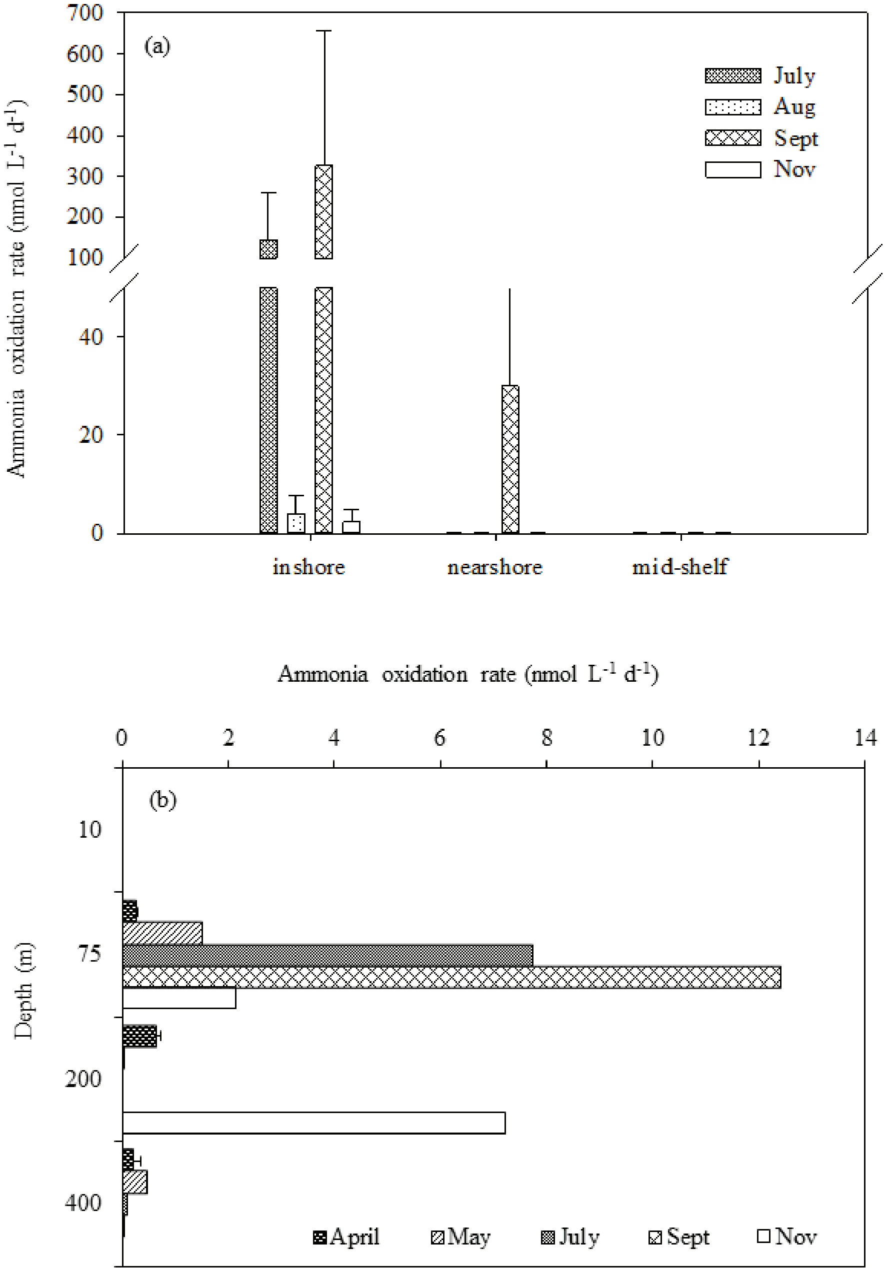
(a)
700
600
500
400
300
200
100
40
20
0
Ammonia oxidation rate (nmol L^{-1} d^{-1})
July
Aug
Sept
Nov
inshore
nearshore
mid-shelf
Ammonia oxidation rate (nmol L^{-1} d^{-1})
0
2
4
6
8
10
12
14
(b)
10
75
200
400
Depth (m)
April
May
July
Sept
Nov

Fig. 4.6. Spearman's rank correlations between ammonia oxidation rates and a) [NO_2^-], b) [NH_4^+] and c) Archaea *amoA* gene abundances. Correlation coefficients (R) are shown in each figure.

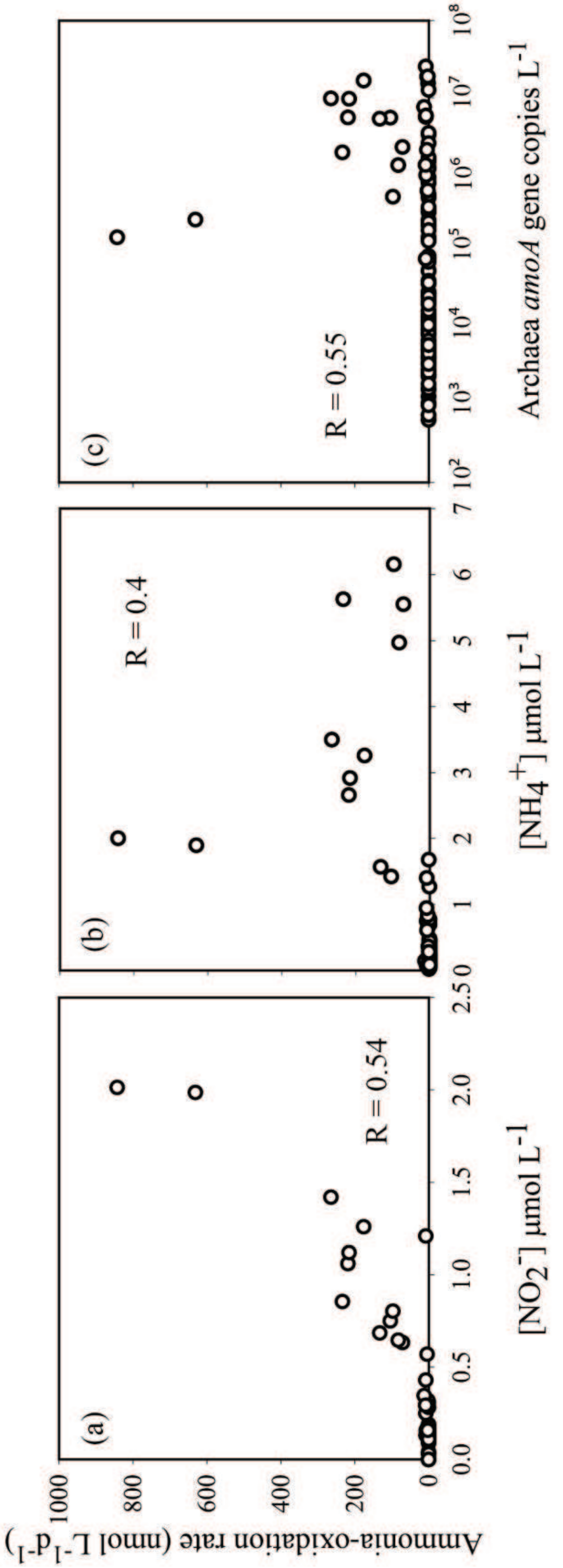
Ammonia-oxidation rate (nmol L-1d-1)
0
200
400
600
800
1000
(a)
R = 0.54
0.0
0.5
1.0
1.5
2.0
2.5
[NO2-] μmol L-1
(b)
R = 0.4
0
1
2
3
4
5
6
7
[NH4+] μmol L-1
(c)
R = 0.55
10²
10³
10⁴
10⁵
10⁶
10⁷
10⁸
Archaea amoA gene copies L-1

Fig. 4.7: Phylogenetic analysis of Archaea *amoA* genes recovered from DNA collected from surface waters of inshore stations SAPES, DOBES and ALTES, nearshore station C1, mid-shelf station C4, and from 10 m and 200 m at the shelf-break station C10. All samples were collected on the July cruise. The Bayesian tree was constructed using MrBayes 3.2.1 (Huelsenbeck and Ronquist 2001) based on an alignment of 586 unambiguous bp of *amoA* sequence with the HKY85 substitution model and the *Ca.* "Nitrososphaera gargensis" *amoA* gene as the outgroup. The posterior probabilities were shown if >0.75. a) Archaea *amoA* sequences we recovered that were assigned to 4 clades are highlighted with different branch colors: red, hot spring/soil group; green, water column group; dark red, water/sediment group; blue, open ocean group. The sub-trees of "open ocean group" show b) the shallow water ecotype "Cluster A" and c) the deep water ecotype "Cluster B" (after Francis et al. 2005). One representative of OTUs (≥ 98% identical) from each library was shown with the total number of clones represented by this sequence in the brackets.

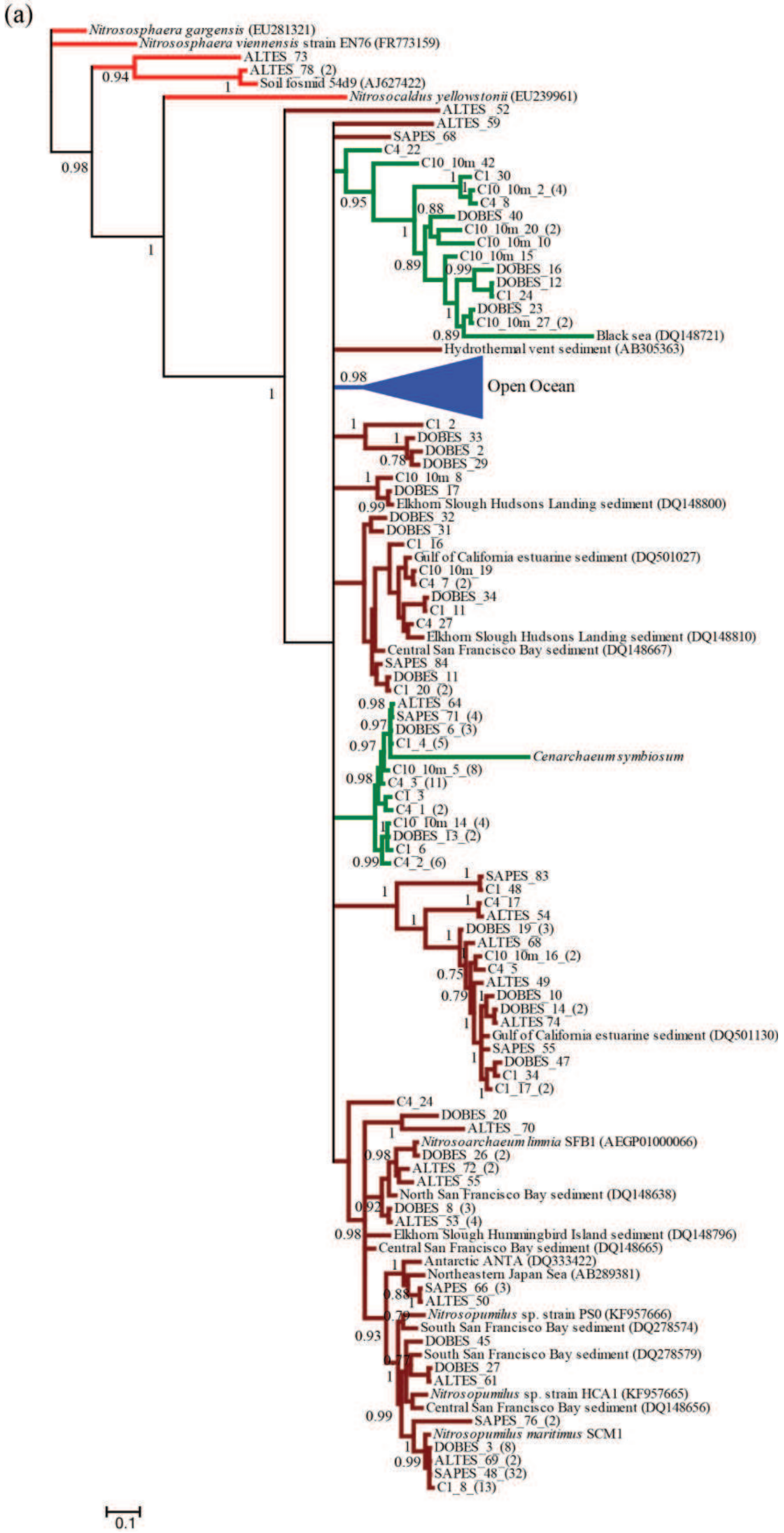
(a)
Nitrososphaera gargensis (EU281321)
Nitrososphaera viennensis strain EN76 (FR773159)
ALTES_73
0.94
ALTES_78_(2)
1
Soil fosmid 54d9 (AJ627422)
Nitrosocaldus yellowstonii (EU239961)
0.98
1
ALTES_52
ALTES_59
SAPES_68
C4_22
C10_10m_42
1
C1_30
1
C10_10m_2_(4)
0.95
C4_8
0.88
DOBES_40
1
C10_10m_20_(2)
C10_10m_10
C10_10m_15
0.89
0.99
DOBES_16
DOBES_12
C1_24
1
DOBES_23
C10_10m_27_(2)
0.89
Black sea (DQ148721)
Hydrothermal vent sediment (AB305363)
0.98
Open Ocean
1
1
C1_2
1
DOBES_33
DOBES_2
0.78
DOBES_29
1
C10_10m_8
DOBES_17
0.99
Elkhorn Slough Hudsons Landing sediment (DQ148800)
DOBES_32
DOBES_31
C1_16
Gulf of California estuarine sediment (DQ501027)
C10_10m_19
C4_7_(2)
DOBES_34
C1_11
C4_27
Elkhorn Slough Hudsons Landing sediment (DQ148810)
Central San Francisco Bay sediment (DQ148667)
SAPES_84
DOBES_11
C1_20_(2)
0.98
ALTES_64
SAPES_71_(4)
0.97
DOBES_6_(3)
0.97
C1_4_(5)
Cenarchaeum symbiosum
C10_10m_5_(8)
0.98
C4_3_(11)
C1_3
C4_1_(2)
C10_10m_14_(4)
1
DOBES_13_(2)
C1_6
0.99
C4_2_(6)
1
SAPES_83
1
C1_48
1
C4_17
1
ALTES_54
DOBES_19_(3)
1
ALTES_68
1
C10_10m_16_(2)
C4_5
0.75
ALTES_49
0.79
1
DOBES_10
DOBES_14_(2)
1
ALTES_74
Gulf of California estuarine sediment (DQ501130)
SAPES_55
1
DOBES_47
C1_34
1
C1_17_(2)
C4_24
DOBES_20
1
ALTES_70
Nitrosoarchaeum limnia SFB1 (AEGP01000066)
0.98
DOBES_26_(2)
ALTES_72_(2)
ALTES_55
North San Francisco Bay sediment (DQ148638)
0.92
DOBES_8_(3)
ALTES_53_(4)
0.98
Elkhorn Slough Hummingbird Island sediment (DQ148796)
Central San Francisco Bay sediment (DQ148665)
1
Antarctic ANTA (DQ333422)
Northeastern Japan Sea (AB289381)
0.88
SAPES_66_(3)
1
ALTES_50
0.79
Nitrosopumilus sp. strain PS0 (KF957666)
South San Francisco Bay sediment (DQ278574)
0.93
DOBES_45
South San Francisco Bay sediment (DQ278579)
0.77
DOBES_27
1
ALTES_61
Nitrosopumilus sp. strain HCA1 (KF957665)
Central San Francisco Bay sediment (DQ148656)
0.99
SAPES_76_(2)
Nitrosopumilus maritimus SCM1
1
DOBES_3_(8)
0.99
ALTES_69_(2)
SAPES_48_(32)
C1_8_(13)
0.1

(b)

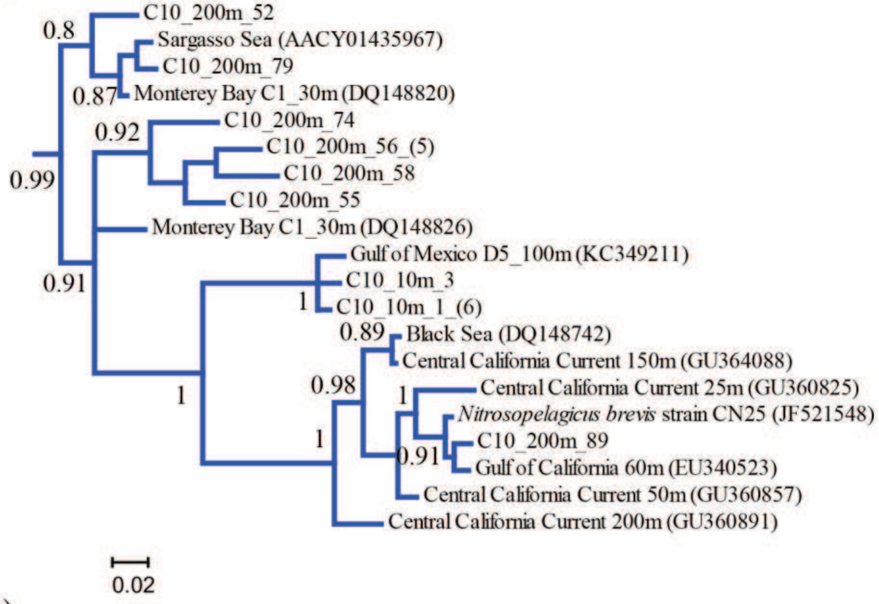
C10_200m_52
0.8
Sargasso Sea (AACY01435967)
C10_200m_79
0.87
Monterey Bay C1_30m (DQ148820)
C10_200m_74
0.92
C10_200m_56_(5)
C10_200m_58
0.99
C10_200m_55
Monterey Bay C1_30m (DQ148826)
Gulf of Mexico D5_100m (KC349211)
0.91
C10_10m_3
1
C10_10m_1_(6)
0.89
Black Sea (DQ148742)
Central California Current 150m (GU364088)
0.98
Central California Current 25m (GU360825)
1
1
Nitrosopelagicus brevis strain CN25 (JF521548)
1
C10_200m_89
0.91
Gulf of California 60m (EU340523)
Central California Current 50m (GU360857)
Central California Current 200m (GU360891)
0.02

(c)

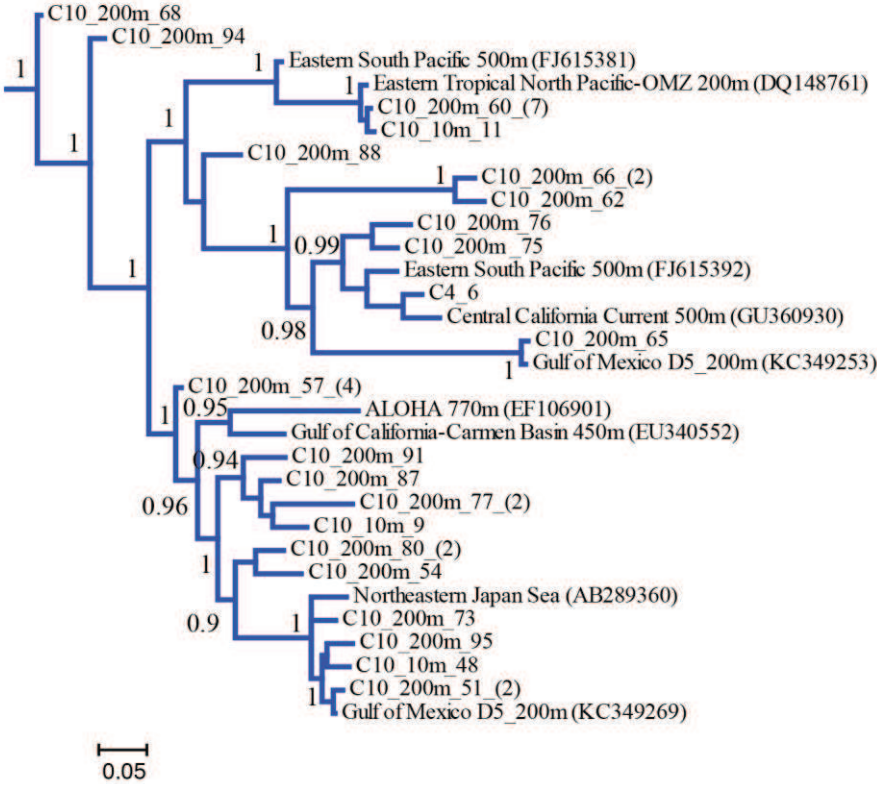
C10_200m_68
C10_200m_94
1
1
Eastern South Pacific 500m (FJ615381)
1
Eastern Tropical North Pacific-OMZ 200m (DQ148761)
C10_200m_60_(7)
1
C10_10m_11
1
C10_200m_88
1
C10_200m_66_(2)
C10_200m_62
1
C10_200m_76
0.99
C10_200m_75
Eastern South Pacific 500m (FJ615392)
C4_6
Central California Current 500m (GU360930)
0.98
C10_200m_65
1
Gulf of Mexico D5_200m (KC349253)
C10_200m_57_(4)
1
0.95
ALOHA 770m (EF106901)
Gulf of California-Carmen Basin 450m (EU340552)
0.94
C10_200m_91
C10_200m_87
0.96
C10_200m_77_(2)
C10_10m_9
C10_200m_80_(2)
1
C10_200m_54
Northeastern Japan Sea (AB289360)
0.9
1
C10_200m_73
C10_200m_95
C10_10m_48
C10_200m_51_(2)
1
Gulf of Mexico D5_200m (KC349269)
0.05

Fig. 4.8: Phylogenetic analysis of Thaumarchaeota 16S rRNA genes recovered from DNA collected from surface waters of inshore stations SAPES, DOBES and ALTES, nearshore station C1, mid-shelf station C4, and from 10 m and 200 m at the shelf-break station C10. All samples were collected on the July cruise. The Bayesian tree was constructed using MrBayes 3.2.1 (Huelsenbeck and Ronquist 2001) based on the alignment of 474 unambiguous bp of sequence with the HKY85 substitution model and the "pSL12_ (UCU63343)" 16S rRNA gene as the outgroup. The posterior probabilities were shown if >0.75. Thaumarchaeota *rrs* sequences retrieved from shelf-break Sta. C10 (10 m and 200 m) were in blue, while those from inshore to mid-shelf stations were in dark red. One representative of OTUs (≥ 99% identical) from each library was shown with the total number of clones represented by this sequence in the brackets.

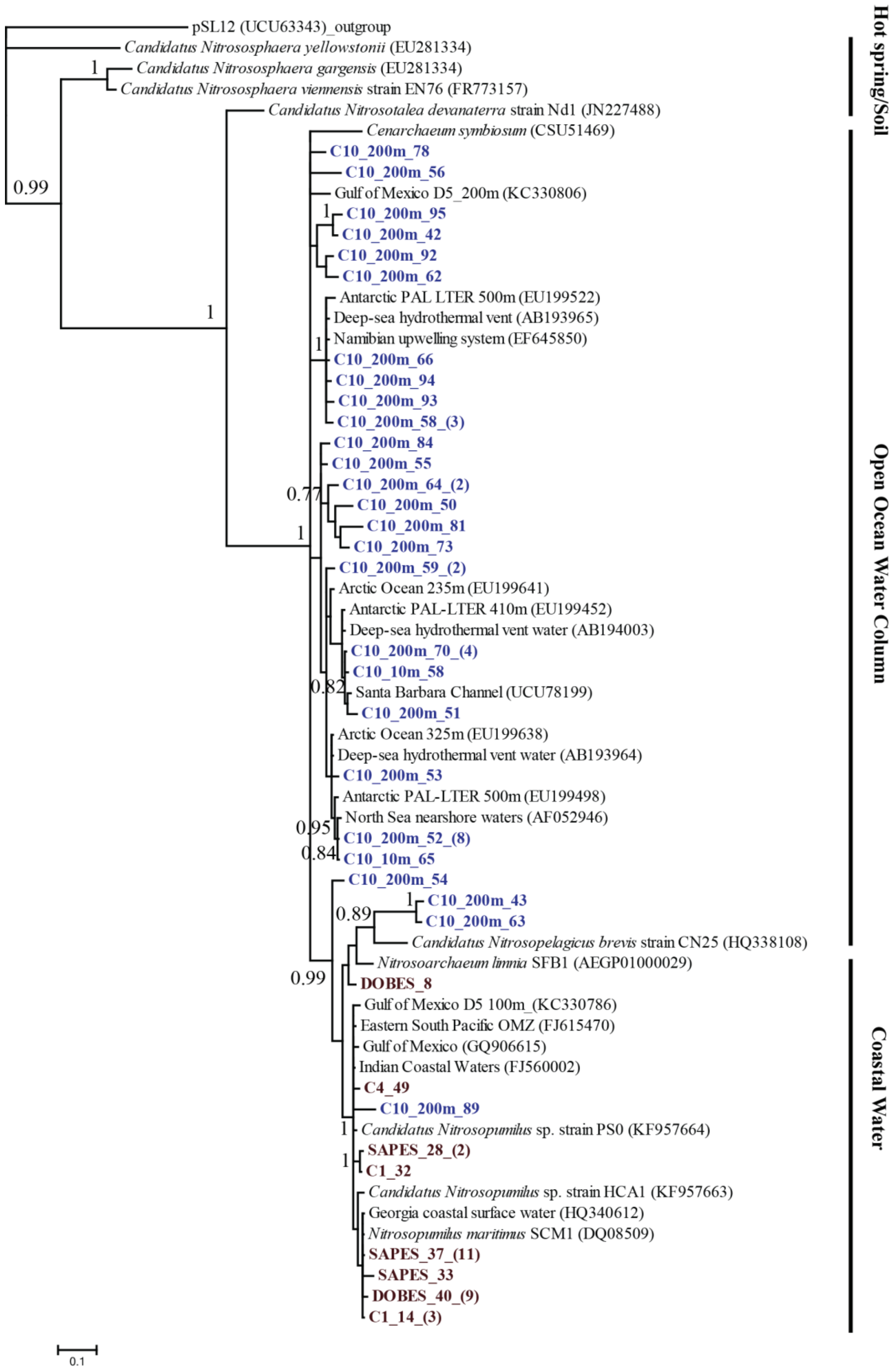
pSL12 (UCU63343)_outgroup
Candidatus Nitrososphaera yellowstonii (EU281334)
Candidatus Nitrososphaera gargensis (EU281334)
Candidatus Nitrososphaera viennensis strain EN76 (FR773157)
Candidatus Nitrosotalea devanaterra strain Nd1 (JN227488)
Cenarchaeum symbiosum (CSU51469)
C10_200m_78
C10_200m_56
Gulf of Mexico D5_200m (KC330806)
C10_200m_95
C10_200m_42
C10_200m_92
C10_200m_62
Antarctic PAL LTER 500m (EU199522)
Deep-sea hydrothermal vent (AB193965)
Namibian upwelling system (EF645850)
C10_200m_66
C10_200m_94
C10_200m_93
C10_200m_58_(3)
C10_200m_84
C10_200m_55
C10_200m_64_(2)
C10_200m_50
C10_200m_81
C10_200m_73
C10_200m_59_(2)
Arctic Ocean 235m (EU199641)
Antarctic PAL-LTER 410m (EU199452)
Deep-sea hydrothermal vent water (AB194003)
C10_200m_70_(4)
C10_10m_58
Santa Barbara Channel (UCU78199)
C10_200m_51
Arctic Ocean 325m (EU199638)
Deep-sea hydrothermal vent water (AB193964)
C10_200m_53
Antarctic PAL-LTER 500m (EU199498)
North Sea nearshore waters (AF052946)
C10_200m_52_(8)
C10_10m_65
C10_200m_54
C10_200m_43
C10_200m_63
Candidatus Nitrosopelagicus brevis strain CN25 (HQ338108)
Nitrosoarchaeum limnia SFB1 (AEGP01000029)
DOBES_8
Gulf of Mexico D5 100m_(KC330786)
Eastern South Pacific OMZ (FJ615470)
Gulf of Mexico (GQ906615)
Indian Coastal Waters (FJ560002)
C4_49
C10_200m_89
Candidatus Nitrosopumilus sp. strain PS0 (KF957664)
SAPES_28_(2)
C1_32
Candidatus Nitrosopumilus sp. strain HCA1 (KF957663)
Georgia coastal surface water (HQ340612)
Nitrosopumilus maritimus SCM1 (DQ08509)
SAPES_37_(11)
SAPES_33
DOBES_40_(9)
C1_14_(3)
1
0.99
1
1
0.77
1
1
0.82
0.95
0.84
1
0.89
0.99
1
1
0.1
Hot spring/Soil
Open Ocean Water Column
Coastal Water

Fig. 4.9: Redundancy analysis (RDA) ordination plots of a) Thaumarchaeota 16S rRNA and Archaea *amoA* genes versus environmental factors in the surface waters of the SAB; and b) Thaumarchaeota 16S rRNA and Archaea *amoA* versus environmental factors with depth at the shelf-break station. The length and angle of arrows show the contribution of each variable to the RDA axes. RF, relative fluorescence; T, temperature; S, salinity; DO, dissolved oxygen concentration; Bacteria 16S, Bacteria 16S rRNA gene abundance*; rrs,* Thaumarchaeota 16S rRNA gene abundance*; amoA,* Archaea *amoA* gene abundance.

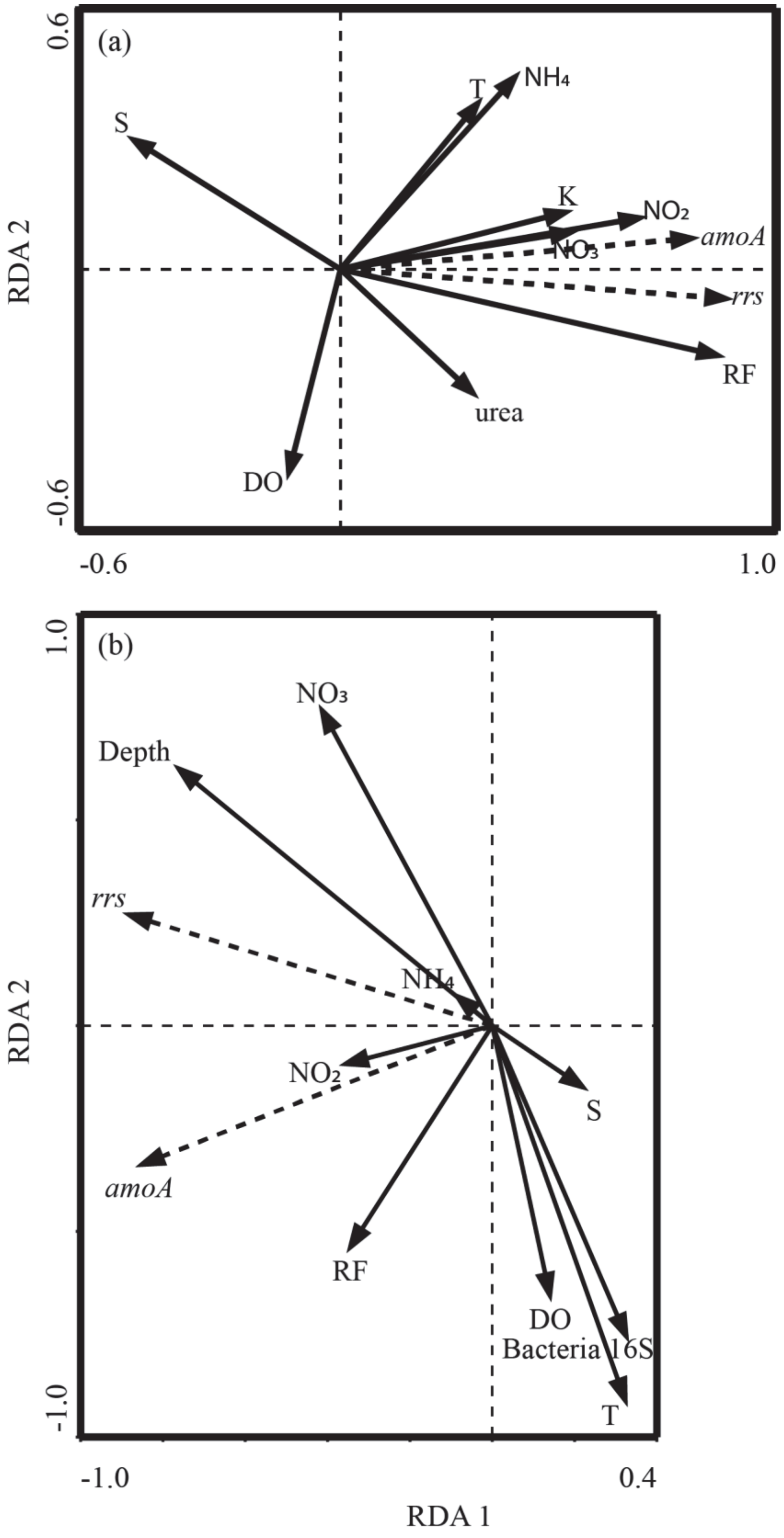
(a)
0.6
-0.6
RDA 2
-0.6
1.0
S
T
NH₄
K
NO₂
NO₃
amoA
rrs
RF
urea
DO
(b)
1.0
-1.0
RDA 2
-1.0
0.4
RDA 1
NO₃
Depth
rrs
NH₄
NO₂
amoA
S
RF
DO
Bacteria 16S
T

CHAPTER 5

CONCLUSIONS

I have investigated the dynamics and metabolism of polyamines in a marine ecosystem, the South Atlantic Bight. The experiments were divided into two areas of concentration, one focused on determining the spatial and temporal variability of polyamine fluxes in the SAB and the contribution of polyamine C and N to bacterioplankton C and N demand there; and the second focused on laboratory investigations of polyamine synthesis, release and uptake by phytoplankton. I collected samples from inner shelf to the shelf-break of the SAB during two cruises (April and October 2011) and from SAB estuaries during August 2011 and April 2012. I conducted experiments with radio-labeled polyamines to determine the turnover rates of polyamines *in situ* in different water mass and I calculated polyamine uptake rates by multiplying turnover rates with *in situ* polyamine concentrations, measured by high performance liquid chromatograph (HPLC). The contribution of polyamines to bacterial C and N demands were estimated by dividing bacterial C and N assimilated from polyamines by the total bacterial C and N demand, estimated from L-leucine incorporation, respectively.

The goal of the second study was to identify the factors governing polyamine dynamics in seawater, specifically production of dissolved polyamines by phytoplankton. I selected representative phytoplankton species from the ocean and measured the concentrations and composition of polyamines in axenic phytoplankton cultures. We manipulated experimental conditions in order to track the responses of intracellular and extracellular polyamine pools to the environmental variables and attempted to connect the results with the field observations.

This dissertation makes several key contributions to our understanding of the role of small dissolved organic nitrogen compounds in oceanic environments.

Firstly, we found that all polyamines we examined (PUT: putrescine, SPD: spermidine and SPM: spermine) can be readily used by bacterioplankton and their roles are similar to dissolved free amino acids (DFAA), supplying nutrients and energy to bacterioplankton. They have comparable turnover rates to DFAA, but the dissolved pools (mostly < 5 nmol L^{-1}) were much smaller than DFAA (10- to 100-fold), resulting in relatively slow uptake fluxes in seawater. The dynamics of polyamines were compound-specific and varied spatially and temporally in the SAB. PUT and SPD were commonly detected, while SPM was sporadically distributed. SPD and SPM were better substrates for bacterioplankton than PUT according to their higher turnover rates. In contrast to their consistently low concentrations, polyamines turned over more rapidly at inner-shelf and estuarine stations in the SAB, leading to the much greater fluxes at those sites than at mid-shelf and shelf-break stations, and rates were about 2-fold greater in spring than in fall. This study also evaluated the fate of polyamine carbon after being assimilated and I concluded that carbon was mostly incorporated into biomass (> 50%), but the short incubation time (~1h) may underestimate the carbon respired from polyamines. I estimated the proportions of bacterial N and C demand contributed met by polyamines. Polyamines could potentially provide more N (≤ 10%) than C (≤ 5%) to bacterial demand, and this contribution seemed to be more important in the offshore water column with relatively low nutrient concentrations. Correlations between polyamine turnover or uptake rates with environmental variables suggested that the spatial and temporal variability of polyamine dynamics was significantly associated with phytoplankton biomass. This differed from DFAA which was more closely tied to bacterial production. This suggested that phytoplankton, the sources of polyamines, were in charge of controlling the bacterial uptake of polyamines.

Secondly, my research on the metabolism of polyamines in phytoplankton cells suggested that the variability of polyamine composition and concentrations in seawater was a consequence of species specific variation in the composition and concentration of polyamines in phytoplankton, modulated by environmental conditions like nutrient limitation and salinity. This work demonstrated that polyamine release to the water by phytoplankton was affected by their physiological conditions. I also demonstrated the capability of phytoplankton to take up dissolved polyamines from culture medium at nM concentrations. I found a strong connection between polyamine metabolism and diatom cell wall synthesis. Polyamines accumulated in *Thalassiosira pseudonana* during the late stationary phase, in contrast to their dynamics in other groups, such as dinoflagellates. This was explained as a consequence of low polyamine demands for building diatom silica cell walls once growth had ceased. Thus, in seawater, bloom terminations may contribute a significant amount of polyamines into the dissolved polyamine pools.

I detected changes of polyamine pools in response to different environmental or nutrient limitations, which may be helpful to explain the correlations between polyamine dynamics and environmental variables (e.g. T, S) in field observations. The internal and external polyamine pools co-varied and increased as temperature increased or salinity decreased. Polyamine release was enhanced under N-limitation, a common situation in the ocean, and the composition of dissolved polyamine pools changed from being dominated by NSPD to SPD, although SPD was only a minor component of the intracellular pool. Thus, the changes in size and composition of dissolved polyamine pool under different conditions may directly affect the polyamine availability to bacterioplankton.

I also tested the ability of the diatom *T. pseudonana* to take up polyamines under two salinity conditions (22 vs 32) and nitrate concentrations (20 vs 50 µmol L^{-1}). The results of these experiments suggested a potential for phytoplankton to use polyamines in seawater and that uptake was controlled by environmental and nutrient conditions. This finding complicates the relationship between polyamine concentrations found *in situ* and phytoplankton. Several factors, including selective release from phytoplankton, environmental conditions and nutrient limitation, and the preferential uptake of specific polyamines by bacteria and phytoplankton, all need to be considered.

Last but not least, polyamine dynamics are further complicated by the potential oxidation of polyamines by ammonia-oxidizing Archaea (Thaumarchaeota). I surveyed the abundances of Thaumarchaeota and measured the ammonia oxidation rates to estimate the activities of Thaumarchaeota in the SAB. I concluded that Thaumarchaeota are an important group of microorganisms in the SAB, and they are the major ammonia-oxidizer there. They were prevalent (16S rRNA and Archaea *amoA* genes typically > 10^4 gene copies L^{-1}) in the water column from inshore to offshore. A mid-summer peak in abundance (up to 10^8 gene copies L^{-1}) was restricted to inshore and nearshore stations. Thaumarchaeota were also abundant and varied little throughout the year (~ 10^6-10^7 gene copies L^{-1}) at the bottom of euphotic zone at the shelf-break. Thaumarchaeota abundance covaried with depth, chlorophyll a, temperature and salinity.

High ammonia oxidation rates (0.6-842 nmol $L^{-1}d^{-1}$) were seen at inshore and nearshore stations during summer and at the bottom euphotic zone of the shelf-break (0.3-12 nmol $L^{-1}d^{-1}$), and ammonia oxidation was slower (undetectable to 0.64 nmol $L^{-1}d^{-1}$) in other regions. The availability of the substrate (NH_4^+) may be the key factor driving ammonia-oxidation rates.

We analyzed the phylogeny of Thaumarchaeota 16S rRNA genes in different water mass and found that the inshore and shelf-break populations contained distinct species. Sequences of *amoA* genes from these two populations were also different from those retrieved from mid-shelf surface waters. Thus, differences in the capability for ammonia oxidation by different Thaumarchaeota species may also influence nitrification rates in seawater. Since preliminary experiments performed in 2011 showed that polyamines were oxidized to produce nitrite faster than ammonium, my survey of Thaumarchaeota abundance and ammonia oxidation rates suggests that polyamine oxidation by Thaumarchaeota may be as important as bacterial uptake in limiting polyamine concentrations in seawater. If it is assumed that polyamine oxidation was similar to ammonia oxidation by Thaumarchaeota, polyamine oxidation rates would be higher in summer (up to hundreds of nmol $L^{-1}d^{-1}$ in inshore waters) and lower in spring (undetectable to 1.3 nmol $L^{-1}d^{-1}$) and fall (undetectable to 7 nmol $L^{-1}d^{-1}$; Tolar 2014, chapter 4). In comparison to polyamine uptake rates I measured during 2011 cruises, which ranged from undetectable in offshore waters to ~15 nmol $L^{-1}d^{-1}$ in inshore waters during April and October (chapter 2), the polyamine oxidation rates are in the same range of polyamine uptake rates during April but are 1-2 orders of magnitude larger than polyamine uptake rates at the beginning of October. It suggests that Thaumarchaeota may be majorly responsible for polyamine removal in summer. Moreover, Thaumarchaeota may play a more important role in removing polyamines at the base of mixing layer because of their high abundances and activity in oxidizing ammonia (0.6-12.4 nmol $L^{-1}d^{-1}$) compared with low polyamine uptake rates (< 0.15 nmol $L^{-1}d^{-1}$) there.

In summary, this dissertation provides insights into the dynamics of polyamine from different perspectives. It determined the role of heterotrophic bacteria and photosynthetic phytoplankton in polyamine cycling and identified environmental variables that affect the activity of these groups. I have also raised the potential for control of polyamine dynamics by ammonia-oxidizing Archaea in the SAB.

APPENDIX A

SUPPLEMENTARY MATERIAL: CONCENTRATIONS, TURNOVER RATES AND FLUXES OF POLYAMINES IN COASTAL WATERS OF THE SOUTH ATLANTIC BIGHT[4]

---

[4] Liu, Q., X.X. Lu, B.B. Tolar, X. Mou, and J.T. Hollibaugh. 2015. Biogeochemistry. 123:117-133. Reprinted here with permission of publisher.

Table A.1: Details of stations sampled during April and October cruises, 2011.

Station	Latitude (ºN)	Longitude (ºW)	April		October		Description
			Depth (m)	Time (h)	Depth (m)	Time (h)	
1	32.039	-80.922	-	-	1.5, 13	9:00	Savannah Harbor
2	31.925	-80.967	1.6, 11.8	12:30	-	-	Wassaw Sound
3	31.299	-81.199	2, 6	17:30	4, 11	20:50	Altamaha Plume
4	30.718	-81.356	1.5, 13	23:00	4, 9	16:00	St. Mary's
5	31.670	-80.142	3, 32	19:00	-	-	Savannah Middle Shelf
6	31.271	-80.379	3, 34	10:00	4, 30	17:20	Gray's Middle Shelf
7	31.025	-80.521	2, 27.5	20:45	4, 27	2:00	Altamaha Middle Shelf
8	30.523	-80.712	2, 30.5	03:20	4, 32	11:40	St. Mary's Middle Shelf
9	31.391	-79.338	10, 75, 433	21:40	-	-	Savannah Offshore
10	31.055	-79.553	-	-	4, 80, 250	12:20	Gray's Offshore
11	30.727	-79.760	10, 60, 470	14:35	4, 80, 250	08:40	Altamaha Offshore
12	30.305	-79.933	10, 70, 500	21:40	20, 80, 200	05:50	St. Mary's Offshore
GR	31.425	-80.863	3, 18.5	14:15	4, 17	18:15	Gray's Reef

Table A.2: Weighting coefficients of variables contributing to principal components axes.

Variable	April			October		
	PC1	**PC2**	**PC3**	**PC1**	**PC2**	**PC3**
Temperature (ºC)	0.07	0.77	-0.16	0.49	-0.06	0.04
Salinity	0.50	0.002	-0.34	0.34	0.52	-0.55
Attenuation Coefficient (K)	-0.46	-0.02	-0.19	-0.49	-0.005	0.16
Dissolved Oxygen (mg L^{-1})	0.31	-0.62	-0.13	-0.07	0.76	0.16
Relative Fluorescence (mg m^{-3})	-0.51	-0.14	0.05	-0.44	0.35	0.21
Bacterial 16S	-0.36	-0.07	-0.9	-0.46	-0.13	-0.77

Table A.3: RDA analysis of relationships between turnover rates, concentrations and uptake rates of polyamines and amino acids and environmental conditions in the SAB.

Axes	RDA 1	RDA 2	RDA 3	RDA 4
		Turnover rate		
Eigenvalues	0.72	0.04	0.015	0.004
Turnover-environment correlations	0.93	0.633	0.649	0.447
Cumulative percentage variance				
of turnover data	72.0	76.0	77.5	77.9
of species-environment relationship	92.4	97.5	99.4	99.9
		Concentration		
Eigenvalues	0.178	0.077	0.493	0.252
Concentration-environment correlations	0.631	0.374	0*	0
Cumulative percentage variance				
of concentration data	17.8	25.5	74.8	100
of concentration-environment relationship	69.8	100	0	0
		Uptake rate		
Eigenvalues	0.823	0.021	0.129	0.026
Uptake-environment correlations	0.933	0.620	0	0
Cumulative percentage variance				
of uptake data	82.3	84.4	97.4	100
of uptake-environment relationship	97.5	100	0	0

* Values of 0 for the species-environment relationships mean that eigenvalues were not canonical, since there were only 2 species. In these cases only RDA 1 and RDA 2 were used to draw biplots for the species-environment relationships (Fig. 2.6)

Figure A.1: (a) Stations sampled during April (18-22) and October (2-6) cruises in the South Atlantic Bight (SAB). Stations visited on both cruises are represented with diamonds (purple); stations visited only on the April cruise represented with squares (blue) and those visited only on the October cruise represented with circles (red). (b) GCE-LTER sites located on the central Georgia coast and bounded on the east by the SAB. Samples were collected from the Sapelo Sound (SP, GCE 1, 2 and 3), Marsh Landing (ML) and Altamaha Sound (AL, GCE 7, 8 and 9) during 13-16 August 2011 and 17-20 April 2012

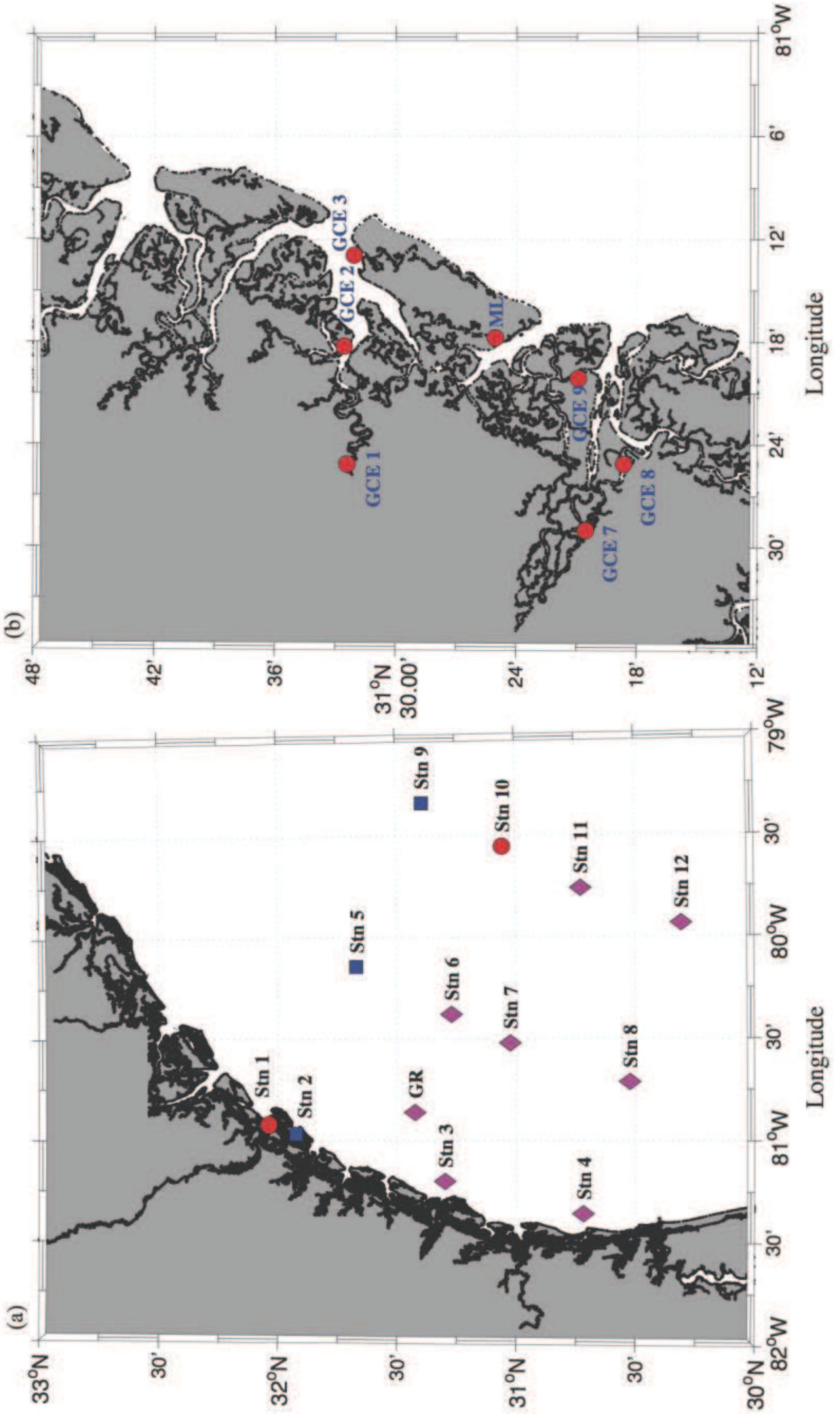
(a)
33°N
30'
32°N
30'
31°N
30'
30°N
Latitude
82°W
30'
81°W
30'
80°W
30'
79°W
Longitude
Stn 1
Stn 2
Stn 3
Stn 4
Stn 5
Stn 6
Stn 7
Stn 8
Stn 9
Stn 10
Stn 11
Stn 12
GR
(b)
48'
42'
36'
31°N 30.00'
24'
18'
12'
30'
24'
18'
12'
6'
81°W
Longitude
GCE 1
GCE 2
GCE 3
ML
GCE 7
GCE 8
GCE 9

Figure A. 2: Relative fluorescence (mg m^{-3}), concentrations of biogenic silica (BSi, µmol L^{-1}), L-leucine incorporation rates (LEU, pmol h^{-1} L^{-1}) and bacterial 16S rRNA gene abundance (copies L^{-1}) in samples collected on the April (a, b) and October (c, d) cruises. *Numbers* on the abscissa identify the station as per Fig. A.1a. *SW* surface water, *MW* mid-water, *BW* bottom water

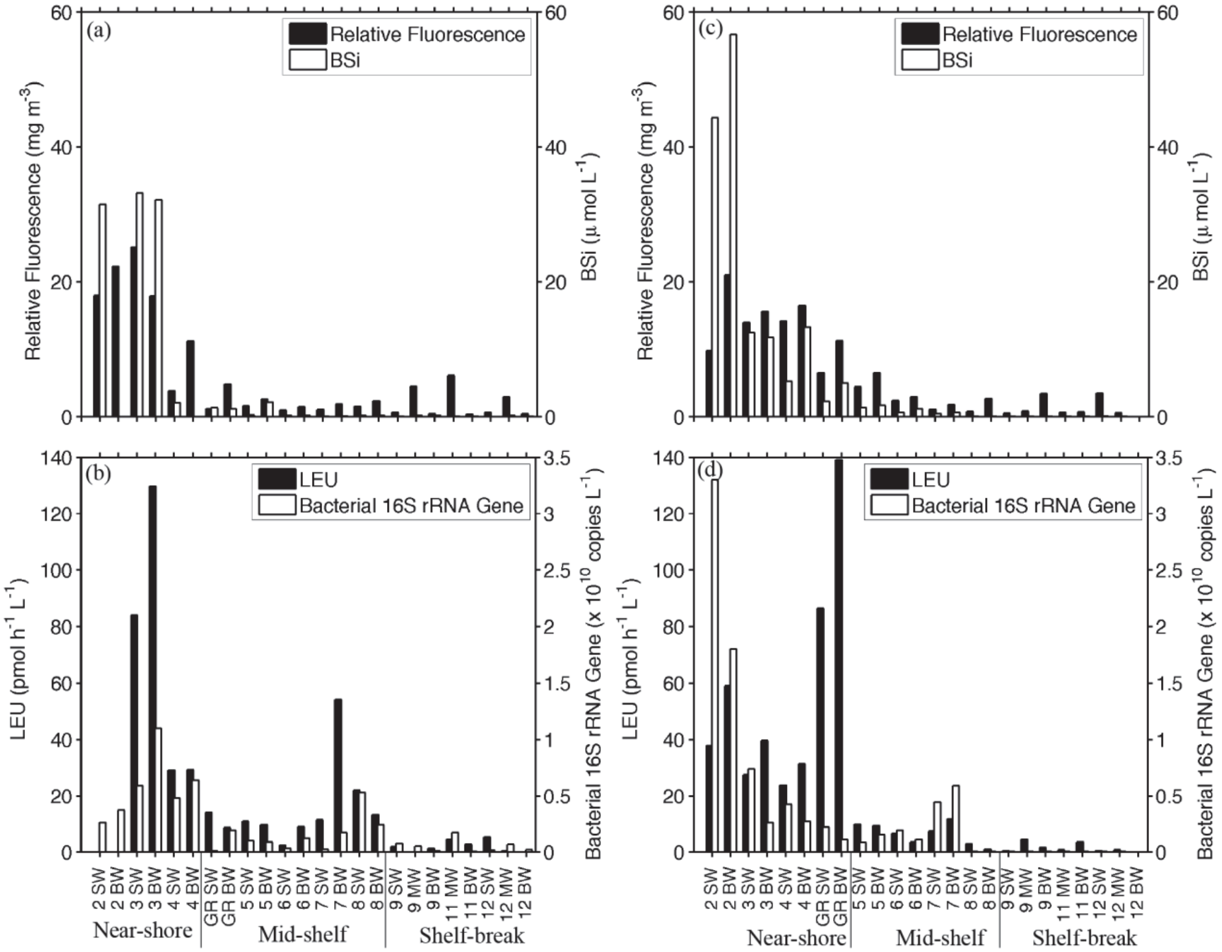
(a)
Relative Fluorescence
BSi
Relative Fluorescence (mg m^{-3})
BSi (μ mol L^{-1})
0
20
40
60
(b)
LEU
Bacterial 16S rRNA Gene
LEU (pmol h^{-1} L^{-1})
Bacterial 16S rRNA Gene (x 10^{10} copies L^{-1})
0
20
40
60
80
100
120
140
0
0.5
1
1.5
2
2.5
3
3.5
2 SW
2 BW
3 SW
3 BW
4 SW
4 BW
GR SW
GR BW
5 SW
5 BW
6 SW
6 BW
7 SW
7 BW
8 SW
8 BW
9 SW
9 MW
9 BW
11 MW
11 BW
12 SW
12 MW
12 BW
Near-shore
Mid-shelf
Shelf-break
(c)
Relative Fluorescence
BSi
Relative Fluorescence (mg m^{-3})
BSi (μ mol L^{-1})
0
20
40
60
(d)
LEU
Bacterial 16S rRNA Gene
LEU (pmol h^{-1} L^{-1})
Bacterial 16S rRNA Gene (x 10^{10} copies L^{-1})
0
20
40
60
80
100
120
140
0
0.5
1
1.5
2
2.5
3
3.5
2 SW
2 BW
3 SW
3 BW
4 SW
4 BW
GR SW
GR BW
5 SW
5 BW
6 SW
6 BW
7 SW
7 BW
8 SW
8 BW
9 SW
9 MW
9 BW
11 MW
11 BW
12 SW
12 MW
12 BW
Near-shore
Mid-shelf
Shelf-break

APPENDIX B

SUPPLEMENTARY MATERIAL: SEASONAL VARIABILITY OF AMMONIA-OXIDIZING ARCHAEA AND AMMONIA-OXIDATION RATES AT THE SOUTH ATLANTIC BIGHT[5]

---

[5] Liu, Q., B.B. Tolar, M.J. Ross, J.B. Cheek, C.M. Sweeney, N.J. Wallsgrove, B.N. Popp, and J.T. Hollibaugh. To be submitted to *Limnology and Oceanography*.

Table B.1: Details of stations during all cruises, 2014. SS, Saint Simons; ALTES, Altamaha Sound; DOBES, Doboy Sounds; SAPES, Sapelo Sound

Region	Site	Latitude (°N)	Longitude (°W)	April		May		July		August		September		November	
				Depth	Time	Depth	Time	Depth	Time	Depth	Time	Depth	Time	Depth	Time
Inshore	SS	31.12746	-81.39836	-	-	2, 9	9:21	-	-	1, 5	19:29	-	-	1, 8	14:56
	ALTES	31.3203	-81.29596	1, 6	10:12	2, 7	9:06	1, 6	7:41	1, 7	16:27	2, 4	16:02	1, 7	18:21
	DOBES	31.37766	-81.28818	1, 14	8:24	2, 17	10:41	2, 10	21:34	1, 10	11:38	1, 8	21:40	1, 10	19:56
	SAPES	31.54262	-81.20922	1, 7	18:09	2, 8	13:21	1,10	18:56	1, 9	20:11	1, 9	20:59	1, 9	21:47
Nearshore	SS1	31.09304	-81.24106	-	-	2,10	14:22	-	-	2, 9	20:31	-	-	1, 7	3:01
	SS2	31.09628	-81.17394	-	-	-	-	-	-	-	-	-	-	1,11	1:57
	A1	31.21216	-81.22748	1, 7	18:45	2, 8	15:52	2, 9	15:21	2, 9	21:45	2, 11	14:11	1, 8	20:03
	A2	31.20534	-81.09502	2, 14	20:26	2,10	17:09	2, 12	17:23	2, 13	22:48	2, 13	15:56	2, 14	18:55
	C1	31.312	-81.19178	2, 8	7:48	2, 10	2:16	2, 9	5:00	2, 11	3:45	1, 9	1:33	1.1, -	13:24
	C2	31.30312	-81.04404	2, 13	9:35	2, 14	0:32	1, 12	6:43	1, 13	5:47	2, 12	3:09	1, 11	14:50
	E1	31.42142	-81.11868	2, 10	1:06	1, 4	4:41	2, 7	19:28	2, 10	19:13	2, 10	11:12	1, -	12:09
	E2	31.41282	-81.00194	2, 13	2:21	2, 12	6:08	2, 12	20:49	2, 14	20:30	2, 13	12:34	1, 10	11:04
	G1	31.5344	-81.05756	2, 9	16:12	2, 10	14:51	2,10	10:42	2, 8	10:16	2, 9	0:46	1, 9	23:46
	G2	31.53132	-80.96024	2, 13	17:20	2, 12	14:09	2, 13	12:19	1, 11	8:59	-	-	1, 11	0:40
Mid-shelf	SS3	31.08498	-81.03222	-	-	-	-	-	-	-	-	-	-	1, 14	0:42
	SS4	31.06576	-80.89528	-	-	-	-	-	-	-	-	-	-	1, 16	23:07
	A3	31.19518	-80.95994	2, 17	22:03	2, 13	18:30	2, 15	18:44	2, 16	23:46	2, 15	17:32	1, 16	17:50
	A4	31.18714	-80.82886	2, 19	23:43	2, 19	19:47	2, 16	20:19	1, 18	0:46	1, 18	19:10	1, 16	16:39
	C3	31.29692	-80.92632	1, 17	10:55	2, 18	23:08	1, 15	8:16	2, 17	6:53	1, 16	4:26	1, 13	16:25
	C4	31.29176	-80.80176	2, 19	12:30	2, 20	21:42	2, 18	10:06	1, 17	8:09	1, 18	6:01	2, 18	17:38
	C5	31.28206	-80.63908	1, 23	14:22	2, 23	20:02	2, 23	13:02	2, 23	9:38	1, 23	7:52	2, 24	19:32
	C6	31.27204	-80.43376	2, 34	16:30	2, 34	17:41	1, 35	15:07	1,40	11:38	2, 35	9:41	1, 30	21:11
	C7	31.26418	-80.30686	2, 35	18:01	2, 35	16:17	-	-	2, 36	12:41	-	-	-	-

Region	Site	Latitude (°N)	Longitude (°W)	April		May		July		August		September		November	
				Depth	Time	Depth	Time	Depth	Time	Depth	Time	Depth	Time	Depth	Time
Mid-shelf	E3	31.39664	-80.86742	2, 17	7:33	2, 17	7:46	2, 15	22:28	2, 17	21:45	1, 17	14:07	1, 18	5:36
	E4	31.3949	-80.69146	2, 19	9:31	2, 22	11:08	2, 20	4:19	2, 19	23:19	1, 21	19:32	1, 21	4:21
	G3	31.52712	-80.88336	-	-	-	-	-	-	-	-	2, 15	2:48	1, 14	2:00
	G4	31.5216	-80.77492	2, 16	20:10	-	-	2, 19	13:43	-	-	-	-	1, 19	3:16
	G5	31.52024	-80.72992	-	-	2, 21	12:13	2, 20	15:19	2, 20	5:52	2, 18	7:10	-	-
	G6	31.5125	-80.58666	-	-	-	-	1, 24	16:50	1, 22	4:42	2, 23	8:41	-	-
	G7	31.5014	-80.36716	-	-	-	-	2, 28	19:01	2, 30	2:31	2, 24	11:17	-	-
Shelf-break	C8	31.24988	-79.99776	2, 45	21:22	2, 45	13:22	2, 44	19:33	-	-	2, 45	13:48	-	-
	C9	31.23324	-79.71604	10, 78, 200	0:40	10, 75, 200	6:15	10, 75, 200	22:43	-	-	10, 50, 200	14:55	10, 75, 225	3:14
	C10	31.21574	-79.59664	10, 75, 200, 400	2:39	10, 75, 200, 400	9:52	10, 75, 200, 400	0:26	-	-	10, 100, 250, 440	18:54	25, 100, 200, 490	5:56

- Samples were not collected.

Table B.2: Primers used in this study

Target Gene	Primer	Sequence (5’→3’)	Q-PCR Efficiency	Reference
Quantitative-PCR				
Thaumarchaeota *rrs* (Taqman)	G1_334F G1_554R TM519AR	AGATGGGTACTGAGACACGGAC CTGTAGGCCCAATAATCATCCT TTACCGCGGCGGCTGGCAC	91-105%	Suzuki *et al.*, 2000
Bacteria *rrs* (Taqman)	BACT1369F PROK1492R TM1389F	CGGTGAATACGTTCYCGG GGWTACCTTGTTACGACTT CTTGTACACACCGCCCGTC	97-110%	Suzuki *et al.*, 2000
Archaea *amoA* (SYBRgreen)	Arch-amoA-for Arch-amoA-rev	CTGAYTGGGCYTGGACATC TTCTTCTTTGTTGCCCAGTA	80-89%	Wuchter *et al.*, 2006
Nitrospina rrs (SYBRgreen)	NitSSU_130F NitSSU_282R	GGGTGAGTAACACGTGAATAA TCAGGCCGGCTAAMCA	93-98%	Mincer *et al.* 2007
β-proteobacterial *amoA* (SYBRgreen)	amoA-1F amoA-r New	GGGGTTTCTACTGGTGGT CCCCTCBGSAAAVCCTTCTTC	81-90%	Rotthauwe *et al.*, 1997 Hornek *et al.*, 2006
PCR and Sequencing				
Archaea *rrs*	21F 958R	TTCCGGTTGATCCYGCCGGA YCCGGCGTTGAMTCCAATT	-	DeLong *et al.*, 1992
Archaea *amoA*	Arch-amoAF Arch-amoAR	STAATGGTCTGGCTTAGACG GCGGCCATCCATCTGTATGT	-	Francis *et al.*, 2005

Table B.3: Mean and ranges of environmental variables at different regions (defined in Table B.1) in the SAB during all cruises. SW, surface water; BW, bottom water; T, temperature; S, salinity; DO, dissolved oxygen; RF, relative fluorescence

Environ. variables	Time	Inshore		Nearshore		Mid-shelf		Shelf-break			
		SW	BW	SW	BW	SW	BW	SW	75 m	200m	400m
T(°C)	Apr	17.3 (16.9-18.1)	17.1 (16.7-17.7)	17 (16.2-17.9)	15.4 (15.2-15.5)	17.2 (16.2-18.5)	16.3 (15.4-18.4)	23.4 (21.8-24.8)	20.8 (19.5-22.7)	12.2 (12.1-12.3)	8.5
	May	24.6 (23.7-25.6)	24.3 (22.8-25.6)	22 (21.4-22.8)	21.7 (21.4-22)	22 (21-23.7)	21.7 (21-22.8)	25.6 (24.2-27)	21.9 (21.5-22.3)	16.2 (14.5-17.9)	9.6
	July	28.8 (28.3-29.4)	28.9 (28.4-29.5)	28.8 (28.4-29.3)	28.8 (28.5-29.2)	28.4 (27.7-28.9)	28.3 (27.4-29)	28.7 (27.8-29.2)	24.6 (23.9-25.5)	13.9 (10.9-16.9)	7.7
	Aug	29.2 (28.8-29.4)	29.1 (28.6-29.4)	29.3 (29-29.9)	29.2 (28.9-29.5)	29 (28.4-29.5)	28.5 (25.4-29.3)	-	-	-	-
	Sept	24.2 (24-24.5)	24.1 (24-24.5)	25.4 (24.6-26)	25.5 (24.7-26)	26.5 (25.9-26.8)	26.5 (25.9-26.8)	28.8 (28.2-29.6)	26.8 (25.5-27.8)	14.1 (13.9-14.3)	8.5
	Nov	19.2 (18.9-19.8)	19.1 (18.8-19.7)	19.7 (18.6-20.9)	19.9 (18.7-20.8)	21.8 (20.9-23.6)	21.8 (20.9-23.6)	27 (26.9-27.1)	26.9 (26.6-27.1)	13.8 (9.7-18)	8.2
S	Apr	21.3 (17.5-25)	24 (22.4-27)	31.2 (29.7-32.3)	33 (31.8-34.4)	33.5 (31.7-36)	35.1 (34-36.1)	36 (35.7-36.2)	36.2	35.4	34.9
	May	27.2 (25.9-27.9)	29.5 (27.4-31.9)	33.4 (31.8-34.4)	33.6 (31.8-34.5)	34.6 (34.5-35)	34.8 (34.5-35.7)	35.8 (35.3-36.1)	36.1 (36.1-36.2)	36 (35.7-36.2)	35
	July	24.4 (13.5-30.4)	24.9 (13.7-31)	34.9 (33.2-35.8)	35.2 (34.1-35.8)	36 (35.9-36.1)	36 (35.9-36.1)	36 (35.9-36.1)	36.1 (36-36.2)	35.6 (35.2-36)	34.8
	Aug	30.5 (27.9-32.4)	31.4 (30.6-32.4)	34.3 (33.3-35.2)	34.6 (33.6-35.2)	35.7 (35.5-36)	35.9 (35.6-36.1)	-	-	-	-
	Sept	25.8 (15.9-32.3)	26.2 (16.3-32.3)	34.1 (33.3-35.1)	34.1 (33.4-35.1)	35.4 (34.6-35.7)	35.4 (34.7-35.7)	35.5 (34.9-36.1)	36 (35.6-36.4)	35.8	35
	Nov	31.3 (30.4-31)	31.4 (30.6-32.3)	33.7 (32.3-34.3)	33.8 (32.5-34.3)	35.5 (34.7-36.2)	35.6 (34.7-36.2)	36.2 (36.1-36.3)	36.4 (36.2-36.6)	35.8 (35.3-36.3)	35

Environ. variables	Time	Inshore		Nearshore		Mid-shlef		Shelf-break			
		SW	BW	SW	BW	SW	BW	SW	75 m	200m	400m
DO (mg L^{-1})	Apr	6.4 (6.1-6.9)	6.5 (6.3-6.7)	6.4 (6-6.9)	6.8 (6.6-7)	6.3 (6-6.7)	6.8 (6.4-7.1)	5.8 (5.7-5.9)	5.7 (5.2-6)	3.7 (3.6-3.8)	3.8
	May	5 (4.6-5.5)	5.3 (4.6-5.6)	6.3 (6-6.8)	6.4 (6.2-6.5)	6 (5.5-6.4)	6.3 (5.8-6.6)	5.9 (5.7-5.9)	5.9 (5.7-6.1)	4.4 (4.2-4.5)	4.1
	July	5 (4.7-5.4)	4.5 (4.1-4.8)	6 (5.3-6.5)	6 (5.6-6.5)	5.8 (4.6-6.3)	6.1 (5.8-6.3)	5.9 (5.8-6)	6.4 (6-6.8)	4.2 (4.1-4.2)	4.2
	Aug	6.2 (5.3-7.1)	6 (4.9-6.5)	5.8 (5.2-6.5)	5.9 (5.7-6.3)	5.5 (4.9-6.2)	6.2 (6.1-6.5)	-	-	-	-
	Sept	5.8 (5.3-6.4)	5.7 (5.1-6.5)	6.4 (6.2-6.7)	6.3 (6.1-6.6)	6.2 (6-6.4)	6.3 (6.2-6.3)	6.2 (6.1-6.3)	6.2 (6.1-6.4)	4.3	4
	Nov	6.7 (6.2-7.4)	7 (6.6-7.6)	7 (6.7-7.4)	7.2 (6.9-7.3)	6.7 (6.2-7)	6.9 (6.6-7.1)	8.1 (6.2-10)	6.2	4.2 (4.1-4.3)	4.1
RF (µg L^{-1})	Apr	7.4 (5.4-8.5)	9.9 (5.7-13.9)	2.5 (1.7-3.6)	2.9 (1.6-4.8)	1 (0.5-2)	1.2 (0.9-1.4)	0.7 (0.5-1)	1.1 (0.8-1.4)	0.4	0.4
	May	12 (10.3-15.6)	11.5 (8.5-14.8)	2.6 (0.8-4.9)	3.6 (1.9-5.9)	1 (0.6-1.8)	1.5 (0.9-2.4)	0.4 (0.3-0.5)	1.6 (0.7-3.1)	0.4 (0.3-0.5)	0.3
	July	8 (5.3-12.7)	11 (7.5-13.1)	4.8 (4-5.6)	5.6 (4.4-6.8)	1.4 (0.6-2.6)	1.7 (1-2.9)	0.4 (0.3-0.5)	1.7 (1-2.3)	0.3 (0.2-0.3)	0.3
	Aug	8.9 (6.6-11.9)	10.1 (6.8-12.8)	3.8 (2.1-4.9)	5.3 (2.6-7.2)	2 (0.6-4.6)	2.5 (1.4-4)	-	-	-	-
	Sept	6.6 (4.7-10.4)	7.7 (5.5-10.9)	3.3 (1.5-5.6)	4.2 (1.8-7)	1.7 (0.9-2.5)	1.9 (1.3-2.8)	0.6 (0.5-0.7)	1.6 (1.2-2.3)	0.5 (0.5-0.6)	0.5
	Nov	6.5 (5.4-8.8)	8.1 (6.5-10.3)	4.6 (3.6-6.2)	5.8 (4.3-9.6)	1.8 (1.1-3.8)	1.9 (1.1-4)	0.7 (0.6-0.7)	0.6	0.4 (0.3-0.4)	0.4

- Samples were not collected

Table B.4: Mean and ranges of gene abundances and concentrations of NH_4^+, NO_2^-, NO_3^- and urea at different regions (defined in Table B.1) in the South Atlantic Bight during all cruises. SW, surface water; BW, bottom water; Thaum. *rrs*, Thaumarchaeota 16S rRNA; Bacteria *amoA*, Betaproteobacteria *amoA*; *Nitrospina rrs, Nitrospina* 16S rRNA

Date	**Location**	**Depth**	**qPCR data (×10^4 copies L^{-1} sample filtered)**				**NH_4 (µmol L^{-1})**	**NO_2 (µmol L^{-1})**	**NO_3 (µmol L^{-1})**	**urea (µmol L^{-1})**	**AO rates (nmol L^{-1} d^{-1})**
			Thaum. *rrs*	**Archaea *amoA***	**Bacteria *amoA***	**Nitrospina *rrs***					
April 2-6	inshore	SW	31 (19-41)	5.8 (1.1-10.4)	0.6 (0.2-1.1)	13.5 (9.3-21)	0.67 (0.37-1.07)	0.14 (0.11-0.2)	0.77 (0.14-1.89)	0.18 (0.08-0.33)	-
		BW	74 (23-172)	37 (2.7-95)	0.9 (0.6-1.4)	34 (9.4-73)	2.3 (0.61-5.41)	0.13	0.19 (0.13-0.25)	0.19 (0.1-0.33)	-
	near-shore	SW	9.5 (0.8-50)	1.5 (0.2-5.8)	0.3 (0.08-0.5)	0.9 (0.1-2.2)	0.35 (0.17-0.46)	0.12 (0.03-0.19)	0.33 (0.06-0.76)	0.2 (0.1-0.3)	-
		BW	9.3 (2.4-25)	2.0 (0.02-5.7)	1.0 (0.4-2.3)	1.5 (0.2-5.0)	0.4 (0.13-0.67)	0.11	0.25 (0.21-0.29)	0.13 (0.12-0.13)	-
	mid-shelf	SW	1.8 (0.4-7.9)	0.3 (0.1-0.6)	0.3 (0.03-1)	0.1 (0.04-0.4)	0.44 (0.16-0.99)	0.09 (0.05-0.11)	0.13 (0.04-0.32)	0.21 (0.01-0.35)	-
		BW	2.8 (0.4-10.7)	0.3 (0.06-0.7)	0.1 (0.02-0.5)	0.1 (0.05-0.2)	0.23 (0.11-0.36)	0.11 (0.1-0.14)	0.22 (0.05-0.33)	0.18 (0.1-0.23)	-
	shelf-break	SW	11.8 (0.4-32)	15.3 (1.1-37)	0.04 (0.03-0.05)	0.2 (0.04-0.5)	0.3 (0.06-0.49)	0.11 (0.06-0.14)	0.09 (0-0.25)	0.24 (0.12-0.32)	-
		75 m	221 (12-462)	274 (33-558)	0.1 (0.02-0.3)	16.4 (0.7-44)	0.22 (0.06-0.37)	0.18 (0.15-0.21)	1.28 (0.08-2.48)	0.28 (0.22-0.33)	0.29
		200 m	734 (270-1470)	122 (97-147)	0.2 (0.06-0.3)	22.2 (12-32)	0.1 (0.09-0.11)	0.13 (0.1-0.15)	8.71 (3.76-13.7)	0.26 (0.22-0.3)	0.64
		400 m	470	5.6	0.004	8	0.07	0.16	17.7	0.33	0.20
May 15-18	inshore	SW	103 (61-150)	24 (8.6-41)	10 (2.6-25)	47 (23-86)	2.24 (1.07-6.35)	0.12 (0.08-0.28)	0.45 (0.19-1.04)	0.05 (0.02-0.15)	-
		BW	149 (69-262)	30.5 (10.5-50.3)	6.7 (2.4-11.4)	66 (25.6-118)	-	-	-	-	-

Date	Location	Depth	qPCR data (×10^4 copies L^{-1} sample filtered)				NH_4 (µmol L^{-1})	NO_2 (µmol L^{-1})	NO_3 (µmol L^{-1})	urea (µmol L^{-1})	AO rates (nmol L^{-1} d^{-1})
			Thaum. *rrs*	**Archaea *amoA***	**Bacteria *amoA***	**Nitrospina *rrs***					
May 15-18	near-shore	SW	8.9 (2.3-21)	3.9 (0.4-8.1)	2.1 (0.1-5.0)	2.7 (0.2-8.9)	0.1 (0.04-0.15)	0.07 (0.05-0.09)	0.05 (0-0.1)	0.18 (0.02-0.34)	-
		BW	11.2 (2.3-25.7)	4.7 (0.8-10.3)	0.9 (0.1-3.2)	3.2 (0.4-6.1)	0.09	0.09	LD	LD	-
	mid-shelf	SW	3.7 (0.5-8.7)	2.3 (0.3-14)	0.2 (0.08-0.5)	0.3 (0.1-0.4)	0.64 (0.2-0.94)	0.06 (0.04-0.09)	0.17 (0-0.79)	0.25 (0-0.35)	-
		BW	4.9 (1.1-23.5)	4.6 (0.3-36)	0.3 (0.05-0.8)	0.4 (0.2-0.5)	0.06	0.11	LD	LD	-
	shelf-break	SW	2.1 (0.06-5.6)	3.6 (0.1-10)	0.3 (0.06-0.4)	0.1 (0.09-0.2)	0.56 (0.05-1.09)	0.12 (0.05-0.21)	0.05 (0-0.1)	0.06 (0-0.1)	-
		75 m	391 (150-769)	726 (240-1560)	0.1 (0.05-0.2)	10.2 (0.5-25.8)	0.14 (0.02-0.25)	0.34 (0.3-0.37)	0.59 (0.05-1.12)	LD	1.52
		200m	597 (360-835)	116 (109-124)	1.8 (0.07-3.5)	23 (11.5-34.4)	0.22 (0.1-0.34)	0.24 (0.15-0.33)	5.3 (0-10.6)	LD	0.01
		400m	79.3	1.4	-	1.1	0.14	0.18	27.82	0.18	0.47
July 15-19	inshore	SW	1390 (127-2680)	788 (125-1680)	4.1 (2.0-8.1)	10.8 (5.7-14)	2.39 (1.27-3.26)	0.87 (0.31-1.26)	0.85 (0.08-1.99)	0.12 (0.07-0.19)	131 (0.6-218)
		BW	1197 (259-1740)	695 (128-983)	7.8 (6.7-8.7)	36.2 (26.7-51.9)	2.7 (1.68-3.5)	0.95 (0.32-1.42)	0.88 (0.15-1.82)	0.16 (0.12-0.26)	161 (2.4-264)
	near-shore	SW	102 (3.6-433)	69 (0.6-335)	0.5 (0.2-0.9)	2.0 (0.1-5.4)	0.25 (0.09-0.41)	0.13 (0.05-0.16)	0.1 (0-0.36)	0.1 (0-0.4)	0.1 (LD-0.3)
		BW	61.8 (0.7-412)	26.8 (0.3-168)	0.5 (0.2-0.8)	3.0 (0.2-7.9)	0.76 (0.1-2.53)	0.16 (0.14-0.19)	0.05 (0-0.18)	0.01 (0-0.03)	0.04 (LD-0.08)
	mid-shelf	SW	2.4 (0.3-7.5)	0.5 (0.07-1.0)	0.2 (0.04-0.7)	0.1 (0.02-0.4)	0.32 (0.11-0.74)	0.13 (0.05-0.18)	0.11 (0-0.46)	0.09 (0-0.36)	0.01 (LD-0.01)
		BW	2.4 (0.4-4.9)	0.4 (0.08-0.8)	0.2 (0.02-0.6)	0.1 (0.06-0.3)	0.11 (0.07-0.22)	0.15 (0.12-0.17)	0.16 (0-0.95)	0.01 (0-0.01)	LD
	shelf-break	SW	0.4 (0.2-0.8)	0.3 (0.06-0.7)	0.04 (0.02-0.06)	0.06 (0.05-0.07)	0.32 (0.05-0.46)	0.08 (0.04-0.14)	0.35 (0-0.54)	0.22 (0-0.34)	-

Date	**Location**	**Depth**	**qPCR data (×10^4 copies L^{-1} sample filtered)**				**NH_4 (µmol L^{-1})**	**NO_2 (µmol L^{-1})**	**NO_3 (µmol L^{-1})**	**urea (µmol L^{-1})**	**AO rates (nmol L^{-1} d^{-1})**
			Thaum. *rrs*	**Archaea *amoA***	**Bacteria *amoA***	**Nitrospina *rrs***					
July 15-19	shelf-break	75 m	148 (53.4-255)	250 (47.1-565)	0.07 (0.04-0.1)	0.9 (0.2-1.5)	0.14 (0.08-0.21)	0.25 (0.24-0.25)	0.09 (0.07-0.1)	LD	7.76
		200m	1197 (1026-1368)	239 (127-351)	0.03 (0.03-0.03)	37.6 (23.2-52)	0.08 (0.04-0.13)	0.15 (0.12-0.18)	21.4 (14.2-28.7)	LD	LD
		400m	889	8.8	0.6	6.1	0.06	0.12	32.6	LD	0.10
August 4-7	inshore	SW	4320 (551-10500)	1750 (95-5750)	2.7 (0.1-10.8)	16 (2.3-33.4)	0.65 (0.35-0.96)	1.2 (0.12-3.28)	0.39 (0.24-0.45)	0.33 (0.23-0.48)	LD
		BW	4012 (1827-7369)	2406 (986-4180)	4.4 (2.0-10.4)	40.6 (16.1-51.6)	0.95 (0.56-1.83)	1.35 (0.43-3.18)	1 (0.12-3.32)	0.41 (0.23-0.64)	6 (4.1-7.7)
	near-shore	SW	115 (15-601)	47 (0.6-334)	1.1 (0.03-3.3)	3.5 (0.5-11.3)	0.21 (0.19-0.26)	0.01 (0-0.01)	0.15 (0.12-0.17)	0.48 (0.09-0.99)	LD
		BW	61.7 (21.1-143)	13.6 (0.3-55.4)	1.0 (0.1-2.0)	6.1 (0.7-21.7)	0.25 (0.18-0.33)	LD	0.18 (0.15-0.2)	0.18 (0.11-0.27)	0.1 (0.01-0.2)
	mid-shelf	SW	10.8 (0.3-32)	1.4 (0.1-5.0)	0.06 (0.07-1.7)	1.0 (0.1-3.2)	0.36 (0.19-0.45)	0.17 (0.16-0.18)	0.03 (0-0.1)	0.15 (0.08-0.27)	0.06 (LD-0.06)
		BW	22.6 (3.2-84.8)	2.5 (0.2-7.3)	0.5 (0.03-1.4)	1.6 (0.2-3.4)	0.49 (0.3-0.78)	0.18	0.07 (0-0.12)	0.13 (0.08-0.2)	0.04 (LD-0.04)
September 23-30	inshore	SW	1120 (361-2370)	103 (26-231)	3.1 (0.5-6.1)	28 (15-41)	3.97 (1.46-5.51)	1.17 (0.66-2.02)	3.08 (0.41-7.33)	0.34 (0.24-0.41)	266 (71-631)
		BW	937 (396-1727)	115 (15.5-197)	1.9 (1.1-2.8)	30.1 (18.7-45.3)	3.64 (1.58-4.99)	1.2 (0.68-2.04)	3.42 (0.63-8.28)	0.35 (0.23-0.44)	386 (82-842)
	near-shore	SW	509 (28-1590)	126 (1.3-554)	2.1 (0.5-6.5)	7.2 (0.3-20)	0.53 (0.08-1.24)	0.28 (0.05-0.78)	0.27 (0-0.66)	0.24 (0.09-0.41)	104 (LD-104)
		BW	490 (32.6-1424)	119 (2.9-535)	2.7 (0.9-4.9)	12.2 (0.7-25.6)	0.45 (0.14-1.09)	0.33 (0.12-0.72)	0.12 (0-0.47)	0.2 (0.09-0.26)	68 (LD-132)
	mid-shelf	SW	11 (1.6-25)	0.9 (0.1-2.9)	0.3 (0.06-0.7)	0.3 (0.1-0.6)	0.33 (0-1.36)	0.13 (0.07-0.18)	0.17 (0-0.68)	0.23 (0.08-0.36)	0.15 (LD-0.15)
		BW	15.2 (2.1-33.4)	1.1 (0.04-2.3)	0.5 (0.03-1.4)	0.5 (0.2-1.3)	0.14 (0-0.34)	0.15 (0.11-0.17)	0.01 (0-0.04)	0.16 (0.08-0.26)	0.04 (LD-0.06)

Date	Location	Depth	qPCR data (×10^4 copies L^{-1} sample filtered)				NH_4 (µmol L^{-1})	NO_2 (µmol L^{-1})	NO_3 (µmol L^{-1})	urea (µmol L^{-1})	AO rates (nmol L^{-1} d^{-1})
			Thaum. *rrs*	**Archaea *amoA***	**Bacteria *amoA***	**Nitrospina *rrs***					
September 23-30	shelf-break	SW	21 (0.3-36)	3 (0.06-7.7)	0.2 (0.06-0.2)	0.2 (0.08-0.3)	0.24 (0.05-0.37)	0.1 (0.08-0.12)	0.34 (0.03-0.57)	0.3 (0.15-0.39)	-
		75 m	367 (32.3-680)	296 (7.4-764)	0.3 (0.04-0.5)	0.7 (0.4-1.3)	0.29 (0.14-0.45)	0.24 (0.12-0.35)	0.34 (0.05-0.77)	0.28 (0.21-0.35)	12.42
		200m	2279 (1180-3378)	458 (122-794)	3.8 (0.7-6.8)	73.1 (28.3-118)	0.1 (0.04-0.16)	0.17 (0.16-0.18)	21.3 (14.6-28)	0.24 (0.21-0.27)	LD
		400m	2367	21.8	1	25.9	0.12	0.17	31.6	0.21	0.01
November 3-7	inshore	SW	287 (179-373)	61 (8.1-93)	3.4 (0.03-11)	19 (2.6-29)	0.55 (0.22-1.4)	0.23 (0.16-0.43)	0.52 (0.1-1.18)	0.35 (0.32-0.38)	1 (0.3-3.1)
		BW	430 (248-629)	93.8 (62.8-135)	5.4 (2.7-8.7)	34 (13.9-58.6)	0.57 (0.28-0.95)	0.19 (0.16-0.29)	0.52 (0.1-1.03)	0.37 (0.34-0.4)	3 (0.3-6.9)
	near-shore	SW	78 (16-327)	5.2 (0.1-17)	1.5 (0.3-5)	2.8 (0.4-7.2)	0.21 (0.07-0.1)	0.14 (0.12-0.18)	0.06 (0-0.12)	0.12 (0.08-0.24)	0.01 (LD-0.01)
		BW	107 (0.1-485)	33.1 (0.1-206)	3.9 (0.8-13.7)	9.0 (0.4-45.7)	0.13 (0.09-0.19)	0.16 (0.12-0.2)	0.07 (0-0.13)	0.19 (0.13-0.24)	0.01 (LD-0.01)
	mid-shelf	SW	19 (0.3-41)	1.7 (0.3-3.3)	1.6 (0.03-1.5)	0.6 (0.2-2.3)	0.2 (0.07-0.42)	0.13 (0.11-0.21)	0.04 (0-0.14)	0.16 (0-0.27)	0.01 (LD-0.2)
		BW	20.9 (6.0-36.2)	2.5 (0.7-9.3)	0.6 (0.03-1.8)	0.7 (0.3-2.0)	0.12 (0.06-0.26)	0.14 (0.11-0.18)	0.03 (0-0.14)	0.18 (0-0.29)	0.01 (LD-0.02)
	shelf-break	SW	27 (25-30)	32 (30-35)	0.1 (0.04-0.2)	0.2 (0.2-0.3)	0.3 (0.22-0.38)	0.18	0.93 (0.12-1.73)	0.12 (0.09-0.15)	-
		75 m	656 (12.5-1300)	959 (16.8-1901)	1.3 (0.3-2.3)	29.4 (14.9-43.9)	1.66 (0.12-3.2)	0.14 (0.12-0.16)	3.32 (0.03-6.6)	0.16 (0.12-0.19)	2.15
		200m	1069 (924-1214)	312 (35.8-589)	1.3 (0.3-2.3)	29.4 (14.9-43.9)	0.28 (0.07-0.5)	0.13	21.2 (13.2-29.2)	0.08 (0.07-0.09)	7.22
		400m	334	2.7	0.007	2.6	0.13	0.21	22.4	LD	LD

Table B.5: Richness and diversity indices of Archaea *amoA* and Thaumarchaeota *rrs* sequences in surface waters at several stations spanning from inshore to shelf-break and in depth of 200 m of the shelf-break station C10 during July cruise. SAPES, Sapelo Sound; DOBES, Doboy Sounds; ALTES, Altamaha Sound

Station #	# of Clones	# of OTUs	Chao1	Shannon H'	# of Unique OTUs	% of Unique OTUs
Archaea *amoA*						
SAPES	45	8	11	1.1	4	50
DOBES	40	24	58	2.9	13	54
ALTES	22	16	38	2.6	9	56
C1	31	13	25	1.9	5	38
C4	29	12	17.3	2.0	6	50
C10 10 m	38	17	28.3	2.5	8	47
C10 200 m	48	27	52.5	3.0	24	89
Thaumarchaeota *rrs*						
SAPES	14	3	3	1.5	2	67
DOBES	10	2	2	0.3	1	50
ALTES	-	-	-	-	-	-
C1	4	2	2	0.6	1	50
C4	1	1	1			
C10 10 m	2	2	3	0.7	1	50
C10 200 m	40	25	88	2.9	24	96

- No clone retrieved from the sample

Table B.6: Redundancy analysis (RDA) ordination plots of Thaumarchaeota 16S rRNA and Archaea *amoA* genes versus environmental factors in the surface waters of the SAB and versus environmental factors with depth at the shelf-break station in the South Atlantic Bight.

	RDA analysis	
Surface water environmental variables (Fig. 4.9a)	**Variance**	**p-value**
Fluorescence	0.53	0.002
NO_2^-	0.08	0.002
S	0.04	0.004
urea	0.02	0.006
T	0.02	0.008
Axes	**RDA 1**	**RDA 2**
Eigenvalues	0.71	0.01
Gene abundance-environment correlations	0.87	0.3
Cumulative percentage variance		
of gene abundance data	71	72
of gene abundance-environment relation	99.3	100
Shelf-break environmental variables (Fig. 4.9b)	**Variance**	**p-value**
Depth	0.47	0.002
T	0.25	0.002
Bacteria 16S	0.05	0.04
NO_3^-	0.05	0.02
Axes	**RDA 1**	**RDA 2**
Eigenvalues	0.76	0.09
Gene abundance-environment correlations	0.93	0.88
Cumulative percentage variance		
of gene abundance data	76	85
of gene abundance-environment relation	89.2	100

Figure B.1: Sampling stations in the South Atlantic Bight. Inshore stations: Saint Simons (SS), Altamaha Sound (ALTES), Doboy Sound (DOBES) and Sapelo Sound (SAPES); nearshore stations: SS1-SS2, A1-A2, C1-C2, E1-E2 and G1-G2; mid-shelf stations: SS3-SS4, A3-A4, C3-C7, E3-E4, G3-G7; shelf-break stations: C8-C10. The contour lines are 20 m, 50 m and 200 m isobath.

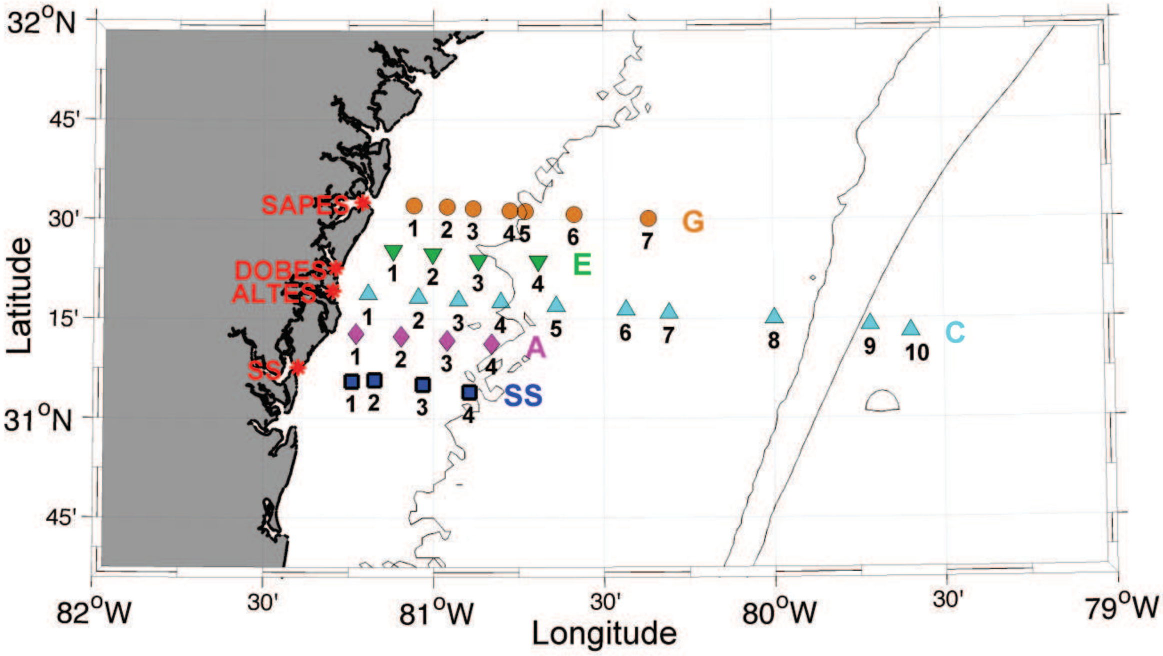
32°N
45'
30'
15'
31°N
45'
82°W
30'
81°W
30'
80°W
30'
79°W
Latitude
Longitude
SAPES
DOBES
ALTES
SS
G
1
2
3
4
5
6
7
E
1
2
3
4
C
1
2
3
4
5
6
7
8
9
10
A
1
2
3
4
SS
1
2
3
4

Fig. B.2: The satellite image of the continental shelf in the South Atlantic Bight taken on March 2, 2014 (graph provided by Dr. John Schalles from Creighton University, Omaha, NE)

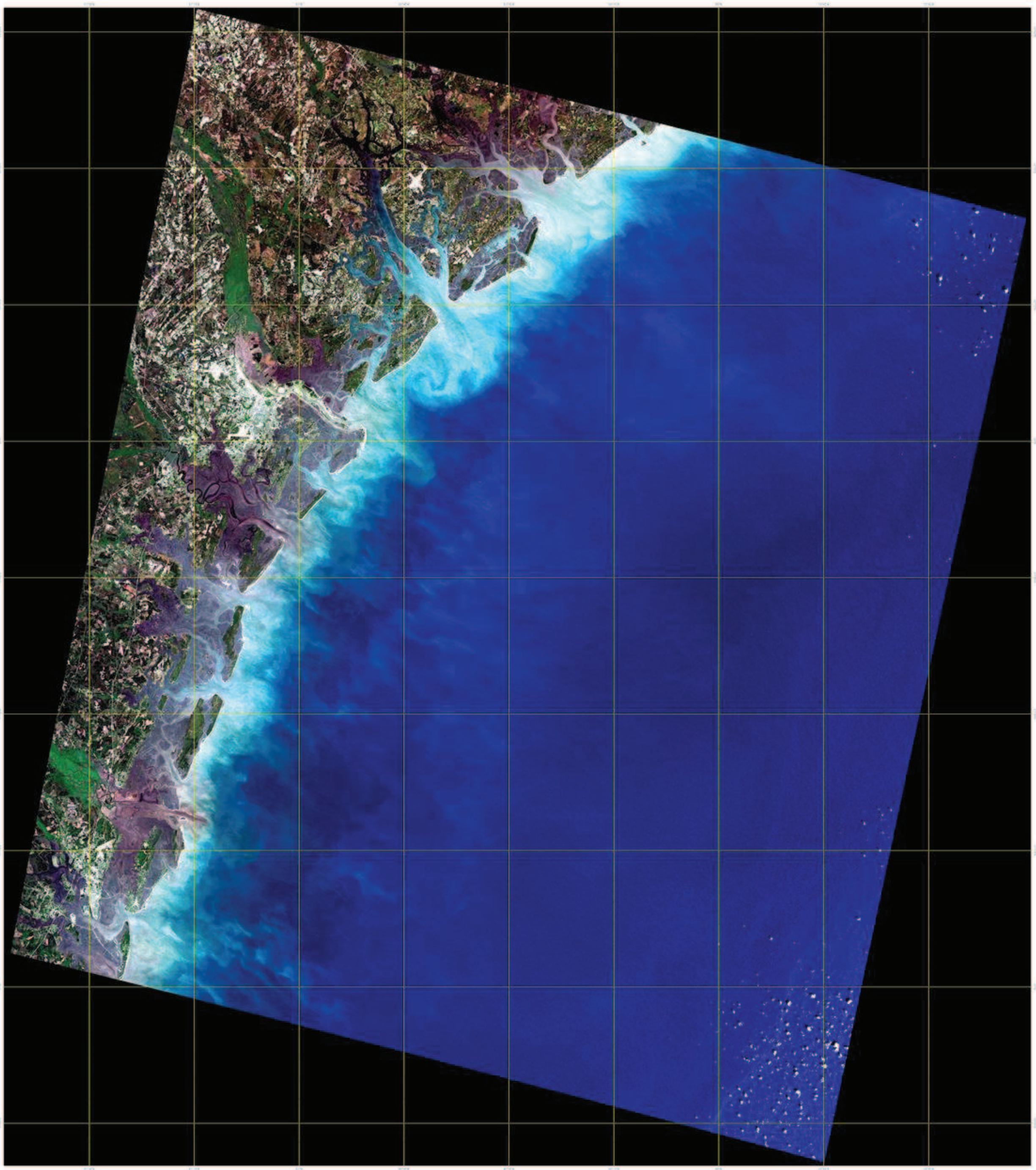

Fig. B.3: Rarefaction curve of Archaea *amoA* gene sequences recovered from DNA collected on the July cruise from surface water samples at inshore stations SAPES, DOBES and ALTES, nearshore station C1; mid-shelf station C4; and 10 m and 200 m at the shelf-break station C10. OTUs were defined with ≥ 98% similarity. SAPES, Sapelo Sound; DOBES, Doboy Sound; ALTES, Altamaha Sound.

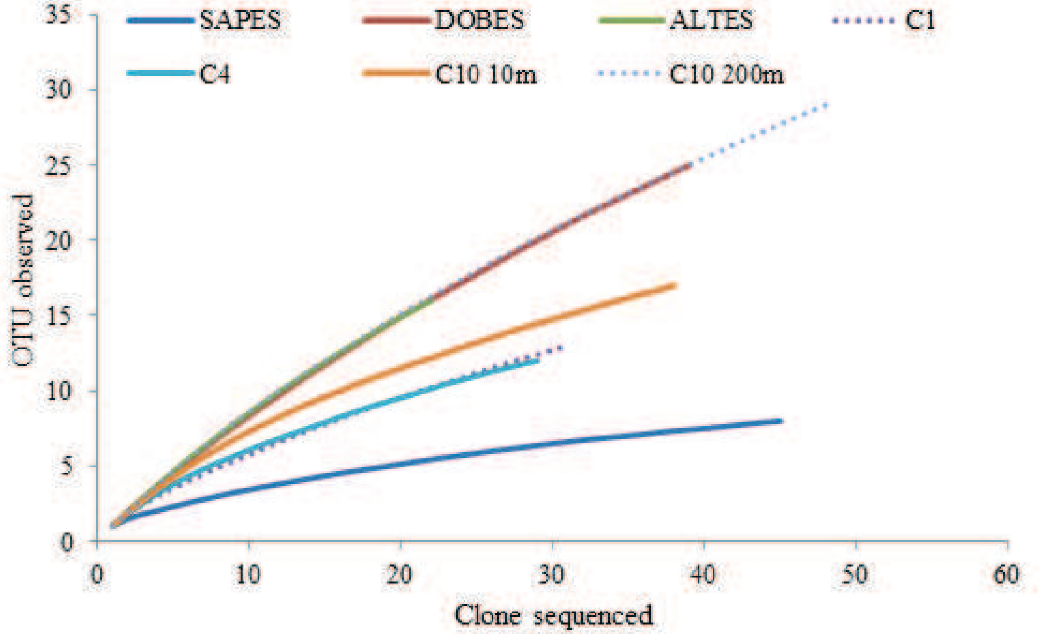
SAPES
DOBES
ALTES
C1
C4
C10 10m
C10 200m
OTU observed
Clone sequenced
0
5
10
15
20
25
30
35
0
10
20
30
40
50
60